This thesis is dedicated to my parents, my wife.

Acknowledgments

Praise and gratitude be to ALLAH, almighty, without whose gracious help it would have been impossible to accomplish this work. Acknowledgment is due to King Fahd University of Petroleum & Minerals for extending the facilities to carry out this research.

I would like to express my gratitude and appreciation to my advisor Dr. Ashraf Fatehi for his guidance and helpful suggestions throughout this study and prior to his leaving KFUPM. Special thanks are due to Dr. Kevin Loughlin for his invaluable contribution to the theoretical aspects of the work and for being my advisor in the remainder of the research. Thanks are due to the committee members Dr. Ramazan Kahraman and Dr. Nadhir Al-Baghli for their invaluable suggestions and significant contributions. I am also deeply thankful to the department chairman Dr. Mohammed Bakr Amin and department technicians, Mr. Mariano and Mr. Mahdi Al-Saffar for the strenuous efforts they exerted and sincere cooperation extended during the experiment work.

I would like to thank SABIC Engineering and Projects Management (E&PM) for giving me this opportunity for studying M.S. as a part time student and for supporting and continuous encouragement throughout the thesis work. Special thanks goes to E&PM management, namely, Mr. Abdulkareem Al-Othman, General Manager of E&PM organization, Mr. Saleh Bahamdan, Engineering Manager, Mr. Ahmed Al-Ghamdi, Design Manager, and Mr. Abdullah Al-Abdulgader, Projects Manager for their continuous encouragement and corporation. I would also like to thank SADAF Company and in particularly process engineering department for providing information regarding the problem studied in this thesis work. Special thanks goes to Mr. Hussain Ghurab, General Manager for Operations & Projects at PDM for his corporation.

My special gratitude to my parents, brothers, and sister whose love and affection is the source of inspiration and encouragement for my studies. Last, but not least, I extend thanks and appreciation to everyone who helped directly or indirectly to get this work done.

TABLE OF CONTENTS

LIST OF TABLES

LIST OF FIGURES

ABSTRACT

Name: FAHAD HUSSAIN FALQI

Title: KINETICS AND EQUILIBRIUM ADSORPTION OF PHOSPHATES ON ACTIVATED ALUMINA

Degree: MASTER OF SCIENCE

Major Field: CHEMICAL ENGINEERING

Date: October 2004

The present work is a part of an overall objective to establish the feasibility for removal of phosphates from the simulated wastewater stream using Activated almunia adsorbent AA400G (14x28 Mesh) and (28x48 Mesh) in order that it can be recycled and re-used for industrial purposes.

Activated alumina is an ion exchanger sorbent rather than an adsorbent for phosphoric acid. Equilibrium isotherms for liquid phase ion exchange are generated for phosphate on Activated Alumina. Data are obtained at variable as well as controlled pH of 4.5 and 6.0. Three temperature levels of 25, 40 and 80 °C are conducted for equilibrium isotherms. Data are fitted based on Freundlich Isotherm. Maximum equilibrium ion exchange loading (mg PO_4^{3-}/g sorbent) is found for the case of no pH control at high phosphorous equilibrium concentration but initial and final control of pH at 6.0 is found to be the best choice of lowering the equilibrium concentration of phosphorous to less than 1 ppm at 80 °C with high adsorbent loading level. It is observed that pH control condition affects the equilibrium adsorbent loading significantly due to competing ions resulting from the addition of buffer solutions 0.1M NaOH and 0.1M H_2SO_4 that decrease the active adsorption sites of phosphate ions to the surface of the activated alumina adsorbent.

Kinetic data are generated and modeled by HSDM model and the diffusion coefficients D_s were found from the fit. The diffusivity increases with increasing initial phosphate solution as well as increasing the temperature as it is expected from Arrhenius's equation. It was found in the case of pH control that the diffusivity is higher than that with no pH control due to promotion by the buffer ions.

Master of Science Degree

King Fahd University of Petroleum & Minerals

Dhahran, Saudi Arabia

October 2004

CHAPTER ONE

INTRODUCTION

1.1 Introduction

Wastewater or contaminated water is a big environmental problem all over the world. Not only does wastewater pollute but also those materials that enter into wastewater produce bacteria. It is known that wastewater not only causes environmental pollution but also, if it is permanently discarded, causes water shortage. For these reasons, disposal of wastewater has caught attention of modern engineers. In addition, attention has been devoted to industrial wastewater contamination since the technologist is interested in minimizing this quantity for the down stream processing costs.

In industrial plants, contaminants may be a result of side reactions, rendering the water stream an effluent status. The industrial wastewater streams contain contaminants such as heavy metals, suspended solids and organic chemicals. These impurities are at low-level concentration but still need to be further reduced to levels acceptable by various destinations in the plant, the most rigid among them being the boiler feed water (BFW). In general, treated water is an expensive commodity; hence there is a need to ensure its economical usage. There has been increasing attention directed towards alternative methods for wastewater treatment. Those contaminants are often resistant to degradation by biological methods, and are not removed effectively by conventional

physicochemical treatment methods, such as coagulation/flocculation, sedimentation, filtration and ozonation. Usually, chemical precipitation is tried first and in this process all materials in wastewater cannot settle out during settlement process. Some materials dissolve in water and so will never settle; others are so small that they would require an uneconomic time period to permit their settlement. These soluble materials can be removed from the liquid by conversion in biological cells. However, as compared to the preceding procedure, adsorption process is widely used since it is has more advantages.

It has been found that the kind of treatment depends on the type of wastewater and also its reuse. Some treated wastewater can be used for industrial purposes and some cannot be used. Moreover, contamination in industrial process water stream is selective and process dependent, hence the water treatment process is also quite specific. The process water tends to get contaminated down stream and requires suitable treatment prior to reusing. One such contaminant in industrial process water is inorganic and organic phosphates. The following is a summarized problem statement concerning a Crude Industrial Ethanol plant:

"Crude industrial ethanol is made by ethylene reaction with steam over phosphoric acid catalyst on silica gel carrier. One of the side reactions results in inorganic and organic phosphate formation. A large quantity of water carries this contaminant and hence it cannot be re-used. This results in loss running into a couple of million riyals per annum. Total phosphates' concentration in water is about 400 ppm. If this wastewater is treated to reduce the phosphates to less than 10 ppm level, then it can be used in most of the plant destinations with the exception of boiler feed water (BFW). The treatment

method could be mechanical, chemical, biochemical or any other provided it is cost effective. For example, separation by adsorbent is proposed, and then it should one which can be regenerated." (SADAF, 2000)

The above statement forms the basis of this research problem, which is to establish, evaluate and present a treatment method for removing inorganic and organic phosphates using an adsorbent, which can be regenerated and re-used so that the process is cost effective. The present study is a part of an overall study to establish techno-economic feasibility for using Alumina for removing phosphate contaminates in water so that it can be recycled. The approach to solve the above problem rests mainly with the testing of a commercial adsorbent suitable for the process through the laboratory and field studies and its applicability to the actual process. One such category of adsorbent is commercial Activated Alumina series from Alcan group in Canada that has reported removal of phosphorous related compounds to single digit ppm concentration and can be effectively regenerated. A suitable treatment process for removing phosphates could help control the cost and save natural resources. For this the treatment should be cost effective and secondary effluent must be much less than the treated effluent.

1.2 Diffusion Theory

There are two diffusion processes in a particle. It is possible that either or them or both of them control the uptake depending on the system parameter and operating condition.

According to the IUPAC classification, pores are divided into three categories based on their size.

Micropores	$d < 20$ Å
Mesopores	20 Å $< d < 500$ Å
Macropores	$d > 500$ Å

1) Micropore Diffusion: This is the case when the diffusion in the particle interior through the large void between the microparticles is very fast. The uptake is controlled by the diffusion of adsorbed molecules into the interior of the microparticle. This is expected for small particle or molecules having molecular dimensions close to the size of micropores.
2) Macropore Diffusion: In this case when the diffusion into the microparticles is fast and hence the uptake is controlled by the ability of the molecules to get through the macropore and mesopore. This is expected for large particle and molecules having size much smaller than the pore size of the macropore.
3) Macropore-Micropore Diffusion: This is often called the bimodal diffusion model. In this case two diffusion processes both control the uptake. This is expected when the particle size is intermediate.

The rates of adsorption and desorption in porous adsorbents are generally controlled by transport within the pore network, rather than by the intrinsic kinetics of sorption at the surface. Since there is little bulk flow through the process it is convenient to consider intraparticle transport as a diffusive process and to correlate kinetic data in terms of diffusivity defined in accordance with Fick's law. It relates the molar flux due to diffusive transport and the concentration gradient by the following expression:

$$J = - D(C) \frac{\partial C}{\partial x} \tag{1.1}$$

Fick's second law describes change of concentration as a function of time as follows:

$$\frac{\partial C}{\partial t} = \frac{\partial}{\partial x}\left[D(C) \frac{\partial C}{\partial x} \right] \tag{1.2}$$

When the diffusivity is a constant, the appropriate expression is:

$$\frac{\partial C}{\partial t} = D \frac{\partial^2 C}{\partial x^2} \tag{1.3}$$

Such definition provides a convenient mathematical representation implying only that the diffusivity is not dependent on concentration gradient. Since the true driving force for any transport process is the gradient of chemical potential, rather than the gradient of concentration, ideal Fickian behavior, in which the diffusivity is independent of sorbate concentration, is realized only when the system is thermodynamically ideal (Ruthven, 1984).

1.3 Characteristic of Activated Alumina Adsorbent

1.3.1 Preparation of Activated Alumina

Alumina is a generic name for the oxides and hydroxides of aluminum. The phase chemistry is complex with five thermodynamically stable phases, plus a large number of metastable and transition forms.

Activated alumina is high surface area adsorbent; porous aluminas are prepared by low temperature calcinations of alumina hydroxide compounds such as the trihydroxides (gibbsite, bayarite) and oxyhydroxides (boehmite, pseudoboehmite). Gibbsite, $Al(OH)_3$ is the aluminum hydroxide phase produced by the Bayer process. Table 1.1 shows the conversion steps of gibbsite to α-alumina. On static calcination in air, dehydration and eventual conversion to α -alumina occurs as follows: At 170 – 200 ºC part of the gibbsite is converted to boehmite, AlOOH, by intragranular hydrothermal pressure. The quantity of boehmite formed depends on a number of factors, including heating rate, soda content, bed depth and atmospheric moisture content. On further heating, to about 250 ºC, the reminder of the gibbsite forms χ-alumina. At about 450 ºC the boehmite starts dehydrating to γ-alumina resulting in another tubular micropore system. As the calcination temperature increases a number of other transition aluminas, of lower surface area, are passed through before α-alumina is finally reached at about 1150 ºC. Bayerite, another $Al(OH)_3$ phase, dehydrates in a similar fashion to gibbsite but via boehmite and η -alumina (instead of χ-alumina). Flash calcination of gibbsite, as used by Alcan Chemicals, produces predominantly χ-alumina, avoiding the boehmite dehydration path. The porosity is very similar to that obtained by static calcination. Some of these aluminas

Table 1.1: Conversion Steps of Gibbsite to Alpha -alumina

Temperature (ºC)	Conversion step
170 - 200	Part of gibbsite → boehmite
250 - 450	The remainder of Gibbsite → χ-alumina
450 - 800	Boehmite → γ-alumina
800 - 1150	χ-alumina → κ-alumina γ-alumina → β-alumina → θ-alumina
1150	κ-alumina → α-alumina θ-alumina → α-alumina

are named AA100 or AA101 produced with a surface area of about 270 m^2/g, or finer product of 260 m^2/g (Azizian, 1992).

By varying the type of the pelletisers and production technique it is possible to produce activated alumina products with a very wide range of physical characteristics; typical examples include the Alcan standard grades AA300 and AA400. AA300 is stronger, has higher density and is less macroporous, an ideal combination for applications as a desiccant. AA400 has a higher macroporosity and is better suited to applications in catalysts, catalyst supports or as general adsorbents (Azizian, 1992).

1.3.2 Properties and Applications of Activated Alumina

Sorption behavior varies extensively, depending upon the morphology and synthesis methodology of the particular material. Adsorption of molecular species on aluminas from bulk liquid water medium represents a special case in adsorption with aluminas. It has been well established that affinity for water on aluminas is stronger than virtually all other species. When placed in water, surface hydroxyls are formed by chemisorption. A further layer of water is bound to these hydroxyls by hydrogen bonding. The surface of activated alumina is very heterogeneous in terms of groupings of cations, hydroxyls and oxygen ion vacancies and this leads to the surface hydroxyls ranging from very basic to partially acidic. The surfaces are also amphotric in nature, as the surface hydroxyls can be protonated in acidic media giving a positively charged surface and deprotonated in basic media to give a negatively charged surface. This behavior can be modified by incorporation of other ions (Fleming, 1986). Their adsorbent properties lead to a wide variety of applications including catalyst, catalyst supports,

desiccants and water purification. Other uses for activated alumina include chromatography and drying of liquids such as kerosene, aromatics, gasoline fractions and chlorinated hydrocarbons. Table 1.2 shows physical properties of activated alumina AA400G (Azizian, 1992).

1.3.3 Mechanism of Phosphorous removal by Activated Alumina

The adsorption of phosphates on activated alumina occurs through an ion exchange mechanism. The ion exchange selectivity sequence for activated alumina has been determined for a range of typical cations and anions as follows (Fleming, 1990):

$$OH^- > PO_4^{3-} > C_2O_4^{2-} > F^- > CrO_4^{2-} > SO_4^{2-} > Cr_2O_7^{2-} > Cl^- > NO_3^- \qquad (1.4)$$

This sequence indicates that only hydroxyl ions are preferentially adsorbed to phosphate ions from water. It also shows that activated alumina surface can adsorb more than one component leading to multicomponent adsorption process. The reaction between the phosphate and the alumina surface is probably best represented by (Fleming, 1990):

$$Al(OH)_3 + H_2PO_4^- \rightarrow AlPO_4 + OH^- + 2H_2O \qquad (1.5)$$

This reaction is slow. It has been suggested that the generation of hydroxyl ions as phosphate is adsorbed by activated alumina results in an increase in pH (Brattebo and Odegaard, 1986).

Inorganic phosphates exist in several forms. The most common forms are the orthophosphates ($H_2PO_4^-$, HPO_4^{2-}, PO_4^{3-}), pyrophosphate ($P_2O_7^{4-}$), tripolyphosphate ($P_3O_{10}^{5-}$), and hexametaphoshpate [$(PO_3)_6^{3-}$]. All these phosphates eventually hydrolyze in an aqueous solution and revert to the orthophosphate form. The resulting three

Table 1.2: Physical Properties of Activated Alumina AA400G (Azizian, 1992).

Surface Area	254 m^2 / g
Apparent Density	2.79 cc / g
Micropore Volume (Pore less than 30 Å)	0.04 cc / g
Macropore Volume (Pore greater than 30 Å)	0.44 cc / g
Total Pore Volume	0.48 cc / g
Average Pore Diameter	72 Å

orthophosphate species exist in equilibrium with each other and depend on the pH of the solution (Azizian, 1992). Analysis of various phosphorous compounds in biological treatment effluents showed that 99.4% of the total phosphorous is soluble, of which 98% is present as inorganic orthophosphates. All equilibrium isotherms results are expressed as PO_4^{3-} without regard to the actual form present. The mechanism of orthophosphate removal on activated alumina is mainly ion exchange accompanied by chemical reactions, precipitation and formation of complexes. The pH affects the importance of secondary reactions in addition to ion exchange (Narkis and Mordehai, 1986).

1.4 Research Objectives

This work is a part of a comprehensive study on economic re-utilization of a phosphate contaminated industrial water stream in a typical petrochemical plant in the Kingdom of Saudi Arabia. The objectives of the thesis are summarized as follows:

- To establish the feasibility for removal of phosphates from the simulated wastewater by adsorption on Activated Alumina AA400G.
- To reduce the concentration of phosphates on the contaminated water stream to less than 1 ppm so that it can be reused.
- To study kinetics and equilibrium adsorption of phosphates on AA400G to enable the adsorption system to be modeled.

CHAPTER TWO

LITERATURE SURVEY

1.2 Introduction

This literature review clearly establishes that phosphate removal using activated alumina is a technically feasible process and phosphate concentration can be brought down to less than 1 mg/L. Recently certain grades of commercial activated alumina, such as AA 400G from Alcan International, report reduction of phosphate levels up to 0.03 mg/L. An adsorption capacity of 100-mg P/g adsorbent is reachable under appropriate pH condition (Azizian, 1992). Although the technical feasibility exists, the economic viability can only be established if the adsorbent can be successfully reused for the waste water stream without its pretreatment (with alum etc.) and also a minimum amount of secondary waste stream should be generated. The industrial scale design can be done from the results of the study as well as available literature (Cooney, 1999).

Water treatment for phosphate removal is a very old and established process, although most of the processes are dedicated to drinking and sewage water treatments. Little attention has been given to the industrial wastewater contamination since these processes are quite specific in nature. Most of the processes however were established and dedicated to municipal wastewater treatment where the emphasis is more on

ecological considerations. Industrial wastewater treatment is done with a dual motive of environmental as well as economic consideration (De Renzo, 1981).

One of the current problems associated with water pollution involves the control of the level of undesirable nutrients, which are responsible for the excess growth of algaes or biological slimes in estuaries and lakes. Some of the biological treatment processes for reduction of phosphate concentration in wastewater involve the use of activated sludge. These methods do not fulfill the rigid requirements for tertiary treatment. In rivers and ground waters, local geology (and pollution), have resulted in levels of ions such as fluoride and arsenic exceeding those deemed safe for drinking water. There is an increasing requirement for cost-effective methods for lowering the levels of these pollutants. More effective for phosphate removal are chemical treatments, which are still subject to the costs and problems of sludge handling and its disposal (Fleming, 1986; Ronald and Thodos, 1969).

Removal of phosphate from wastewater has been practiced a long time in order to prevent eutrophication of lakes and water bodies. Presently economical means of removing phosphate in wastewater treatment plant is precipitation of the phosphate using metal salts, i.e. alum, ferric chloride, or lime and subsequent sedimentation of the phosphate floc in the treatment plant clarifiers. Application of aluminas in water treatment is quite common. Concentration of phosphates can be reduced to 1 mg/L by use of this method. Further reduction is possible with the use of activated alumina but it is a relatively expensive process for municipal wastewater. The main disadvantages of chemical precipitation are the high sensitivity to pH, increase in the electrolyte

concentrations and problems associated with sludge handling while a major advantage of using activated alumina is no sludge. Further the alumina can be regenerated using sodium hydroxide solution (Fleming, 1986).

Alumina oxides are well known as sorbents in industries varying from petroleum refining to pharmaceutical manufacture. Along with zeolites, silica, and carbons, these materials constitute the vast majority of adsorption media in use today. It is somewhat ironic, however, that aluminas are typically not considered to be a significant media in water treatment. Not only are particular aluminas well-suited for solving some existing separation problems in process and waste water, current advances in pore structure control and the ability to modify surface chemistry have led to the development of alumina materials applicable for water processes (Fleming, 1986).

Activated alumina has been examined as a phosphorus selective adsorbent for the removal of orthophosphate from aqueous solutions and effluents of biological treatment of domestic sewage and numerous studies have indicated the technical feasibility of Activated Alumina as an absorbent for phosphate removal (Urano and Tachikawa, 1991). The use of conventional ion exchange resins for selective phosphorus removal from effluents is not practical for the removal of phosphates alone, because of the extensive removal of nearly all other anions, which reduces the efficiency and capacity of the resin to remove phosphates. All these resins have a high sensitivity towards the pH (Ames and Dean, 1970).

It seems that the pH, the activated alumina granule size and the column length are very important parameters in minimizing the operating costs of a fixed-bed system for phosphorus removal. One of the earliest techno-economic study for selective removal of mixed phosphates on activated alumina was done by Yee (1966). The forms of phosphates studied for removal from wastewater included sodium orthophosphates and a variety of mixed polyphosphates. Three types of alumina varying in properties and with surface area ranging from 250 – 500 m^2/g were deployed. Exhausted column was regenerated in a three step process by re-circulating 1M NaOH solution followed by re-acidification with HNO_3. Polyphosphates were hydrolyzed to convert to orthophosphates for accurate analysis. 99% of orthophosphates was removed by 3000 bed volumes (BV) and isotherm capacities up to 30 mg PO_4^{3-} /g adsorbent were reached. 12 BV of waste NaOH solution is generated during regeneration, which indicates the high volume reduction factor (rate of product water to regenerated waste) that can be achieved.

Narkis and Mordehai (1986) showed that activated alumina effectively removed orthophosphates from effluent of biological sewage plant and from synthetic aqueous solutions. Their research purpose was to study the possibility of phosphorus removal from effluents using activated aluminas, manufactured by Merck and Alcoa. The adsorption isotherms of Merck and Alcoa F-1 activated aluminas for orthophosphate adsorption from extended aeration effluents were studied with respect to Langmuir and Freundlich adsorption isotherms. They found that the acidic and basic Alcoa F-1 activated aluminas have higher sorption capacities of orthophosphates than Merck activated alumina.

The results presented in literature indicate that the alumina system behaves very similar to a granular activated carbon (GAC) system. In addition special attention obviously has to be taken concerning the pH, since the adsorption capacity is strongly pH-dependent and since the adsorption itself affects pH significantly. The adsorption capacity of activated alumina increases with decreasing pH to a pH of 4. Below pH 4, the adsorption capacity decreases due to significant solubility of the alumina adsorbent (Brattebo and Odegaard, 1986). The pH-dependency is both related to the amphoteric properties of the alumina surface and to the polyprotic nature of phosphate; however, several explanations to these phenomena are proposed in literature. The highest adsorption capacity is observed at pH 4.0 – 6.0 (Azizian, 1992).

Orthophosphoric acid (H_3PO_4) is considered as a weak polybasic acid which has three dissociation equilibrium constants and undergoes successive ionizations:

$$H_3PO_4 \overset{pK_1=2.1}{\leftrightarrow} H_2PO_4^- \overset{pK_2=7.2}{\leftrightarrow} HPO_4^{2-} \overset{pK_3=12.3}{\leftrightarrow} PO_4^{3-}$$

where pK is defined as the negative common logarithm of the dissociation constant K (Laidler and Meiser, 1995). Bhandari et al. (1997) considered phosphoric acid as an example of a weak polybasic acid which has three dissociation equilibrium constants. They reported in their sorption equilibrium results by ion-exchange studies on weak resins that the sorbed species is not monovalent $H_2PO_4^-$ ion but divalent HPO_4^{2-} ion because it is more strongly anchored on the resin sites than the monovalent ion. Furthermore, they ruled out the possibility of sorption of H_3PO_4 as PO_4^{3-} on three sites in the weak base resins but acknowledged that this sorption cannot be overlooked in anion exchange resins of high basicity.

2.2 Equilibrium Study

The basic data needed for a good design of a packed bed adsorption system includes the equilibrium and kinetic parameters. The equilibrium data is a relation between the solute concentration in the adsorbent to that in the liquid phase. This data of q (solute concentration in the solid phase) versus C (solute concentration in the fluid phase) is normally fitted to one or more standard "isotherm" equations. Inspection of the adsorption isotherm plot can provide much valuable information. Five important properties of the adsorption isotherm are (Slejko, 1985):

1. The adsorbability of a component or, in other words, its relative affinity for the adsorbent.
2. The uptake or the concentration of the adsorbate on the adsorbent. This is expressed as weight of contaminant adsorbed per weight of adsorbent or the percentages.
3. The degree of removal achievable as indicated by the equilibrium adsorbate concentration. A constant concentration indicates a nonadsorbable component.
4. The presence of competing adsorbates indicated by nonlinear or multi-line isotherm plots.
5. The effect of pH on the adsorption isotherm.

Experimental isotherms are useful for describing adsorption capacity to facilitate evaluation of the feasibility of this process for a given application, for selection of the most appropriate adsorbent, and for preliminary determination of adsorbent dosage requirements. Moreover, the isotherm plays a crucial functional role in predictive modeling procedures for analysis and design of adsorption system. An additional

potential use of adsorption isotherms is for theoretical evaluation and interpretation of thermodynamic parameters, such as heats of adsorption. A variety of different isotherm equations have been proposed, some of which have a theoretical foundation and some being of a more empirical nature (Slejko, 1985).

The Langmuir Isotherm

The simplest theoretical model for monolayer adsorption is due to Langmuir (1918). Also, among the isotherms the most widely applicable for the liquid phase adsorption is the Langmuir Isotherm. It was formulated on the basis of dynamic equilibrium between the adsorbent phase and the fluid phase. When a solution is contacted with adsorbent and the system is allowed to attain equilibrium, the rate at which molecules are adsorbing to the surface is equal to the rate at which molecules are leaving the surface. This is what the concept of equilibrium implies. That is, equilibrium does not mean that adsorption and desorption cease to occur, but rather that their rates are equal, so that no there is further net adsorption. The main assumptions are the mono layer coverage, defined sites, equal energy of adsorption and no interaction forces between adjacent sites.

The Langmuir Isotherm can be represented by:

$$\frac{q}{q_m} = \frac{b\ C}{1 + b\ C} \qquad (2.1)$$

where q_m represents the concentration of the adsorbed species on the surface when one complete monomolecular layer of coverage is achieved. This means the surface is fully covered, $\theta = 1$, and $q = q_m$ which is the monolayer coverage (Cooney, 1999). It may be noted that the Langmuir isotherm reduces to a linear relationship under special

conditions. The denominator of the Langmuir isotherm equation (Weber, 1972), for example, approaches a value of unity for dilute solutions, and q_m b then becomes a compound linear partitioning coefficient. This corresponds to such low values of surface concentration ($q << q_m$) that additional adsorption changes the available surface area insignificantly and the reaction is dependent only on the solution phase concentration (Slejko, 1985). Equation (2.1) can be written in a variety of linear forms to facilitate fitting of experimental data for parameter evaluations,

$$\frac{C}{q} = \frac{1}{q_m C} + \frac{C}{q_m} \tag{2.2}$$

$$\frac{1}{q} = \frac{1}{q_m} + \frac{1}{b\, q_m\, C} \tag{2.3}$$

or

$$q = q_m - \frac{q_m}{b\ C} \tag{2.4}$$

These linear forms are equivalent, but one may be preferred to the others for a particular situation, depending on the range and spread of data to be described (Weber, 1972; Reinbold et al., 1979). A variety of equations have been used to fit multicomponent equlibria. Some are based on specific models, such as the Langmuir model, and others are merely empirical.

The Langmuir isotherm equations for a two-solute system are [Butler and Ockrent, 1930]:

$$\frac{q_1}{q_{m1}} = \frac{b_1\ C_1}{1 + b_1\ C_1 + b_2\ C_2} \tag{2.5}$$

$$\frac{q_2}{q_{m2}} = \frac{b_2\ C_2}{1 + b_1\ C_1 + b_2\ C_2} \tag{2.6}$$

The assumption of these equations is that the two solutes compete for exactly the same sites. However, in reality, some sites are involved in noncompetitive adsorption, and thus Jain and Snoeyink (1973) modified these equations for liquid to account for this fact based on the assumption that the first solute has adsorption sites equivalent to ($q_{m1} - q_{m2}$) available to it for noncompetitive adsorption. In practice, multicomponent Langmuir equations, regardless of their exact form, are of limited usefulness, since even single-solute Langmuir equations rarely fit liquid-phase adsorption data well.

The Freundlich Isotherm

It is frequently found that experimental data on adsorption for a liquid phase are fitted better by the so-called Freundlich isotherm equation (Freundlich, 1926):

$$q = k\ C^{1/n} \qquad (2.7)$$

where n is a constant normally greater than 1. The Freundlich isotherms are commonly used to fit data for the adsorption of organic pollutants from aqueous solution into activated carbon. The Freundlich equation does not approach a linear isotherm for very dilute solutions, and it does not approach a limiting asymptotic value observed for many systems. Freundlich attempted to attach rigorous physical significance to the parameters k and 1/n, but was, for the most part, unsuccessful. The value of k can, however, be taken as a relative indicator of adsorption capacity, while 1/n is indicative of the energy or intensity of the reaction (Crittenden and Weber, 1978). The Freundlich isotherm is derivable on a theoretical basis. The main assumptions are the Freundlich model does not impose any requirement that the coverage must approach a constant value corresponding to one complete monomolecular layer as the final concentration of solute in the solution

at equilibrium C gets large. It also implies that the energy distribution for the adsorption sites is of essentially an exponential type, rather than of the uniform type assumed in the Langmuir development.

The Langmuir-Freundlich Isotherm

While the Langmuir and Freundlich isotherm equations are by far the most common single-solute expressions used, there are other single-solute equations which are sometimes employed. One of these isotherm equations is the so-called Langmuir-Freundlich equation:

$$q = \frac{b\ q_m\ C^{1/n}}{1 + b\ C^{1/n}} \tag{2.8}$$

This equation has three parameters: b, q_m and 1/n. Although not thermodynamically consistent, this equation has been shown to provide a reasonably good empirical correlation of binary equilibrium for a number of simple gases on molecular sieve adsorbents; and is widely used for design purposes. However, because of the lack of a proper theoretical foundation this approach should be treated with caution (Cooney, 1999).

Langmuir-Freundlich equations for a two-solute system are of the form (Conney, 1999):

$$q_1 = \frac{a_1\ C_1^{1/n1}}{1 + b_1\ C_1^{1/n1} + b_2\ C_2^{1/n2}} \tag{2.9}$$

$$q_2 = \frac{a_2\ C_2^{1/n2}}{1 + b_1\ C_1^{1/n1} + b_2\ C_2^{1/n2}} \tag{2.10}$$

The Redlich-Peterson Isotherm

The Redlich-Peterson isotherm equation is an empirical equation and has the following form:

$$q = \frac{A\ C}{1 + B\ C^{n}} \tag{2.11}$$

Crittenden and Weber (1978) used this equation to fit data on phenol, p-bromophenol, p-toluene sulfonate, and dodecylbenzene sulfonate adsorption on Filtrasorb 400 activated carbon.

BET Isotherm

Brunauer et al. (1938) extended the Langmuir isotherm to include multi-layer adsorption phenomena. The essential assumptions of the BET isotherm are that any given layer need not be complete before a subsequent layer can form, no interaction between neighboring adsorbed molecules; and the heat evolved during the filling of the second and subsequent layers of molecules equals the heat of adsorption for monolayer attachment. If the layers beyond the first are assumed to have equal energies of adsorption, the BET equation takes the form (Slejko, 1985):

$$q = \frac{B\ C\ q_{\max}}{(C_s - C)\left[1 + (B - 1)\left(C / C_s\right)\right]} \tag{2.12}$$

2.3 Kinetic Study

Diffusion at the atomic or molecular level is a universal phenomenon. It occurs in all states of matter on time scales that vary over many orders of magnitude. Diffusion also controls the overall rate of a wide variety of physical, chemical and biochemical processes. Diffusion is a very significant phenomenon in porous solids such as catalysts or adsorbents. Such materials generally have very fine pores to achieve the large surface areas required for high activity. Transport through these pores occurs mainly by diffusion and often affects or even controls the overall reaction rate of the process. The mechanisms by which diffusion may proceed are highly affected by the nature of the diffusing molecules and their interactions with the surroundings. Depending on the particular system and the conditions, diffusion in microporous system may show features common to diffusion in vapor or liquid phase (Ruthven, 1984).

Diffusion Mechanism

1. Molecular Diffusion

When pore diameter is large relative to the mean free path, collision between diffusing molecules occurs far more frequently than collisions between the molecule and the pore wall. Under these conditions, the influence of the pore wall is negligible and diffusion occurs by the same mechanism as in the bulk fluid. A wide range of empirical and semiempirical correlations are available but it is generally necessary to select the appropriate correlation with care, taking due account of the nature of the components.

2. Pore Diffusion

In analyzing diffusivity it is assumed that the transport occurs only through the pores and the flux through the solid can be neglected. It is therefore convenient to define pore diffusivity based on the pore cross-sectional area:

$$J = -\varepsilon_p D_p \frac{\partial C}{\partial x} \tag{2.13}$$

The pore diffusivity is smaller than the diffusivity in a straight cylinder pore as a result of two effects; (i) Random orientation of the pores which gives a longer diffusion path and a reduced concentration gradient in the direction of flow, and (ii) the variation in the pore diameter. Both effects are commonly accounted for by a tortuosity factor (τ):

$$D_p = \frac{D}{\tau} \tag{2.14}$$

where D is the diffusivity under the same condition in a straight cylindrical pore. Tortuosity is a geometric factor and is independent of either temperature or the nature of the diffusing specie. If the pore structure is characterized in detail, a reasonably accurate theoretical prediction of tortuosity may be made but this requires detailed measurement of both the pore shape and pore size distribution.

3. Surface Diffusion

If there is significant adsorption on the pore wall there is the possibility of an additional flux due to the diffusion through the adsorbed phase or surface diffusion. Physically adsorbed molecules are relatively mobile and the mobility is substantially smaller than in the vapor phase. If adsorption equilibrium is favorable, the molecular density in the adsorbed layer may be relatively high. The fluxes through the gas phase and the adsorbed

phase are to a first approximation independent and therefore additive so that the diffusivity will be given by the sum of the pore and surface contribution, duly weighted to account of the difference in molecular densities between the adsorbed and vapor phases (Ruthven, 1984).

Surface diffusion can be described by the flux expression as follows:

$$J = - D_s \frac{\partial C}{\partial x} \tag{2.15}$$

4. Surface and Pore Diffusion

In porous adsorbents, the intraparticle transport can occur with pore and solid diffusion in parallel. The dominant transport process is the faster one and this depends on the relative diffusivities and concentrations in the pore fluid and in the adsorbed phase. Equilibrium between the pore fluid and the solid phase can be assumed to exit locally at each point within a particle. Then, the mass transfer flux is expressed by (Perry and Green, 1997):

$$J = - \left[\varepsilon_P D_P + \rho_P D_s \frac{dn}{dC} \right] = - D_e (C_p) \frac{\partial C_P}{\partial r} \tag{2.16}$$

where dn/dC is the derivative of the adsorption isotherm and it has ben assumed that at equilibrium $C_P = C$.

Isothermal Single Component Sorption in Batch system

Physical adsorption is an extremely rapid process so that in a porous catalyst or adsorbent the overall rate of adsorption is almost controlled by mass or heat transfer resistance rather than by the intrinsic rate of sorption at the active surface. Diffusion controlled processes may exhibit many of the features commonly associated with the slow activated surface adsorption process. There are several distinct resistances to mass

and heat transfer. There are essentially three consecutive mass transport steps associated with the adsorption of solutes by porous adsorbents. The first step, bulk transport of solute in the solution phase, is usually rapid because of mixing and convective flow. The second step, film transport, involves diffusion of the solute through a hypothetical "film" or hydrodynamic boundary layer. Except for a small amount of adsorption that occurs on the exterior of the adsorbent, the solute then must diffuse within the pore volume of the adsorbent and/or along pore-wall surfaces to an active adsorption site (intraparticle transport) (Ruthven, 1984; Slejko, 1985).

Film and intraparticle transports are thus the major factors controlling rates of adsorption from solute by porous adsorbents. Transfer of solute across the film can only occur by molecular diffusion, an intrinsically slow process. If the intensity of mixing is increased, the film thickness δ can be made smaller, and the mass transfer resistance, which is proportional to $\delta/D_{AB,}$ reduced. Once a solute molecule reaches the opening of a pore at the particle surface, it must diffuse through the liquid, which fills a typically tortuous network of interconnected pores, until it reaches a vacant adsorption site, where it can attach itself to the solid surface. As adsorption proceeds, successive solute molecules must travel farther and farther into the particle in order to find vacant sites. Thus, the process of reaching all the surface sites in a particle is a slow one. Two major resistances to mass transfer then should be considered: the external resistance in the liquid phase and the internal resistance in the solid phase (Cooney, 1999).

Assuming the liner driving force approximation, the liquid phase mass flux equation can be written for a finite volume batch system as:

$$V \frac{dC}{dt} = -k_f A \left(C - C_s\right) \tag{2.17}$$

where C is the uniform concentration of the solute in the bulk of the liquid, far from the surface, C_s is the concentration of the solute at the adsorbent particle surface, V is the volume of the solution, A is the surface area of the adsorbent particle and k_f is the film mass transfer coefficient. Theoretical boundary layer studies have led to functional correlations for external mass transfer coefficient in terms of system parameters; two that have been suggested by Williamson et al. [1963] for different flow regimes in fixed beds are given as follows:

$$\frac{k_f}{v_s} Sc^{0.58} = 2.40\ \mathrm{Re}^{-0.66} \quad (for \quad 0.08 < \mathrm{Re} < 125) \tag{2.18}$$

$$\frac{k_f}{v_s} Sc^{0.58} = 2.40\ \mathrm{Re}^{-0.31} \quad (for \quad 125 < \mathrm{Re} < 5000) \tag{2.19}$$

$$Sc = \frac{u}{\rho D_l} \tag{2.20}$$

$$\mathrm{Re} = \frac{\rho a_p v_s}{\varepsilon u} \tag{2.21}$$

where u, ρ, and v_s represent fluid viscosity, density and superficial velocity in the adsorption bed respectively. Adsorbent particle radius is designated a_p, adsorbent bed interparticle void fraction, ε, and Sc and Re denote the Schmidt and Reynolds numbers of the particle, respectively. An estimate for the free liquid diffusivity, D_l, of the solute is also required for calculation of k_f. More recently, Weber and Liu. (1980) proposed an experimental short-bed adsorber technique for direct and more accurate determination of k_f.

Intraparticle transport actually involves two mass transfer processes, pore and surface diffusion which act in parallel. The mass balance equation describing both pore and

surface diffusion for a spherical particle is derived based on the following assumptions (Yoshida and Galinada, 2000):

- Solid-phase and pore diffusion occur in parallel within the adsorbent particle.
- Pore and solid-phase diffusivities are constant during the adsorption process.
- The pore diameter and the void fraction of the adsorbent particle are constant throughout the adsorption process.
- The concentration of adsorbed solute inside the pore is in local equilibrium with the concentration of the adsorbed solute on the solid-phase of the pore wall.
- The bulk phase concentration of the solute is constant during the adsorption process.

Theses assumptions lead to the following mass transfer equation:

$$\varepsilon_p \frac{\partial C}{\partial t} + \frac{\partial q}{\partial t} = D_p \varepsilon_p \frac{1}{r^2}\left(r^2 \frac{\partial C}{\partial r} \right) + \frac{D_s}{r^2}\frac{\partial}{\partial r}\left(r^2 \frac{\partial q}{\partial r} \right) \qquad (2.22)$$

Here, C [mol/ m^3] and q [mol/ m^3 adsorbent] are the liquid-phase concentration of a solute in the pore and the adsorbent phase concentration of the solute in the solid-phase, respectively; ε_p is the void fraction of the pore; and D_p [m^2/ s] and D_s [m^2 / s] are the pore and solid-phase diffusivities, respectively.

Assuming surface diffusion is the major intraparticle transport mechanism, the solid phase continuity equation (Equation 2.22) reduces to:

$$\frac{\partial q}{\partial t} = \frac{D_s}{r^2}\frac{\partial}{\partial r}\left(r^2 \frac{\partial q}{\partial r} \right) \qquad (2.23)$$

This equation describes homogeneous diffusion in a sphere, assuming a constant diffusivity, D_s, at all points in the particle (Cooney, 1999).

CHAPTER THREE

APPARATUS AND EXPERIMENTAL PROCEDURES

3.1 Apparatus

The current experiment is divided into two parts: the measurement of equilibrium isotherms and kinetics of adsorption of orthophosphates. The apparatus involved in both parts are described below.

Part I: Equilibrium isotherms

125 ml and 250 ml elementary flasks containing activated alumina adsorbent and experimental solutions of orthophosphates are placed at fixed positions in a bath water shaker manufactured by KARL KOLB, Scientific Technical Suppliers (Model GFL). The shaker bath consists of a temperature controller that controls the temperatures for the experimental runs at 25, 40 and 80 ºC. A temperature indicator provided in the shaker is used to monitor the experiment temperature. Also, shaking rate is maintained at 25% via a shaking rate frequency with a scale ranging from 0 to 100% installed on the shaker bath. The purpose of this controller is to enhance adsorption of phosphate solute into the activated alumina adsorbent as well as aiding in achieving the equilibrium in short time period. Typical schematic of the shaker is shown on Figure 3.1.

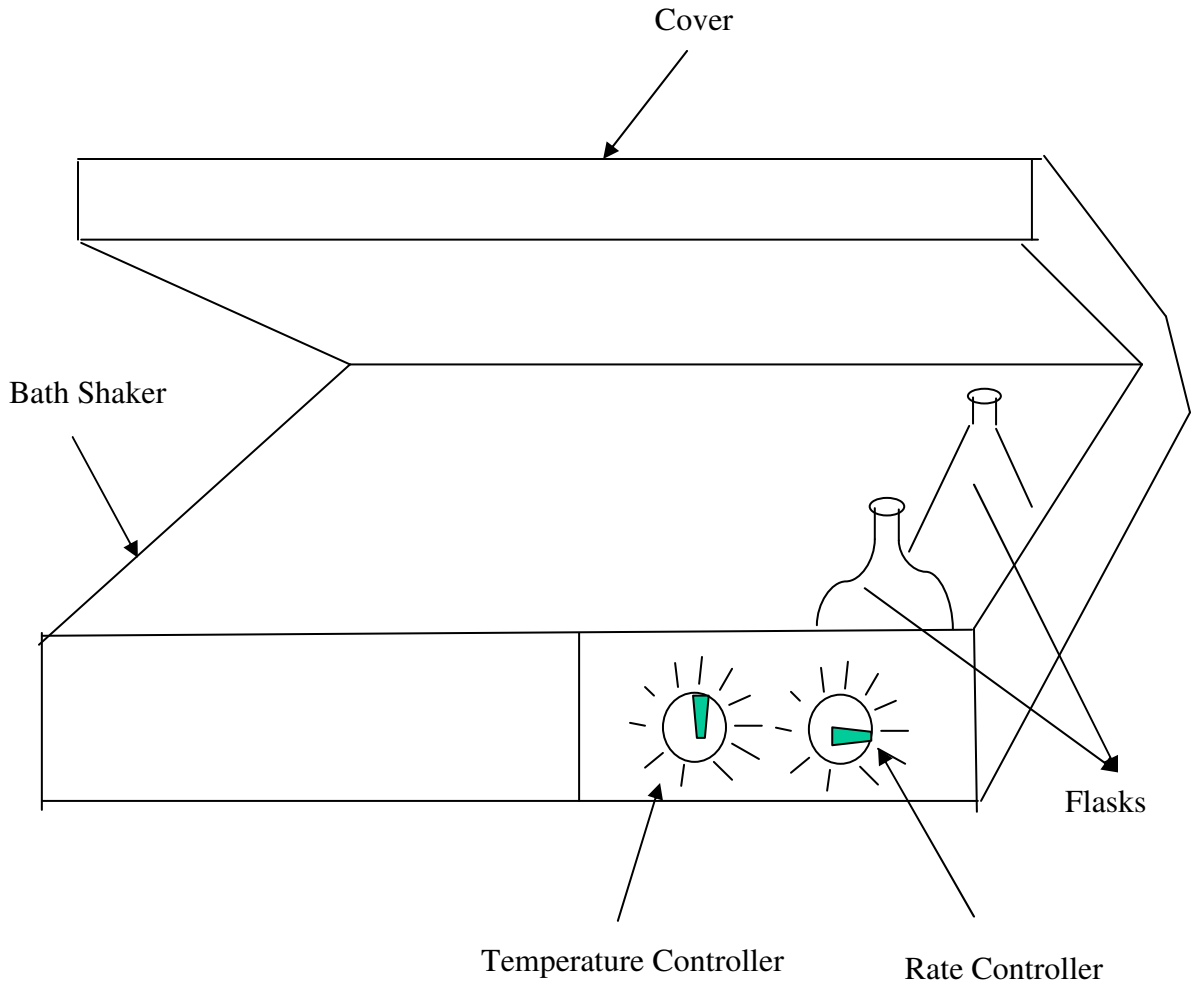

Figure 3.1: A Schematic Diagram of the Equilibrium Experimental Setup.

Part II: Kinetics

Figure 3.2 shows a schematic diagram of the kinetics setup. A tank with about 13 L capacity that was manufactured in the KFUPM workshop and made of plexiglass is used in the setup with two holes on the side for exit and ingress circulation and two on its cover for the pH meter and the mercury thermometer. A variable speed pump manufactured by COLE-PARMER INSTRUMENT Co. (115V DC, 2.0A, 3200RPM) is used to circulate the solution out of and into the tank passing through a column. A speed controller (MASTERFLEX CONTROLLER) giving allowable variation with a scale ranging from 0 to 10 is provided in the pump to maintain the circulation rate at two values of 5 (equivalent to 300 ml/min) and 6 (equivalent to 400 ml/min). The column (21 cm long and 2.8 cm I.D.) made of plexiglass has two meshes at the inlet and the outlet to prevent losing the adsorbent material (1-3 gram of AA400G 28x48/14x28 Mesh) with the flow passing through the column. The tank and the circulation tube lines are not insulated. An electrical heater manufactured by COLE-PARMER INSTRUMENT Co. (Model 1252-00 Circulator) is used to control the temperatures for the experimental runs at 25, 40 and 80 ºC with coils immersed on the tank solution for heating and agitating the experiment solution. A digital pH meter manufactured by EUTECH INSTRUMENT (Model PC300) is used to monitor the pH of the experiment solution with an electrode immersed on the solution from the hole made on the tank roof.

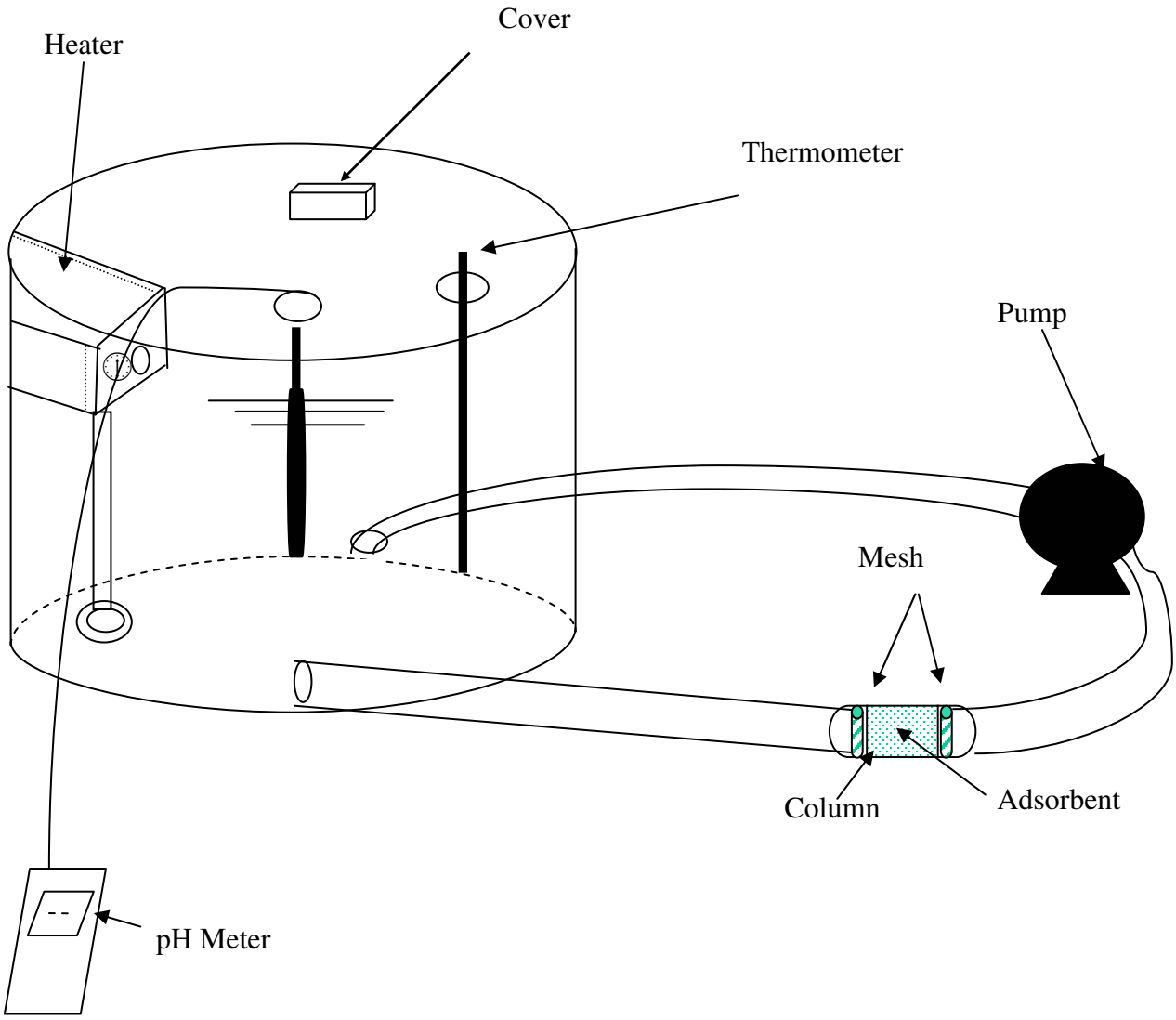

Figure 3.2: A Schematic Diagram of the Kinetics Experimental Setup.

3.2 Experimental Procedure

3.2.1 Preparation of Experiment Solutions & Activation of Adsorbents

0.00146 M orthophosphoric acid (85% by wt., specific gravity = 1.69) is used for preparation of the experiment solutions of 0.0046, 0.0001 and 0.000002 M of stock solution, model solution and calibration solution respectively. The equilibrium concentration of the experimental solutions is expressed as mg of total phosphorous (P) per liter of solution while the adsorbent loading is expressed as mg of orthophosphates ions (PO_4^{3-}) adsorbed per unit gram of activated alumina adsorbent. More details are given in Appendix A.

Preparation of the Model Solution

Orthophosphate solutions containing 10 mg P/L (0.0001 M) were prepared by mixing orthophosphoric acid with deionized water. Stock solution was prepared by adding 1.44 gram of the orthophosphric acid into 2000 ml Erlenmeyer flask. The resulting concentration of phosphorus resulted as 455.32 mg/L (0.0046 M). A quantity of 44 ml from the stock solution was taken and diluted with deionized water into 2000 ml Erlenmeyer flask to get 10 mg P/L solution (0.0001 M). The calculations of the preparation of the stock solution and the model solution are given in Appendix A.

Calibration Curves

A solution of 0.2 mg of P/L (0.000002 M) was prepared for use in the calibration curve data. A quantity of 0.9 ml from the stock solution was taken and diluted with deionize water into 2000 ml Erlenmeyer flask to give 0.2 mg P/L solution. Samples of

phosphorous solutions with concentration of elemental phosphorous varying from 0 to 0.2 mg P/L were prepared and its transmittance measured (see method of analysis). The resulting calibration curve was used for obtaining phosphorous concentration of the experimental samples. A typical calibration curve is given in Figure 3.3. The calculations and data of the calibration curve are given in Appendix A.

Activation of Adsorbents

Alcan Activated alumina AA400G 14x28 Mesh (Sample No. 00093) and AA400G 28x48 Mesh (Sample No. 00094) received from ALCAN CHEMICALS, DIVISION OF ALCAN ALUMINIUM LIMITED, were activated prior to use in the experiment work. A quantity of about 500 mg of activated alumina AA400G (14x28 or 28x48 Mesh) was placed in the bottom of a 500 ml wash bottle that was surrounded by electrical heater tapes for heating purpose. The temperature was maintained at 85 °C via the electrical heater tapes connected to a furnace manufactured by THERMOLYNE CORPORATION (Model No. CP 13315) equipped with a set point controller for setting the desired temperature. A nitrogen stream (40 ml/min) was introduced to the inside tube at the center of the bottle to pass through the adsorbent for activating the activated alumina adsorbent AA400G (14x28 or 28x48 Mesh) for a period of 24 hours. A vent provided on the top of the wash bottle was used to vent the nitrogen that was passed through the adsorbent placed on the bottom of the bottle. The dry activated alumina adsorbent AA400G (14x28 or 28x48 Mesh) was sealed on a glass container with a cap prior to use.

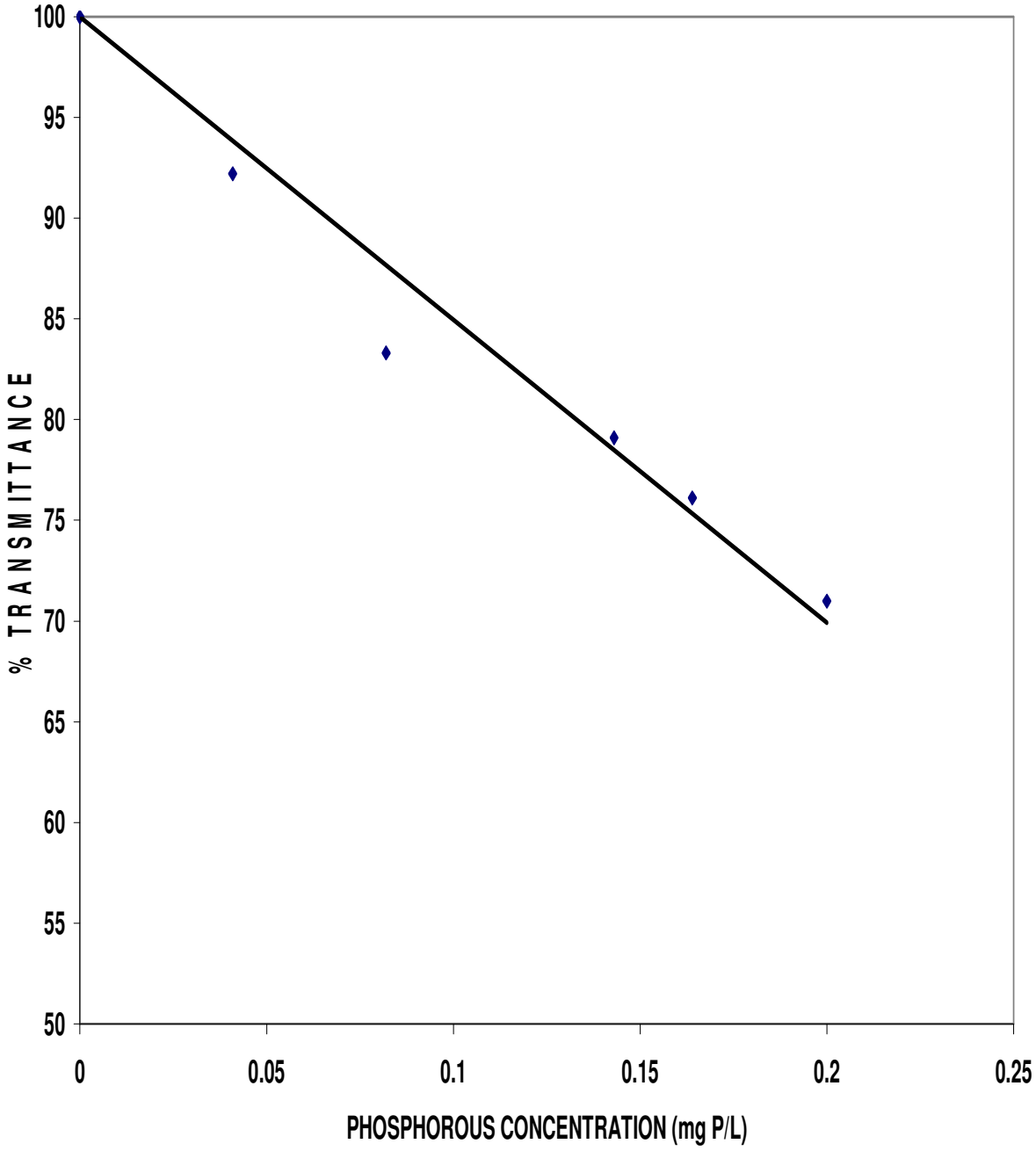

Figure 3.3: A Typical calibration Curve

3.2.2 Measurement of Equilibrium Isotherms

Measured quantities (100 and 200 ml) of solution of 10 mg P/L were added to weighted amounts (0.05, 0.1, 0.2, 0.5, 0.7 and 1.0) of dry activated alumina AA400G (28 x 48 or 14 x 28 Mesh) in glass flasks which are stoppered and placed in the shaker bath partially filled with water. The flasks were put in the shaker and left for sufficient time to permit adsorption to reach equilibrium conditions. Runs with continuous control of pH at 4.5 and 6.0 were conducted for two days while the reminder runs were conducted for five days. Runs were conducted at temperatures of 25, 40 and 80 ºC by adjusting the temperature controller. For runs with controlled pH of 4.5 and 6.0, pH of the solution was measured and controlled by adding droplets of 0.1 M buffer solutions of H_2SO_4 and NaOH respectively as required. pH was initially adjusted upon mixing the experimental solution with the adsorbent and finally one hour prior to samples analysis for the runs with initial and final pH control. Buffer solutions were not added for solutions of no pH control runs.

3.2.3 Generation of Uptake Curves

The tank was initially filled with 3 liter of 10 mg P/L (or 10 mg P/L) for the experiments. The adsorbent was washed several times with deionized water (pH = 4.85) to remove all fines prior to use on experimental runs. The pump and the timer were started simultaneously upon starting the experiment. The circulation of the solution, maintained at 300 ml/min (0.182 cm/sec) (or 400 ml/min= 1.083 cm/sec), was started through the glass column holding 1-3 gram of dry activated alumina adsorbent AA400G (28x48 or 14x28 Mesh) using the variable speed pump. The objective here was to minimize the

concentration gradient across the column by lowering the residence time (26 sec) in the column relative to the total experiment time (24 hours) and to increase the mass transfer process for the system. The specific pH was maintained by careful addition of 0.1 M buffer solutions of H_2SO_4 and NaOH respectively as required for the runs with controlled pH of 4.5. Samples were withdrawn from the tank solution at frequent times and the pH was recorded for each one. When composition analysis indicated that the equilibrium had been reached as no further change was observed, the pump was stopped to terminate the experiment run.

3.3 Method of Analysis

A spectrophotometer manufactured by SHIMADZU CORPORATION, ANALYTICAL INSTRUMENT DIVISION (Model UVmini-1240V), was used to identify the absorbance (or transmittance) of each sample at a wavelength of 690 μm. Standards were prepared in order to draw calibration curves so as to convert absorbances (or transmittances) into concentration readings. The samples were filtered through Whatman filter paper and diluted appropriately into a 25 ml flask using deionized water in order to obtain a reading within the range of the spectrophotometer. 1 ml of ammonium molybdate solution and 2 drops of stannous chloride were added to the diluted sample solution. The solution was mixed and the color was allowed to develop for 10 minutes. The resulting blue colored complex was analyzed by the visible range colorimetry method on the spectrophotometer at a wavelength of 690 μm and the

concentrations of phosphorus remaining in the solutions was found from the calibration curve. Standard procedures are available (ASTM D 515-88, 1992).

CHAPTER FOUR

EQUILIBRIUM STUDIES

4.1 Introduction

Equilibrium studies were performed with the objective of obtaining the adsorption capacities of the activated alumina under varying conditions of temperature and pH. The pH studies were carried out with continuous control as well as initial and final control. Although mesh size was not a parameter of study under conditions of equilibrium, two mesh sizes were tested to see the effect, if any and to use their adsorption isotherms constants for kinetics study part. The discussion and analysis presented will be related to the effect of temperature, mesh size and pH.

The adsorption data at equilibrium is presented as a relation between amount adsorbed in the solid phase expressed as (mg PO_4^{3-} /g of activated alumina sorbent) versus the concentration of the adsorbate in the liquid phase at equilibrium expressed as (mg phosphorous/L). This relation is referred to as an isotherm. A wide variety of isotherms are available for fitting the data in gas adsorption but in case of liquid phase adsorption, the choice is generally limited to Langmuir, Freundlich or their combination as Langmuir-Freundlich isotherm. Based on reported work in literature (Urano and Tachikawa, 1991; Cooney, 1999) where the Freundlich isotherm was used, the present

data was also fitted with Freundlich Isotherm. The fit parameters are presented and discussed in the discussion that follows.

The first runs (1 to 4) of equilibrium adsorption experiments with controlled pH of 4.5 and 6.0 were performed with a contact time of two days. The remainder of runs (5 to 13) was conducted with a contact time of five days. The contact time was chosen to be long enough to permit adsorption to reach equilibrium conditions as reported by (Urano & Tachikawa, 1991) for batchwise adsorption tests of activated alumina adsorbent for phosphorous removal. Brattebo and Odegaard (1986) found that the equilibrium was achieved in alumina-phosphorous systems after five days. Narkis and Mordehai (1986) mentioned an equilibrium time of 6.5 hours. Therefore, their experiments were carried out for 24 or 48 hr to ensure complete equilibrium. Kinetics uptake was studied by a batchwise adsorption tests and it has been found that in 6 hours samples reached equilibrium conditions at ambient temperature with no pH control (Fatehi, 2000). As the kinetic experiments in this study (chapter-5) reached equilibrium generally in 24 hours, the period of 5 days is considered adequate even allowing for the difference of a pulsating mass transfer coefficient compared to a forced convective mass transfer coefficient.

4.2 Experimental Procedure

Thirteen experimental runs were performed to measure the equilibrium isotherms at the experimental conditions as shown in Table 4.1. The raw experimental data is presented in Appendix B. Two sets are reported: (I) pH adjustment readings for

Table 4.1: Conditions of Runs for Equilibrium Isotherm Experiments

Run No.	Mesh Size	Temperature (° C)	pH
1	28 x 48	25	Control pH 4.5
2	28 x 48	25	Control pH 6.0
3	14 x 28	25	Control pH 4.5
4	14 x 28	25	Control pH 6.0
5*	28 x 48	80	Initial & Final Control pH 4.5
6*	28 x 48	40	Initial & Final Control pH 4.5
7*	28 x 48	25	Initial & Final Control pH 4.5
8*	28 x 48	80	Initial & Final Control pH 6.0
9*	28 x 48	25	Initial & Final Control pH 6.0
10*	28 x 48	40	Initial & Final Control pH 6.0
11	28 x 48	25	No pH Control
12	28 x 48	40	No pH Control
13	28 x 48	80	No pH Control

*Note: Runs may not be at equilibrium.

equilibrium isotherm experiments and (II) data of adsorption isotherm experiments.

First four runs were performed at controlled pH of 4.5 and 6.0 while the reminder of the runs were executed with initial and final pH control of 4.5 and 6.0 and no pH control. Runs involving initial and final pH control may not have achieved complete equilibrium due to the addition of buffer solutions that release ions (H^+, OH^-, Na^+, SO_4^{2-}) to the sample solution. The addition of buffer solution was carried out one hour before the analysis. These ions need at least 6.5 hours to reach the complete equilibrium condition of the system. Therefore, these runs [5 to 10] were assumed to have not achieved equilibrium.

Three temperature levels, ambient temperature (about 25 ºC), 40 and 80 ºC are conducted to study the temperature variation effect. Two mesh sizes of activated alumina adsorbent AA400G (14x28 & 28x48 Mesh) are tested in the experiments.

4.3 Results and Discussion of Results

4.3.1 Freundlich Fit of the Isotherms

The data collected for all isotherm runs at different conditions as indicated in Table 4.1 are fitted using Freundlich isotherm which has the following form:

$$q = k\, C^{\frac{1}{n}}$$

where q and C are concentration in the adsorbed and fluid phase respectively. The tabulation of the constant k and the parameter 1/n for all runs are listed in Table 4.2. The correlation coefficients (R) were generally very high for all the runs performed under different conditions.

Table 4.2: Freundlich Isotherms Constants of All Isotherm Runs

Run No.	k $(mg^{1-1/n} L^{1/n} / g)$	1/n (-)	R^2
1	17.85	0.500	0.99
2	11.60	0.704	0.99
3	9.98	0.583	0.99
4	5.01	0.588	0.80
5*	7.08	0.793	0.97
6*	11.38	0.632	0.98
7*	15.73	0.532	0.95
8*	14.81	0.266	0.98
9*	18.48	0.268	0.95
10*	15.80	0.243	0.83
11	26.34	1.010	0.98
12	25.55	1.082	0.99
13	13.04	1.159	0.96

*Note: Runs may not be at equilibrium.

The value of equilibrium adsorbent loading for AA-400G (28x48 Mesh) found from this study compares very comparable with the values reported by Alcan Chemical group. At ambient temperature (25 ºC) and initial and final pH control of 4.5, the equilibrium ion exchange loading at phosphorous equilibrium concentration of 10 mg/L was extrapolated and found to be 54 mg PO_4^{3-} /g AA400G which is comparable to a value of 63 mg PO_4^{3-} /g AA400G reported by Alcan Chemical group (Fleming, 1990). From the literature, it has been found that values of Freundlich constants found were not at same conditions as the current studied conditions. Fleming (1990) reported values of 10 and 0.80 for k and 1/n respectively for isotherms at ambient temperature and with only initial pH control of 4.5 while values of 15.73 and 0.532 (for run 3) were found in this study at similar conditions but with initial and final pH control of 4.5 that may not be at equilibrium condition.

4.3.2 Effect of Temperature Variation

Temperature dependence of the adsorption enhancement phenomenon was investigated by running experiments at 25, 40 and 80 ºC under different pH conditions. Since the temperature of the actual industrial contaminated water stream is close to 80 ºC, temperature variation effect was considered and is studied as well.

Experimental runs were conducted at three different temperature levels of 25, 40 and 80 ºC. Some of these runs were performed with initial and final control at two pH values of 4.5 and pH 6.0 that may not be at equilibrium and some were with no pH control. The equilibrium isotherms at different temperatures for different pH conditions are shown in Figures 4.1, 4.2 and 4.3. The decrease in capacity at high temperature levels

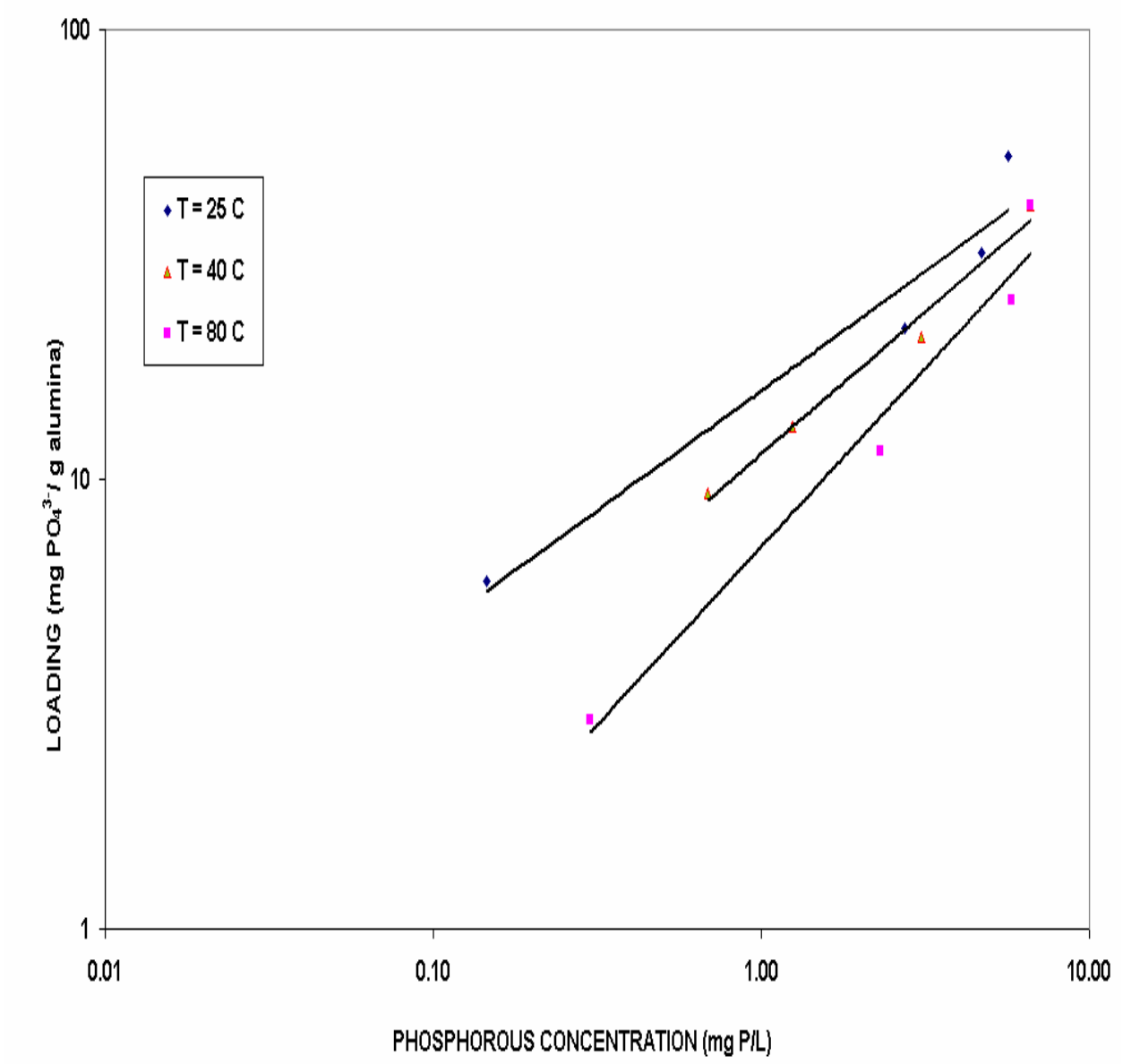

Figure 4.1: Isotherms at Initial and Final pH Control of 4.5 for AA400G 28x48 Mesh at Different Temperatures along with Best Fit Freundlich Curves Using Constants Given in Table 4.2. [Isotherms may not be at Equilibrium]

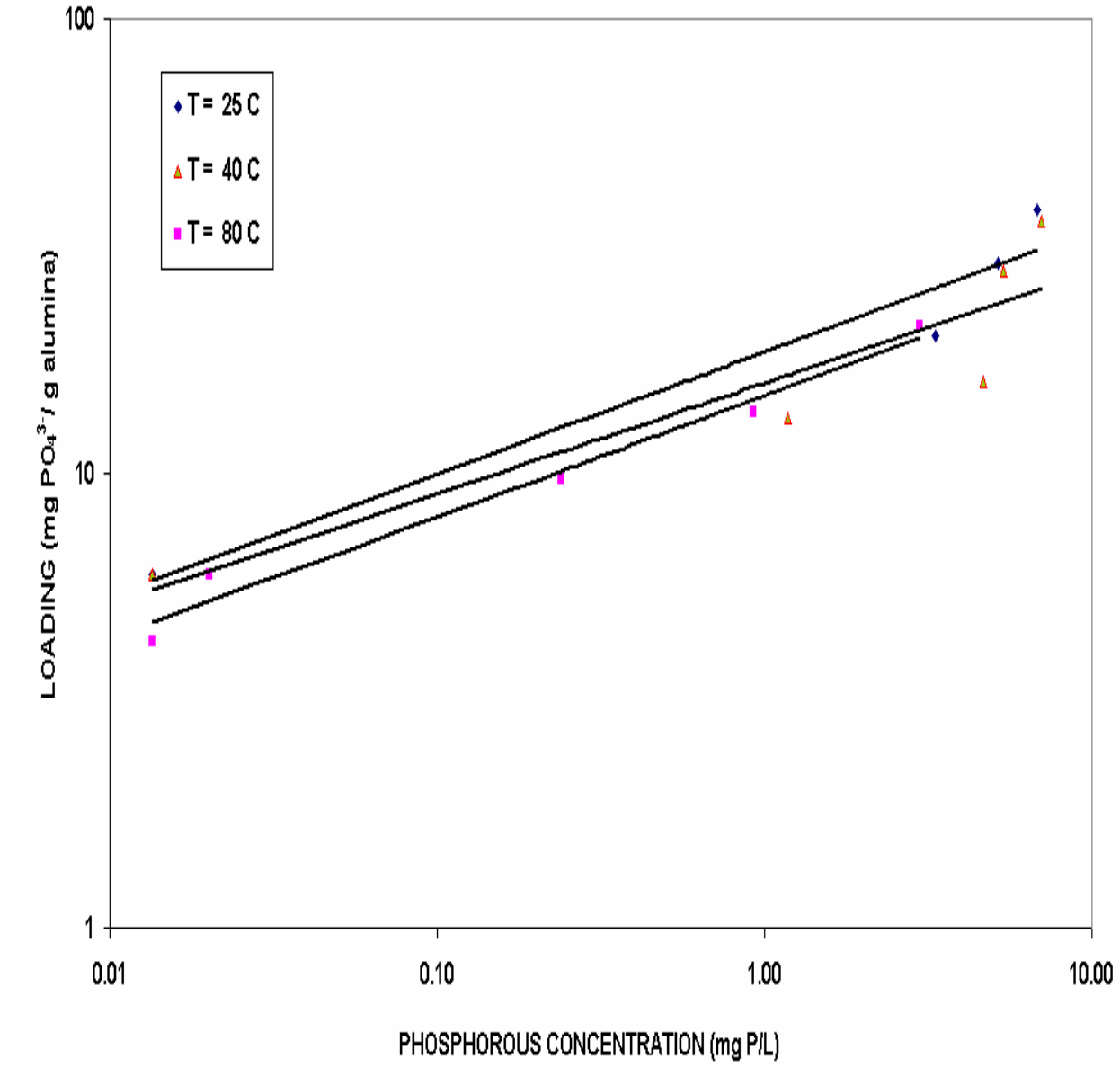

Figure 4.2: Isotherms at Initial and Final pH Control of 6.0 for AA400G 28x48 Mesh at Different Temperatures along with Best Fit Freundlich Curves Using Constants Given in Table 4.2. [Isotherms may not be at Equilibrium]

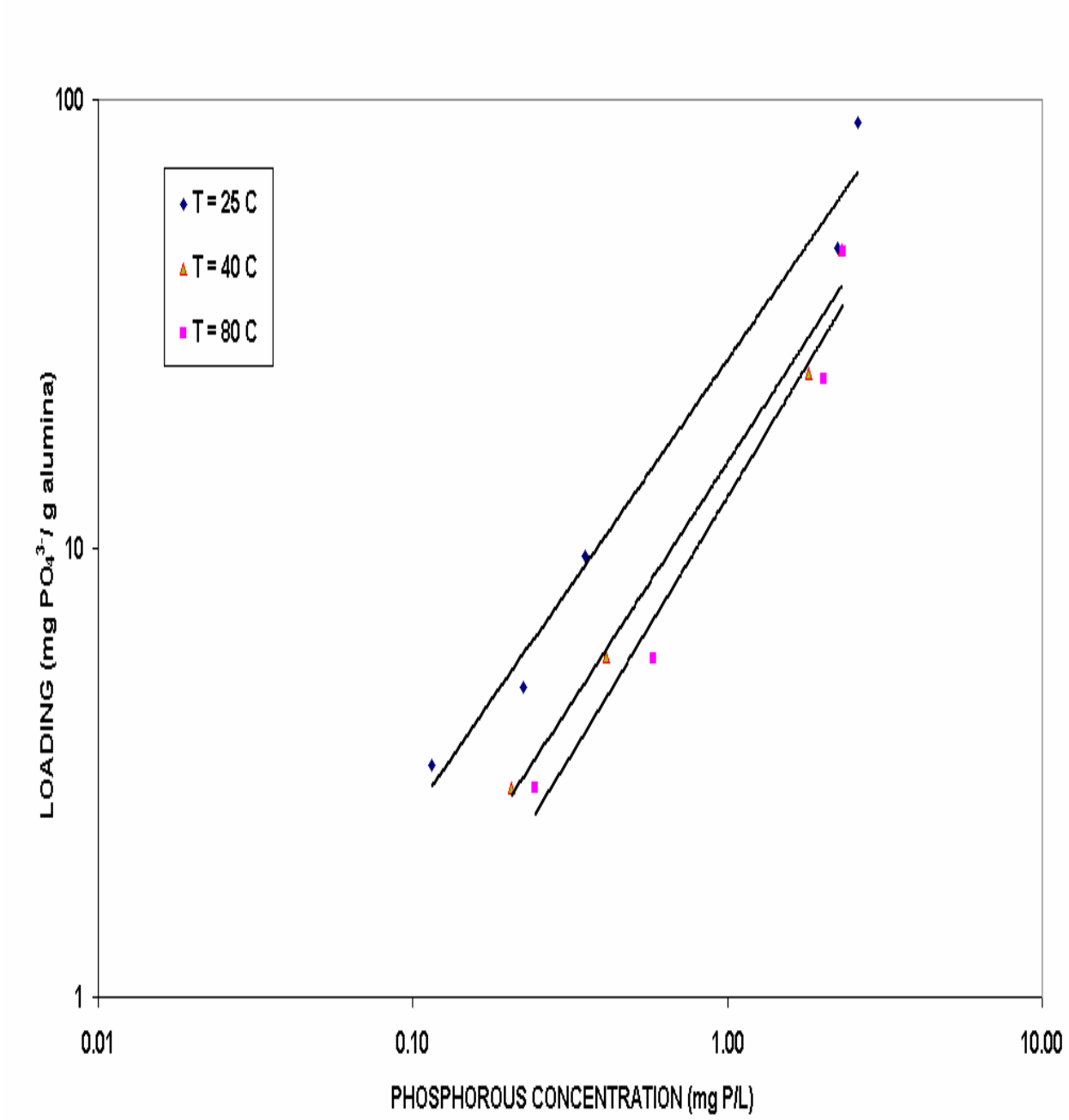

Figure 4.3: Isotherms with no pH Control for AA400G 28x48 Mesh at Different Temperatures along with Best Fit Freundlich Curves Using Constants Given in Table 4.2.

is evident from all plots. That is the sorbent loading is inversely proportional to the temperature as it is expected from Van't Hoff's relation.

Figure 4.1 shows three runs at different temperatures of 25, 40 and 80 ºC with initial and final control pH of 4.5 that may not be at equilibrium. It can be seen from the figure that temperature has an affect on the adsorption of phosphate on the activated alumina adsorbent. The adsorption capacity increases with the decrease of temperature. Same observation can be deduced from Figures 4.2 and 4.3 for initial and final pH control of 6.0 and no pH control respectively. Large scatter in the data can be observed at high phosphorous equilibrium concentration of approximately 8 mg P/L due to the low quantity of activated alumina adsorbent (0.05 gram) used for some samples. Table 4.3 gives values of the equilibrium ion exchange loading (mg PO_4^{3-}/g AA400G) at various levels of equilibrium phosphorous concentration for different temperatures for three set of pH conditions. As shown in the Table, equilibrium loading is high at low temperature of 25 ºC compared to the values at high temperatures of 40 and 80 ºC in all pH conditions. Maximum equilibrium loading was observed for the case of no pH control at 25 ºC at high phosphorous equilibrium concentration loading of 10 mg/L. At low phosphorous equilibrium concentration loading of 0.1 mg/L, highest equilibrium loading was observed for the case of pH at 6.0 compared to pH at 4.5 and no pH control for all three temperature values. Not much difference was found between the values of equilibrium loading for temperatures of 40 and 80 ºC in all range of the equilibrium concentration loading under the three set of pH conditions. Figure 4.3 indicates that the BET isotherm may fit the isotherms better than the Freundlich isotherm at high loadings as the loadings appear to be above the best Freundlich fits at the end of the isotherm.

Table 4.3: Equilibrium Ion Exchange Loading (mg PO_4^{3-} /g AA400G) at Various Phosphorous Equilibrium Concentrations for Different Temperature levels.

Run No.	pH	Temperature (ºC)	Phosphorous Equilibrium Concentration		
			0.1 mg P /L	1 mg P/L	10 mg P/L
1	4.5**	25	5.64	17.85	56.44
7*		25	4.62	15.72	53.51
6*		40	2.64	11.40	44.17
5*		80	1.14	7.08	44.00
2	6.0***	25	2.29	11.60	58.68
9*		25	9.97	18.48	34.25
10*		40	9.02	15.78	27.61
8*		80	8.02	14.79	27.29
11	No Control	25	2.57	26.31	269.23
12		40	1.29	15.54	187.76
13		80	0.90	13.02	187.69

*Note 1: Runs 5 to 10 may not be at equilibrium.

** Note 2: Run 1 is with controlled pH while runs 5, 6 and 7 are with initial and final pH control.

*** Note 3: Run 2 is with controlled pH while runs 8, 9 and 10 are with initial and final pH control.

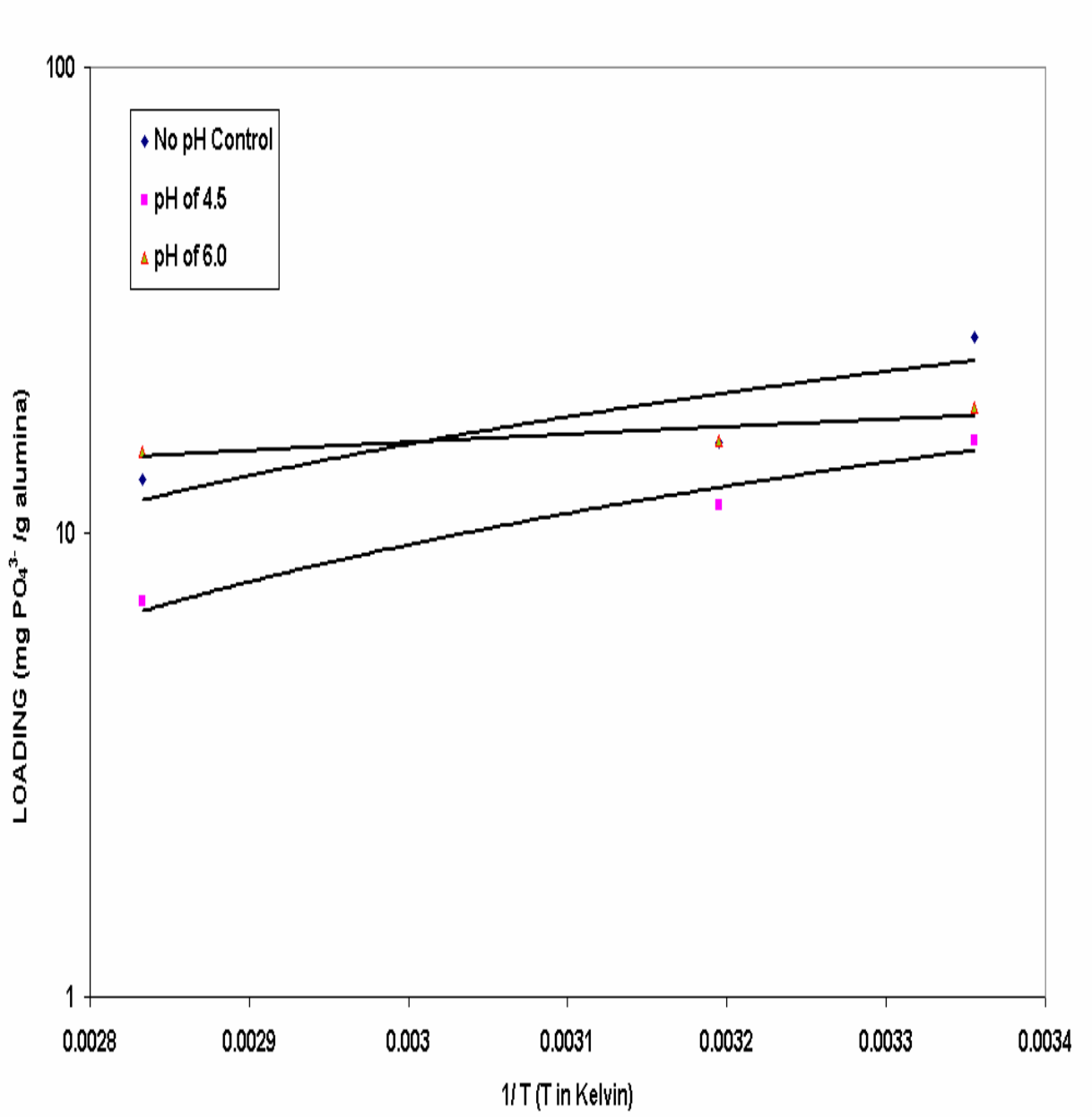

Figure 4.4: Relationship Between the Equilibrium Ion Exchange Loading and the Temperature for AA400G 28x48 Mesh at Phosphorous Equilibrium Concentration of 1 mg P/L for Different pH Conditions along with Line of Best Fit.

This may be due to the formation of polyphosphate species (Lewis and Kydd, 1991).

The relation between the equilibrium ion exchange loading and the temperature was further evaluated and studied based on Van't Hoff's plot at a phosphorous equilibrium concentration of 1 mg P/L as shown in Figures 4.4 for all pH conditions. It is clear from the figure that the equilibrium loading increases with lowering the temperature. Lowest equilibrium loading values were observed for the case with pH control of 4.5. The optimum pH for achieving the research objective of lowering the concentration of the industrial contaminated water to less than 0.1 mg/L was found to be achieved at a pH of 6.0 at which gives highest equilibrium ion exchange loading at temperature of 80 ºC.

4.3.3 Effect of Mesh Size

Mesh size, in principle, should affect only the approach to equilibrium but not the final equilibrium condition. Various types of activated alumina adsorbents with different pore sizes were studied to evaluate the adsorption abilities for phosphate removal on batchwise adsorption tests (Urano & Tachikawa, 1991).

Two mesh types of AA400G (14x28 and 28x48) were experimentally tested under different conditions. Runs 1 and 3 as well as 2 and 4 were done using different mesh sizes of 28x28 and 14x28 under continuous pH control of 4.5 & 6.0 respectively. The finer mesh AA400G (28x48) exhibits higher capacity at both levels of pH as shown in Figures 4.5 and 4.6. This could be attributed to blockage of some pores in coarser particles.

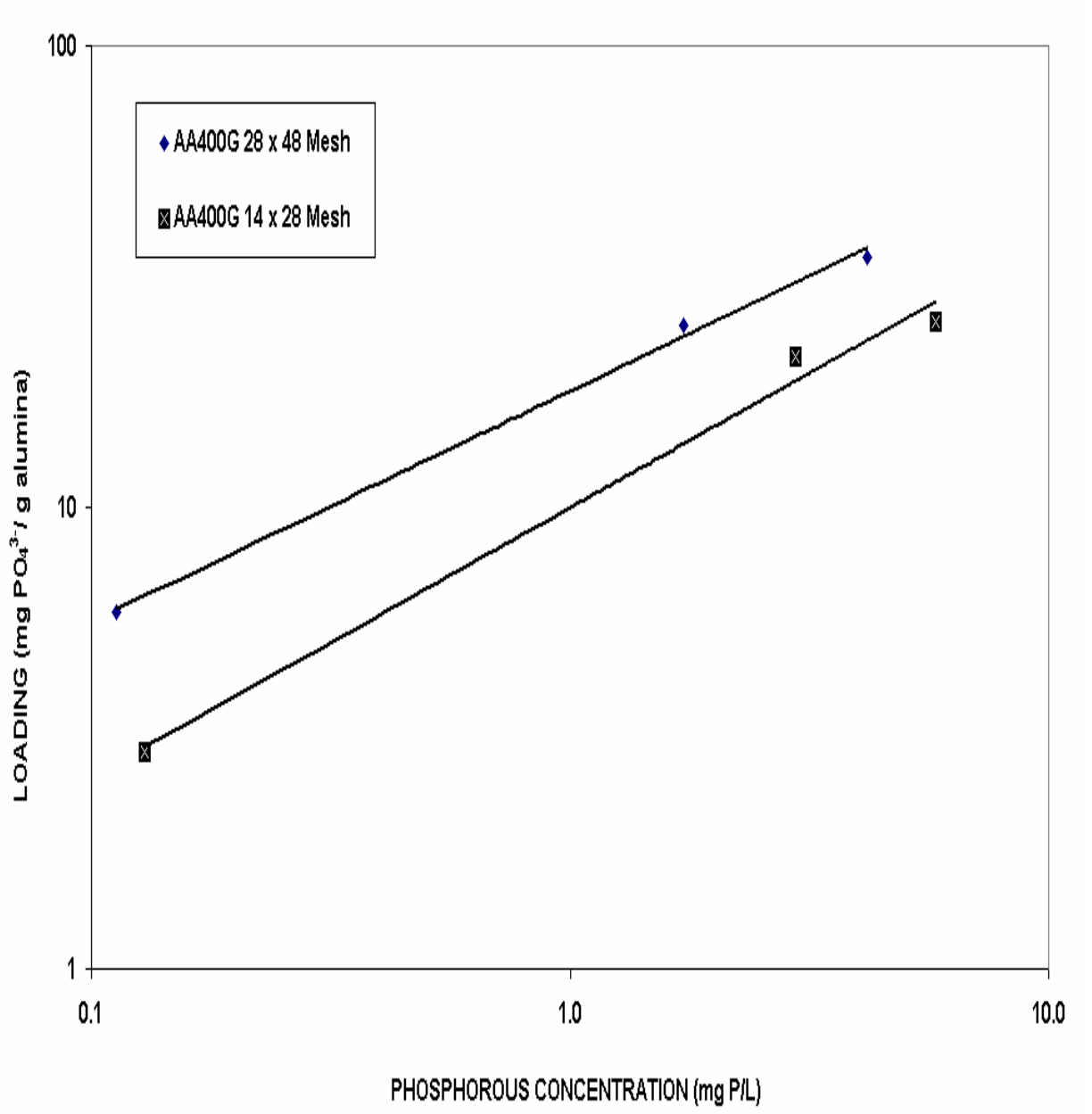

Figure 4.5: Isotherms of Phosphorous at Controlled pH 4.5 at Ambient Temperature along with Best Fit Freundlich Curves Using Constants Given in Table 4.2.

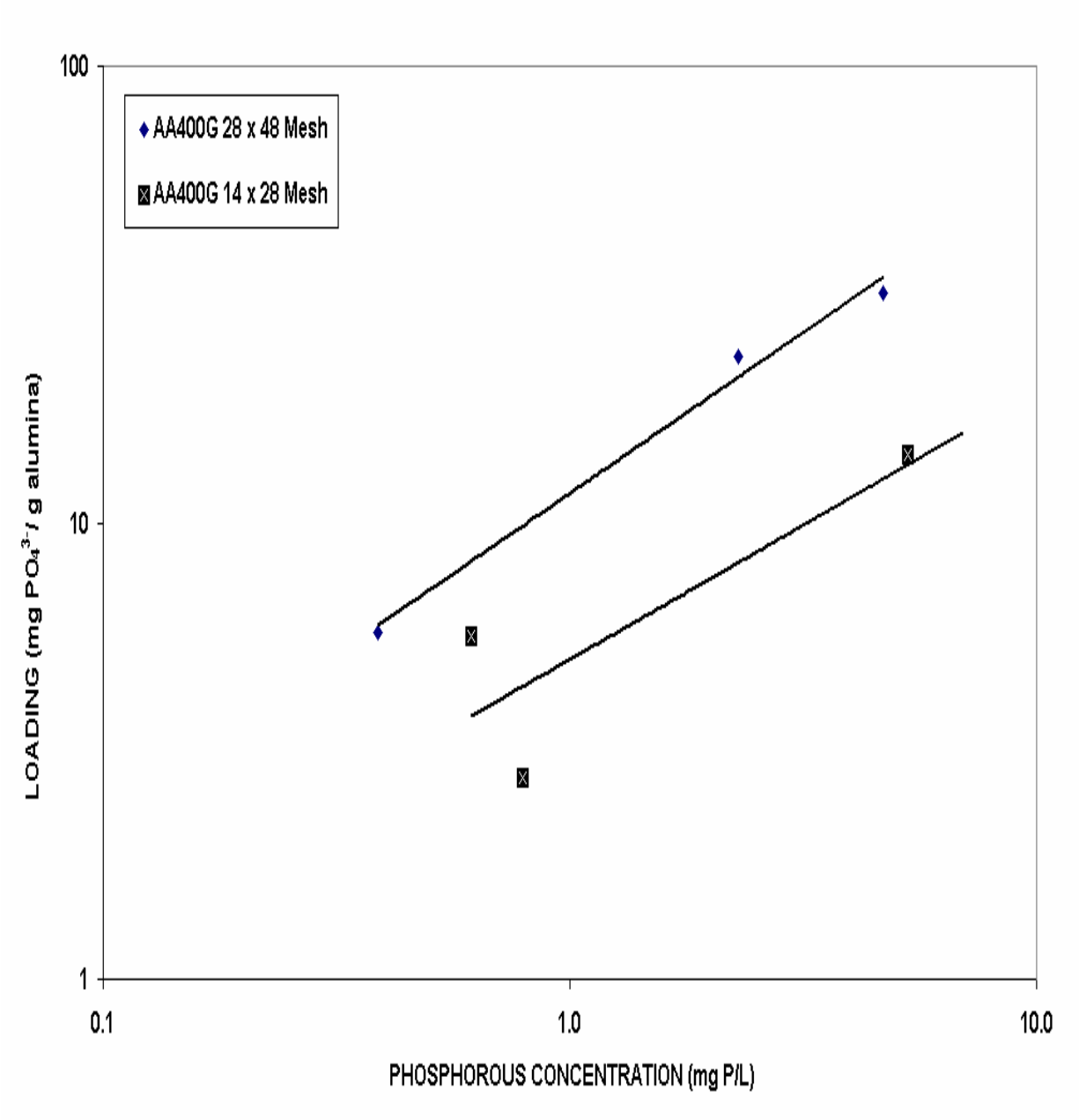

Figure 4.6: Isotherms of Phosphorous at Controlled pH 6.0 at Ambient Temperature along with Best Fit Freundlich Curves Using Constants Given in Table 4.2.

The equilibrium loading at phosphorous equilibrium concentration of 1 mg /L was found to be 17.85 and 9.98 mg PO_4^{3-}/g AA400G for 28x48 and 14x28 Mesh respectively at control pH of 4.5. It is possible that this difference may be attributed to the effect of the pH control of the experiment solution by the frequent addition of droplets of 0.1 M buffer solutions of H_2SO_4 and NaOH for controlling the desired pH. Since the added droplets of buffer solutions to the experiment solutions were not quantified for both mesh sizes runs, difference in results for the two mesh sizes may be due to the controlled pH procedure. This is due to the presence of different numbers of competing ions (H^+, OH^-, Na^+, SO_4^{2-}) generated from buffer solutions for the two cases resulting in different equilibrium data.

4.3.4 Effect of pH

The isotherm runs were conducted at controlled pH of 4.5 and 6.0 as well as with no pH control. Studies were also conducted by only controlling the initial and final pH which was done upon mixing the experimental solution with the adsorbent and finally one hour prior samples analysis.

The data collected at controlled pH of 4.5 and 6.0 for AA400G (28x48 Mesh) and AA400G (14x28 Mesh) at ambient temperature (25 ºC) is plotted in Figures 4.7 and 4.8 respectively. It is observed that controlled pH of 4.5 gives higher equilibrium loading at all phosphorous equilibrium concentration compared to that with pH of 6.0. This observation can also be seen for the other mesh type AA400G (14x28 Mesh) as shown in Figure 4.8.

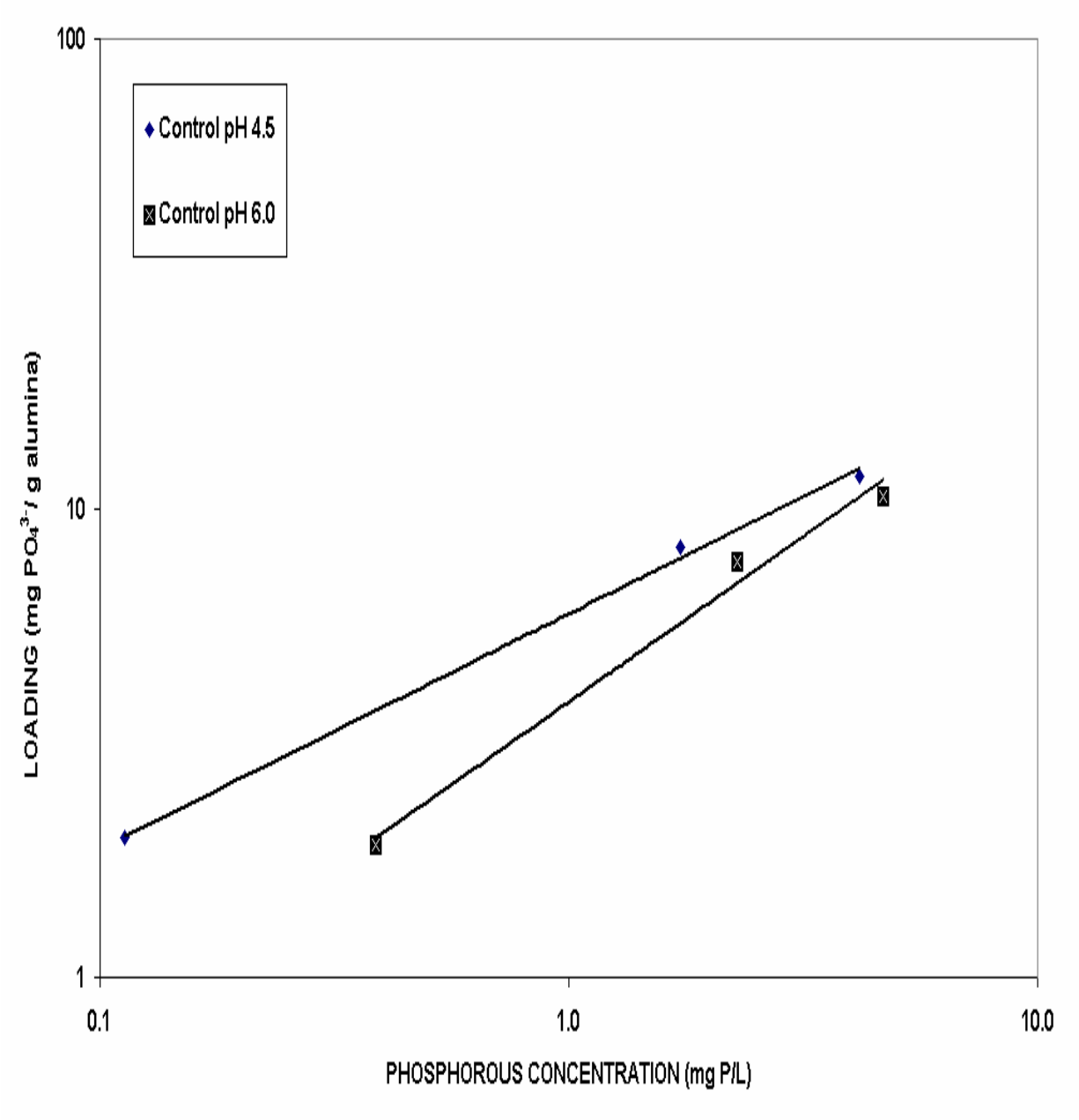

Figure 4.7: Isotherms of Phosphorous for AA400G 28x48 Mesh at Controlled pH and Ambient Temperature along with Best Fit Freundlich Curves Using Constants Given in Table 4.2.

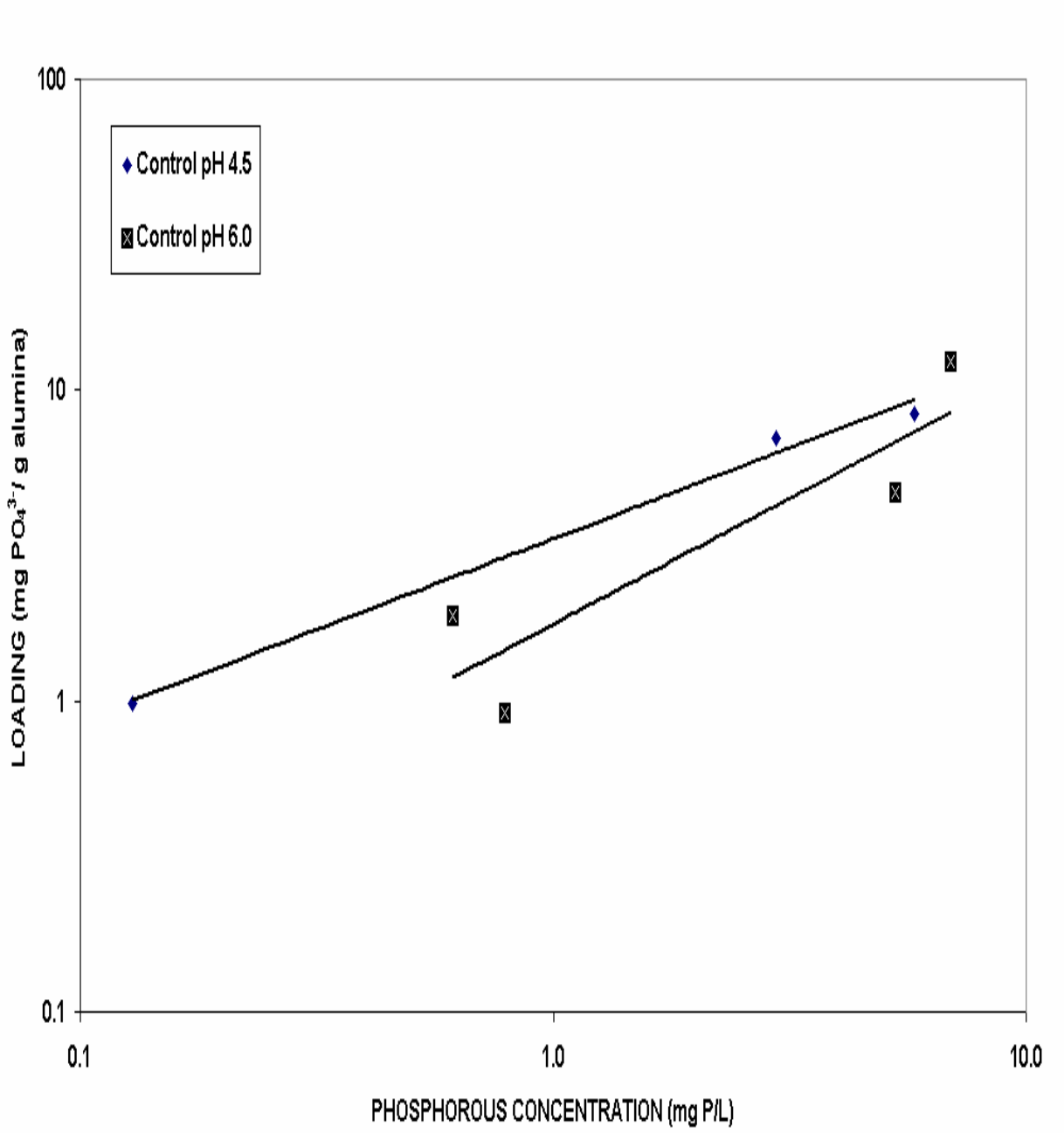

Figure 4.8: Isotherms of Phosphorous for AA400G 14x28 Mesh at Controlled pH and Ambient Temperature along with Best Fit Freundlich Curves Using Constants Given in Table 4.2.

In the case of no pH control, the pH of the solution was not maintained at a fixed value for the different samples in the set. The value of pH ranged from 3.7 at the start of the run rising to values ranging from 6 to 9.0 at equilibrium depending on the adsorbent quantity used in the samples. The pH increased during experimental run due to the release of hydroxyl ions (OH^-) to the solution resulting from the exchange with phosphates ions on the activated alumina adsorbent. Brattebo (1983) and Fleming (1986) mentioned that pH increased during experimental run. Table 4.4 shows the values of final pH for two runs conducted with initial and final pH control of 4.5 and 6.0 that may not be at equilibrium and results reported by Alcan group for only initial pH control. It can be seen from the Table that the final pH was higher than the pH of the starting solution and increased with increasing amount of adsorbent as would be expected. This observation agrees with the results reported by Alcan group and shown in the Table. They explained that sodium is leached from activated alumina samples in association with hydroxyl groups at pH's approaching 10 and that the presence of additional NaOH in solution acts to increase the pH. They also found the concentration of Al in the filtrate increased significantly for a filtrate pH $\geq$ 10 suggesting that activated alumina based materials can only be used in the pH range from 4 to 10 (Fleming, 1986).

Table 4.5 gives the equilibrium ion exchange loading (mg PO_4^{3-}/g AA400G) at three phosphorous equilibrium concentration levels of 0.1, 1 and 10 mg/L for different pH conditions and at various temperature levels. It can be seen from the Table that the equilibrium loading is high in case of initial and final pH control of 4.5 and 6.0 in the low phosphorous equilibrium concentrations range compared to the case of no pH control for all temperature levels in this range. Maximum equilibrium loading was attained with no

Table 4.4: Final pH of Typical Isotherm Runs for AA400G (28x48 Mesh) at Ambient Temperature

Adsorbent Weight (g)	Starting pH = 4.5		Starting pH = 6.0	
	Final pH	Alcan Results	Final pH	Alcan Results
0.05	6.9	7.7	6.3	7.5
0.10	7.4	8.5	6.9	8.3
0.50	8.4	9.4	7.5	9.4
1.00	9.3	9.6	8.5	9.7

Table 4.5: Equilibrium Ion Exchange Loading (mg PO_4^{3-} /g AA400G) at Various Phosphorous Equilibrium Concentrations for Different pH Conditions.

Run No.	Temperature (ºC)	pH	Phosphorous Equilibrium Concentration		
			0.1 mg P/L	1 mg P/L	10 mg P/L
1	25	4.5**	5.64	17.85	56.44
2		4.5**	2.29	11.60	58.68
7*		4.5	4.62	15.72	53.51
9*		6.0	9.97	18.48	34.25
11		No Control	2.57	26.31	269.23
6*	40	4.5	2.64	11.40	49.17
10*		6.0	9.02	15.75	27.61
12		No Control	1.29	15.54	187.69
5*	80	4.5	1.14	3.08	44.00
8*		6.0	8.02	14.79	27.29
13		No Control	0.90	13.02	187.76

*Note 1: Runs may not be at equilibrium.

**Note 2: Runs 1 and 2 with continuous controlled pH of 4.5.

pH control at high equilibrium concentration. This is because the addition of buffer solutions 0.1M NaOH and H_2SO_4 respectively in case of pH control condition resulting in release of competitive ions (H^+, OH^-, Na^+, SO_4^{2-}) to activated alumina surfaces that reduce the active adsorption sites of orthophosphates ions (PO_4^{3-})

The equilibrium loading versus the final pH of the solution is plotted as shown in Figures 4.9, 4.10 and 4.11 for the temperatures of 25, 40 and 80 ºC respectively. The final pH values for the case of no pH control were measured to be 8.7 and 6.5 for phosphorous equilibrium concentrations of 0.1 and 1 mg P/L respectively for all temperature levels. It can be seen that pH of 6.0 gives highest equilibrium ion exchange loading at phosphorous equilibrium concentration of 0.1 g P/L. Not much difference can be observed for the case of 1 mg P/L at temperature of 40 ºC for all pH conditions.

Based on above findings and in terms of achieving the research objectives intended to reduce the industrial contaminated water concentration to less than 0.1 mg P/L, pH of 6.0 is considered to be the optimum value that would be selected for the adsorption process provided that the stream temperature is close to 80 ºC. The configuration of the adsorber column could be divided into two portions. In the first portion, the industrial contaminated water containing 400 ppm of total phosphates compounds can be treated with no pH control up to the point in the column where the concentration reduces to 1 mg/L. In the latter portion of the column where the expected concentration of phosphorous is low, the pH of 9.0 should be adjusted with acid chemical (H_2SO_4) injection to a pH of 6.0 which is the optimum loading at low concentration and high temperature value of 80 ºC.

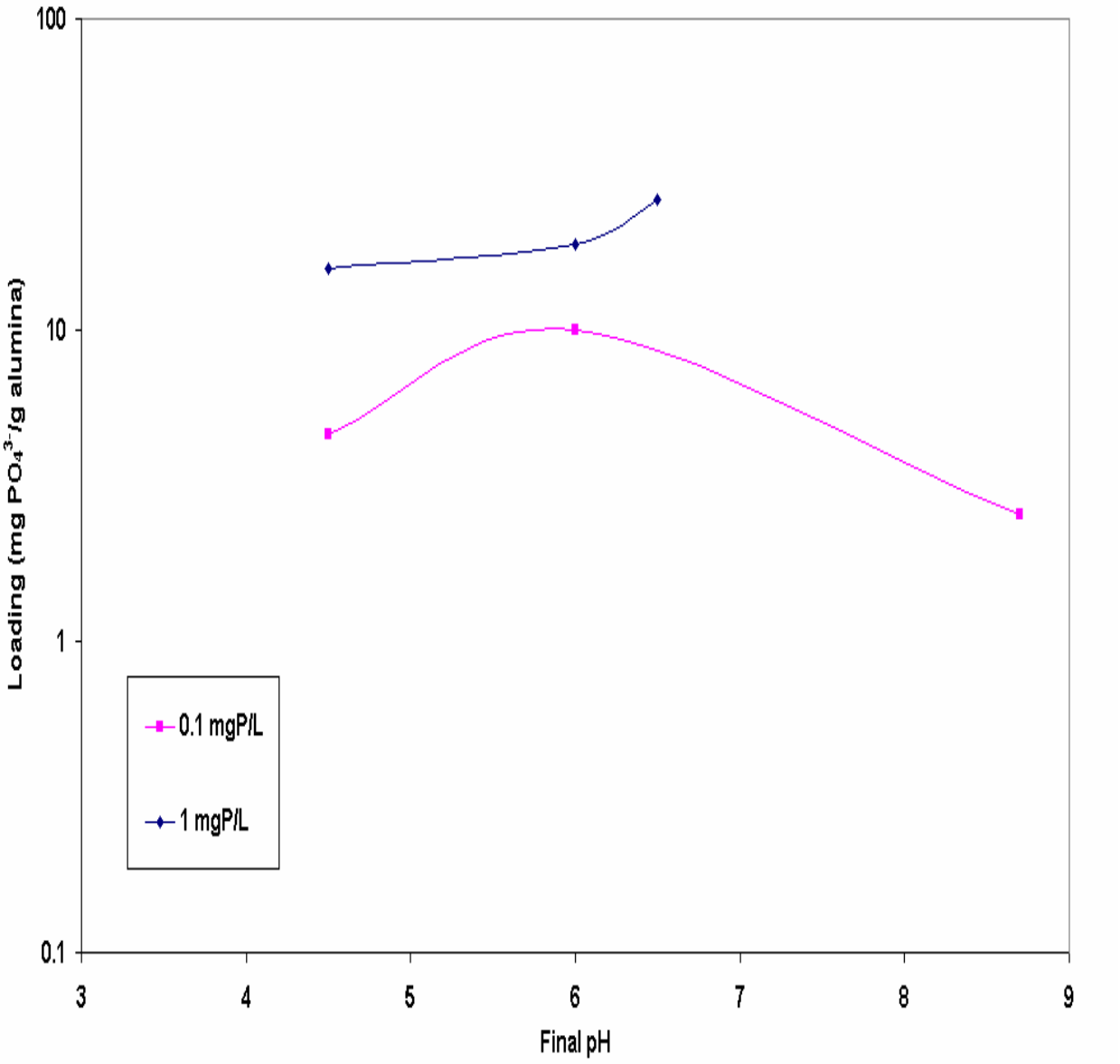

Figure 4.9: Relationship Between the Equilibrium Loading and the Final pH for AA400G 28x48 Mesh with Different Phosphorous Equilibrium Concentration at Ambient Temperature.

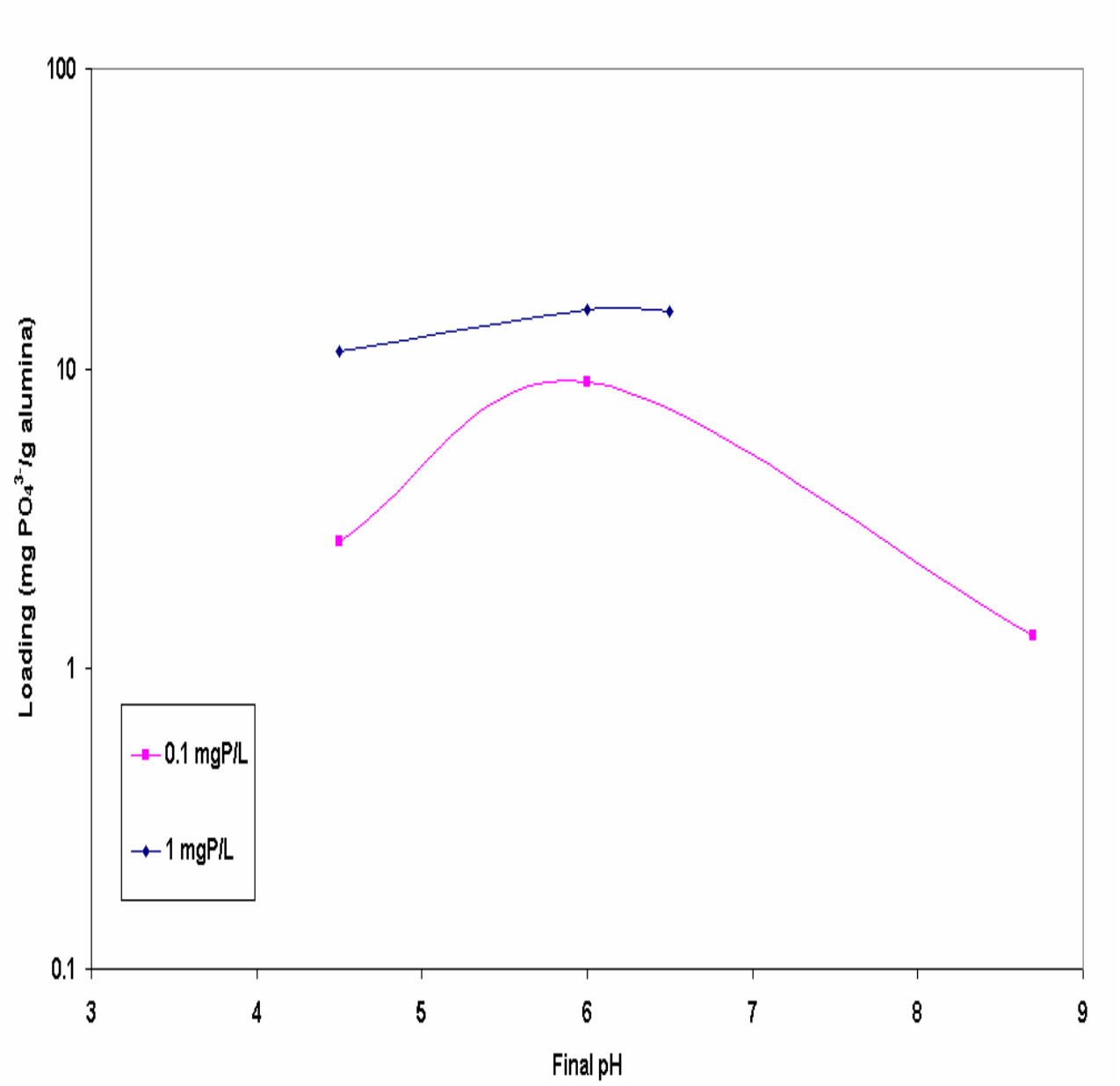

Figure 4.10: Relationship Between the Equilibrium Loading and the Final pH for AA400G 28x48 Mesh with Different Phosphorous Equilibrium Concentration at Temperature of 40 ºC.

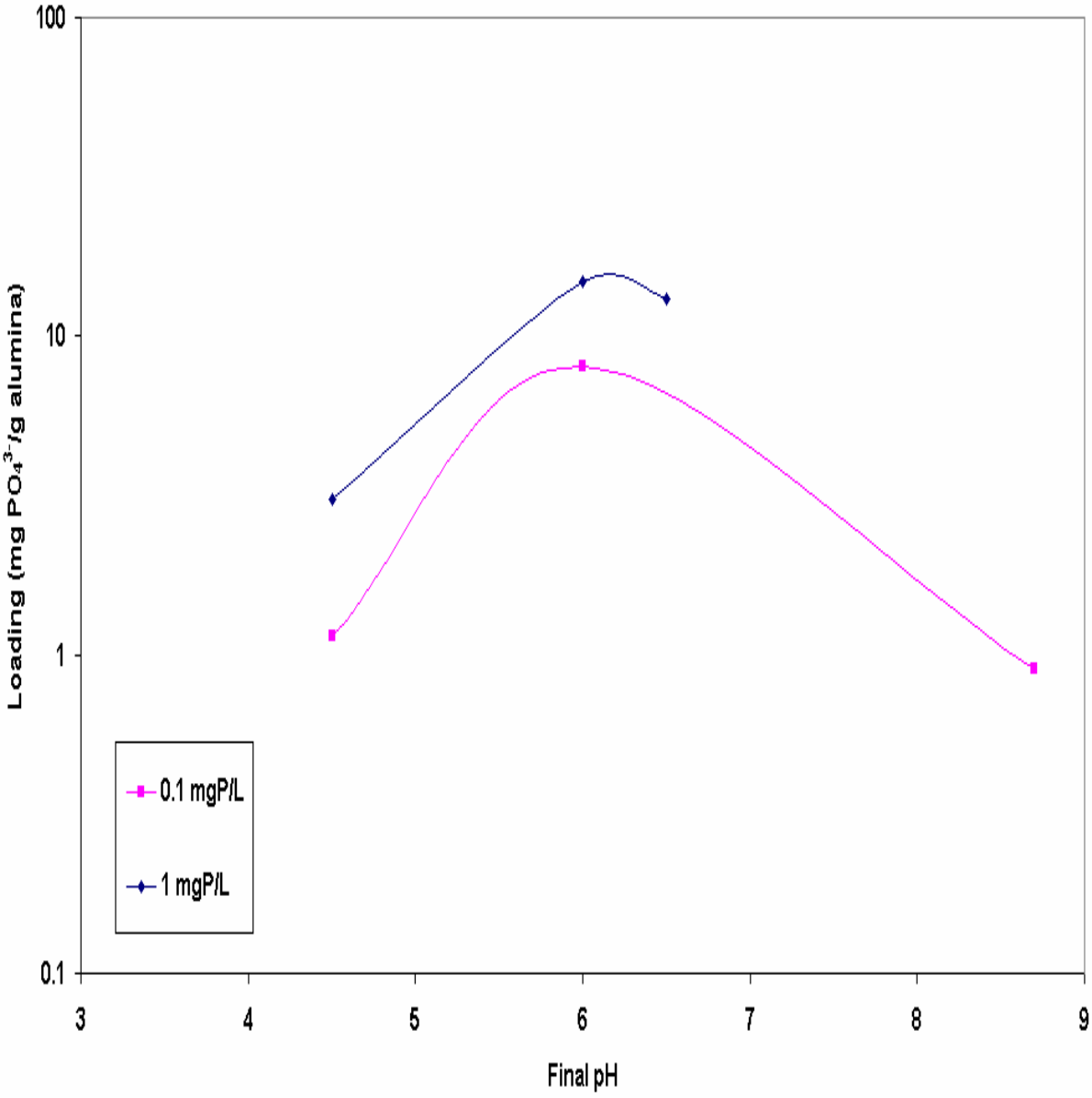

Figure 4.11: Relationship Between the Equilibrium Loading and the Final pH for AA400G 28x48 Mesh with Different Phosphorous Equilibrium Concentration at Temperature of 80 ºC.

CHAPTER FIVE

KINETICS STUDIES

5.1 Introduction

Knowledge of kinetics for adsorption systems is essential for the design and operation of adsorbers. Furthermore, like in the case of equilibrium uptake, it is also important to study factors affecting kinetics such as temperature, pH and circulation rate and influent concentration. The objective of this section is to investigate the effect of the aforementioned variables on the kinetics of the adsorption process. The homogeneous surface diffusion model (HSDM) is used to analyze the experimental data and to calculate the diffusivity coefficients related to the adsorption experiments.

5.2 Theory

Alumina is generally considered as an adsorbent but in the adsorption of orthophosphoric acid it is acting like an ion exchanger with OH^- ions and PO_4^{3-} ions exchanging places.

In ion-exchange systems, electrical coupling effects complicate the diffusion. In a system with various counterions, diffusion rates can be described by the Nernst-Planck equations (Perry, 1997) which are dependent on the ionic self diffusivities $\bar{D}_i$ of the individual species.

For a system with two counterions A and B, with charge z_A and z_B, the Nernst-Planck equations reduce to the following equation:

$$J_A = -\rho_P \overline{D}_{A,B} \frac{\partial n_A}{\partial r} = -\rho_P \frac{\overline{D}_A \overline{D}_B \left[z_A^2 n_A + z_B^2 n_B \right]}{z_A^2 \overline{D}_A n_A + z_B^2 \overline{D}_B n_B} \frac{\partial n_A}{\partial r} \tag{5.1}$$

which shows that the apparent diffusivity $\overline{D}_{A,B}$ varies between $\overline{D}_A$ when ionic fraction of species A in the resin is very small and $\overline{D}_B$ when the ionic fraction of B in the resin approaches unity, indicating that the ion present in smaller concentration has the stronger effect on the local interdiffusion rate. The terms z_A and z_B are the charges of A and B, and n_A and n_B are the concentrations of A and B.

Since the current system consists of a complex mixture containing various ions such as H^+, OH^-, Na^+, SO_4^{2-} and PO_4^{3-} resulting from orthophosphoric acid and buffer solutions of 0.1M NaOH and 0.1M H_2SO_4, the apparent diffusivity is a complex diffusion coefficient comprising the diffusivities of these individual ions. The remainder of the chapter involves determination of the apparent diffusivity of this mixture of ions and it is possible that it varies depending on the composition of the ionic mixture as may be observed from equation 5.1 above.

5.2.1 HSDM Model

A schematic diagram describing the adsorption profile of an adsorbate on an adsorbent particle using the mechanism assumed by the HSDM is shown on Figure 5.1. The HSDM model is based on the following assumptions:

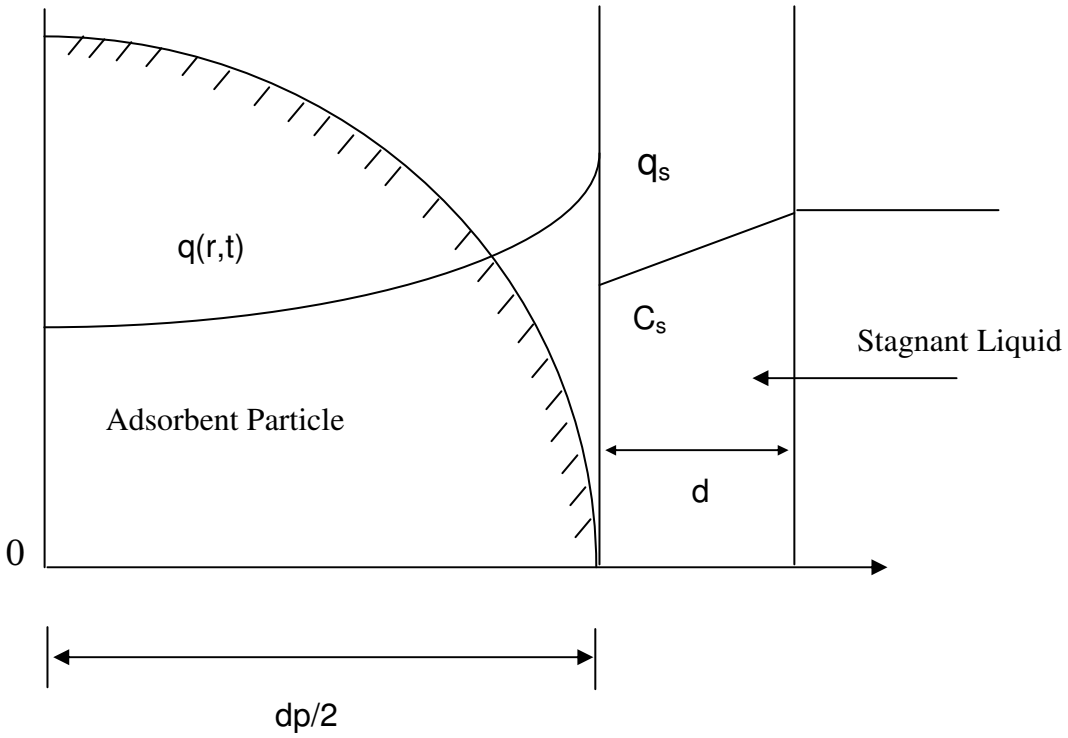

Figure 5.1: Schematic Representation of the HSDM Model

- The equilibrium between the adsorbent and the adsorbate occurs only at the outer surface of the adsorbent particle and is represented by the Freundlich isotherm.
- Intraparticle diffusivity is independent of the phosphate concentration and the particle size.
- Alumina particle is a homogeneous ideal sphere.
- Relative ratio of the time constants for the overall time of experiment, to the time in the packed bed is very large.
- Liquid phase is considered well mixed and recirculation liquid is considered to have the same composition as the bulk liquid.
- The system temperature is considered uniform. A temperature drop of 1 ºC is observed at the exit of the adsorber column compared to the temperature of the solution in the tank. This is due to heat loss from the tank and circulation lines that are not completely insulated and exposed to ambient temperature.

The current adsorber column can be considered as a differential adsorber in which the concentration change across the column is assumed to be very small. Differential reactors or adsorbers such as the continuously stirred tank reactor (CSTR) can be operated in such a way that the initial reactions can be studied (i.e. in differential mode). Since a CSTR is inherently a differential reactor at all levels of conversion, the standard data obtained from its operation are differential rates at a fixed level of conversion. The plug flow reactor (PFR) and bed reactor (BR) can also be operated in a differential mode at any level of conversion by incrementing the space time between composition readings and observing the small increments in conversion that result (Wojciechowski and Rice,

2003). This small concentration change assumes the liquid phase in the packed bed has a constant composition. Table 5.1 gives concentration values of two samples taken simultaneously at two different positions for two times. First sample was taken at the inlet hole of the tank where the solution is coming out from the packed bed adsorber and prior mixing with the tank solution and at the same time the second sample was taken at the exit hole of the tank where the solution is circulated to the packed bed adsorber. It can be seen from the Table that the concentration is almost the same at the two positions meaning that the composition of liquid phase solution in the packed bed adsorber is constant throughout the experiment time.

The kinetic parameters incorporated in this model are the stagnant liquid film mass transfer coefficient, k_f, which describes the rate of diffusion of the adsorbate from the liquid phase through the stagnant liquid film layer around the adsorbent particle, and the surface diffusion coefficient, D_s, which describes the rate of diffusion of the adsorbate on the adsorbent surface.

If the intraparticle mass transfer is described by surface diffusion model HSDM, then the governing mass balance equations of the differential adsorber column and the particle are:

Liquid phase Mass Balance Equation

$$V \frac{\partial C(t)}{\partial t} = -k_f A \left(C(t) - C_s(t)\right) \tag{5.2}$$

Particle Diffusion Mass Balance Equation

$$\frac{\partial q(r,t)}{\partial t} = \frac{D_s}{r^2} \frac{\partial}{\partial r}\left(r^2 \frac{\partial q(r,t)}{\partial r} \right) \tag{5.3}$$

Table 5.1: Concentration Values at Different Positions for AA400G 28x48 Mesh with Initial Concentration of phosphates of 10 mg P/L and Controlled pH of 4.5 at T = 25 ºC.

Run No.	Sample Position	Concentration (mg P/L)	
		First Time (10 minutes)	Second Time (60 minutes)
2	Inlet hole	9.58	8.56
	Exit hole	9.61	8.59
3	Inlet hole	8.64	7.36
	Exit hole	8.61	7.39

In addition, the following initial and boundary conditions apply:

$t = 0$ $\quad q(r, 0) = 0, \quad C(0) = C_0$ (5.4)

$r = 0$ $\quad \partial\, q(0, t) / \partial r = 0$ (5.5)

$r = R$ $\quad D_s A \rho_p \frac{\partial q(R,t)}{\partial r} = k_f A \left(C(t) - C_s(t)\right)$ (5.6)

Defining dimensionless variables (Bhaskar and Bhamidimarri, 1992):

$y = C / C_0$

$u = q / q_0$

$\tau = D_s\, t / R^2$

$\psi = (k_f\, A / V) / (D_s / R^2)$

$x = r / R$

$\gamma = V\, C_o / W\, q_o$

Then, Equations (5.2-5.6) take the following dimensionless forms:

$$\frac{\partial y}{\partial \tau} = \psi \left(y - y_s\right) \tag{5.7}$$

$$\frac{\partial u}{\partial \tau} = \frac{1}{x^2} \frac{\partial}{\partial x}\left(x^2 \frac{\partial u}{\partial x}\right) \tag{5.8}$$

The initial the boundary conditions become:

$\tau = 0$ $\quad u(x, 0) = 0, \quad y(0) = 1$ (5.9)

$x = 0$ $\quad \partial\, u(0, \tau) / \partial\, x = 0$ (5.10)

$x = 1$ $\quad \frac{\partial u(1, \tau)}{\partial x} = \frac{\psi \gamma}{3}\left(y(\tau) - y_s(\tau)\right)$ (5.11)

where ψ is the ratio of film diffusion time to surface diffusion time, γ, the separation factor and W (= ρ_p AR / 3), the weight of the adsorbent.

If fluid and solid phase concentrations are related by a Freundlich isotherm then,

$$q_s = k\, C_s^{\alpha} \tag{5.12}$$

or

$$u_s = y_s^{\alpha} \tag{5.13}$$

5.2.2 Determination of External Mass Transfer Coefficients

The external mass transfer coefficients k_f is evaluated using an appropriate mass transfer correlation for packed beds. Wakao and Funzakri (1978) developed the following forced convective mass transfer correlation for spheres in a packed bed with Reynolds numbers between 3 and 1000:

$$Sh = 2 + 1.1\,\mathrm{Re}^{0.6}\, Sc^{0.333} \tag{5.14}$$

where k_f is the liquid-phase mass transfer coefficient, Sh is Sherwood number, Re is Reynolds number and Sc is Schmidt number. These dimensionless groups are defined in the following equations:

$$\mathrm{Re} = \frac{2\rho_l r v}{\mu} \tag{5.15}$$

$$Sc = \frac{\mu}{\rho_l D_l} \tag{5.16}$$

$$Sh = \frac{2k_f r}{D_l} \tag{5.17}$$

where, μ is viscosity of solution, ρ_l is the density of solution, r is the mean radius of adsorbent particle, ν is the superficial velocity, and D_l is the free liquid diffusivity of adsorbate (in this case the phosphate ion PO_4^{3-}) in the solution.

5.3 Experimental Procedure

Fifteen experimental runs were performed to measure the kinetics at the experimental conditions presented in Table 5.2. The length of the packed beds is 21 cm and the I.D. is 2.8 cm. Since the length was constant, indicate that packed bed was supported at approximately a 50^o angle to ensure packed bed behavior.. Kinetics batch experiments raw data collected at different conditions, as indicated in Table 5.2, is listed in Appendix C. Four runs were performed at controlled pH of 4.5 [runs 1 to 4] while the remainder of the runs was executed with no pH control.

5.4 Calculation Procedure For the Model

The parameter k_f was calculated from the mass transfer correlation [Equation 5.14]. The parameter D_s was calculated by fitting the model equations [Equations 5.7 to 5.13] to the data. The criteria used to calculate the sum of squares by the function called LSQCURVEFIT in MATLAB was:

$$SS = \text{sum (Theoretical uptake data} - \text{Experimental uptake data)}^2 \qquad (5.18)$$

Table 5.2: Experimental Conditions for Kinetics Batch Experiments

Run No.	Adsorbent	Adsorbent Weight (gram)	Initial Solution Concentration (mg/L)	Temperature (ºC)	pH	Circulation Rate (ml/min)
1	AA400G 28x48 Mesh	3	10	25	Control pH 4.5	300
2	AA400G 28x48 Mesh	1	10	25	Control pH 4.5	300
3	AA400G 28x48 Mesh	2	10	25	Control pH 4.5	300
4	AA400G 28x48 Mesh	2	20	25	Control pH 4.5	300
5	AA400G 28x48 Mesh	1	10	25	No Control	300
6	AA400G 28x48 Mesh	3	10	25	No Control	300
7	AA400G 28x48 Mesh	2	10	25	No Control	300
8	AA400G 28x48 Mesh	1	10	25	No Control	400
9	AA400G 28x48 Mesh	1	20	25	No Control	300
10	AA400G 14x28 Mesh	3	10	25	No Control	300
11	AA400G 14x28 Mesh	2	10	25	No Control	300
12	AA400G 28x48 Mesh	3	10	40	No Control	300
13	AA400G 28x48 Mesh	3	10	80	No Control	300

Table 5.2: Experimental Conditions for Kinetics Batch Experiments

Run No.	Adsorbent	Adsorbent Weight (gram)	Solution Concentration (mg/L)	Temperature (ºC)	pH	Circulation Rate (ml/min)
14	AA400G 14x28 Mesh	3	10	80	No Control	300
15	AA400G 14x28 Mesh	3	10	40	No Control	300

The correlation values (R^2) are calculated as follows:

$$R^2 = 1 - \left(\frac{sum(E - T)^2}{sum(E - M)^2} \right) \tag{5.19}$$

where E represents the experimental uptake data, T represents the theoretical uptake data and M is the mean of the experimental uptake data. The relevant parameters are given in Table 5.3.

The model equations (5.6 to 5.12) are solved numerically using orthogonal collocation method. The experimental data is fitted using the function expressed by (Equation 5.18). Values of diffusivity D_s are assumed as initial guess values for the fit function. The parameters included in the solution of the model equations and in the experimental data fitting are γ and α:

$$\gamma = \frac{1}{\lambda} - 1 \tag{5.20}$$

Here, λ is the fractional uptake (λ) calculated using the experimental data as follows:

$$\lambda = \frac{C_o - C_\infty}{C_o} \tag{5.21}$$

where C_o and C_∞ are the initial and the final equilibrium solution concentrations respectively.

The parameter α is found from the Freundlich isotherm equations (Chapter 4). Table 5.4 gives values of γ and α for each run. Other variables such as solution viscosity, velocity and particle size are also given in the Table. The detailed calculation procedure for the model is given in Appendix D.

Table 5.3: Kinetics Parameters of All Kinetics Batch Experiments

Run No.	Diffusion Coefficient D_s (cm^2 /sec)	External Mass Transfer Coefficient k_f (cm/sec)	R^2
1	2.40E-10	4.85E-03	0.98
2	4.21E-08	4.85E-03	0.88
3	1.74E-09	4.85E-03	0.86
4	2.55E-09	4.85E-03	0.90
5	3.00E-09	4.85E-03	0.97
6	7.00E-09	4.85E-03	0.97
7	1.04E-09	4.85E-03	0.97
8	3.36E-09	5.72E-03	0.97
9	3.54E-09	4.85E-03	0.97
10	6.92E-09	3.62E-03	0.96
11	2.04E-08	3.62E-03	0.96
12	2.24E-08	7.96E-03	0.96
13	3.84E-08	1.58E-02	0.93
14	3.72E-08	1.18E-02	0.96
15	2.22E-08	5.94E-03	0.92

Table 5.4: Model Parameters of All Kinetics Batch Experiments

Run No.	Temperature (ºC)	pH	Viscosity Of Solution (cp)	Velocity (cm/sec)	Particle Size (cm)	α	γ
1	25	Controlled at 4.5	1	0.812	0.045	0.50	0.086
2	25	Controlled at 4.5	1	0.812	0.045	0.50	4.26
3	25	Controlled at 4.5	1	0.812	0.045	0.50	0.90
4	25	Controlled at 4.5	1	0.812	0.045	0.50	0.30
5	25	No Control	1	0.812	0.045	1.01	0.80
6	25	No Control	1	0.812	0.045	1.01	0.11
7	25	No Control	1	0.812	0.045	0.50	0.30
8	25	No Control	1	1.083	0.045	1.01	0.72
9	25	No Control	1	0.812	0.045	1.01	0.724
10	25	No Control	1	0.812	0.089	1.01	0.185
11	25	No Control	1	0.812	0.045	1.01	0.499
12	40	No Control	0.62	0.812	0.045	1.081	0.353
13	80	No Control	0.32	0.812	0.045	1.159	0.686
14	80	No Control	0.32	0.812	0.089	1.159	0.500
15	40	No Control	0.62	0.812	0.089	1.081	0.350

5.5 Results and Discussion of Results

5.5.1 Effect of Phosphate Solution Concentration

The dimensionless concentration of the liquid solution at two phosphate concentrations of 10 mg P/L and 20 mg P/L at room temperature (about 25 °C) are presented in Figures 5.2 and 5.3 at a controlled pH condition of 4.5. A plot of phosphate-reduced concentration vs. square root of time is given for variation of initial phosphate concentration in the aforementioned Figures. It is apparent that the intraparticle diffusional resistance is the rate limiting step in the overall uptake of phosphate as shown in Figures 5.2 and 5.3.

In Figure 5.2, with 2 gram of AA400G (28x48 Mesh) and controlled pH of 4.5, residual phosphorous concentration decreased with increasing initial phosphate concentration from 10 mg P/L to 20 mg P/L. Also, large change of the uptake curves was observed for the two concentration levels due to the large concentration gradient applied for both cases. That might be also due to the effect of the pH of the solution maintained by the addition of droplets of buffer solutions of 0.1 M NaOH and H_2SO_4 respectively. For the case of 1 gram of AA400G (28x48 Mesh) and with no pH control, the variation in initial phosphate concentration from 10 mg P/L to 20 mg P/L had no effect on the uptake curves and the uptake curves for both concentrations were similar as shown in Figure 5.3. Figure 5.2 indicates that the uptake curves of both concentration levels had different apparent diffusivity. The apparent diffusivities of both concentration levels were almost same for the case of 1 gram AA400G (28x48 Mesh) and with no pH control as shown in Figure 5.3.

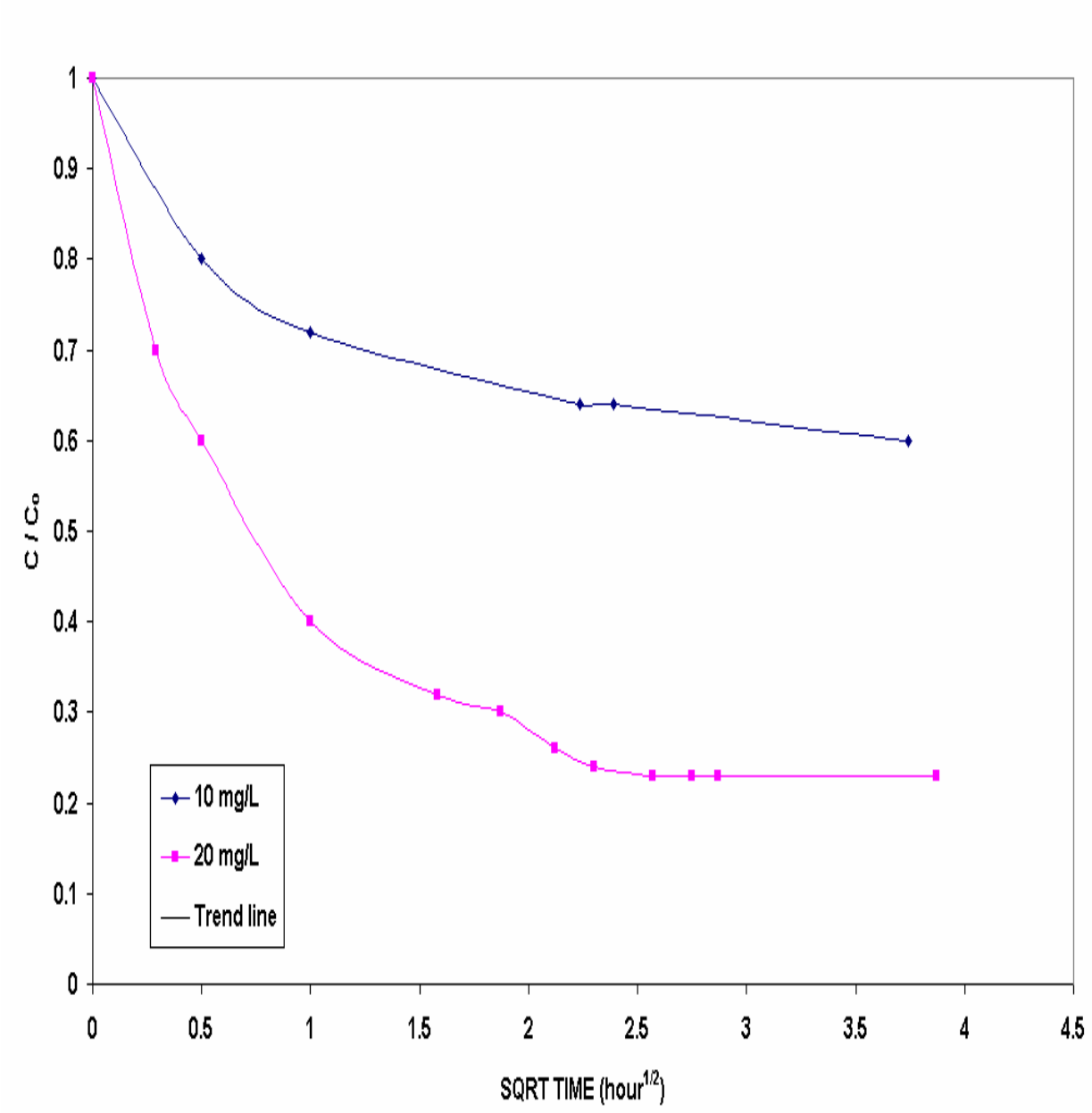

Figure 5.2: Uptake Experiment for Phosphate with 2 gram of AA400G 28x48 Mesh at T = 25 ºC and Controlled pH of 4.5.

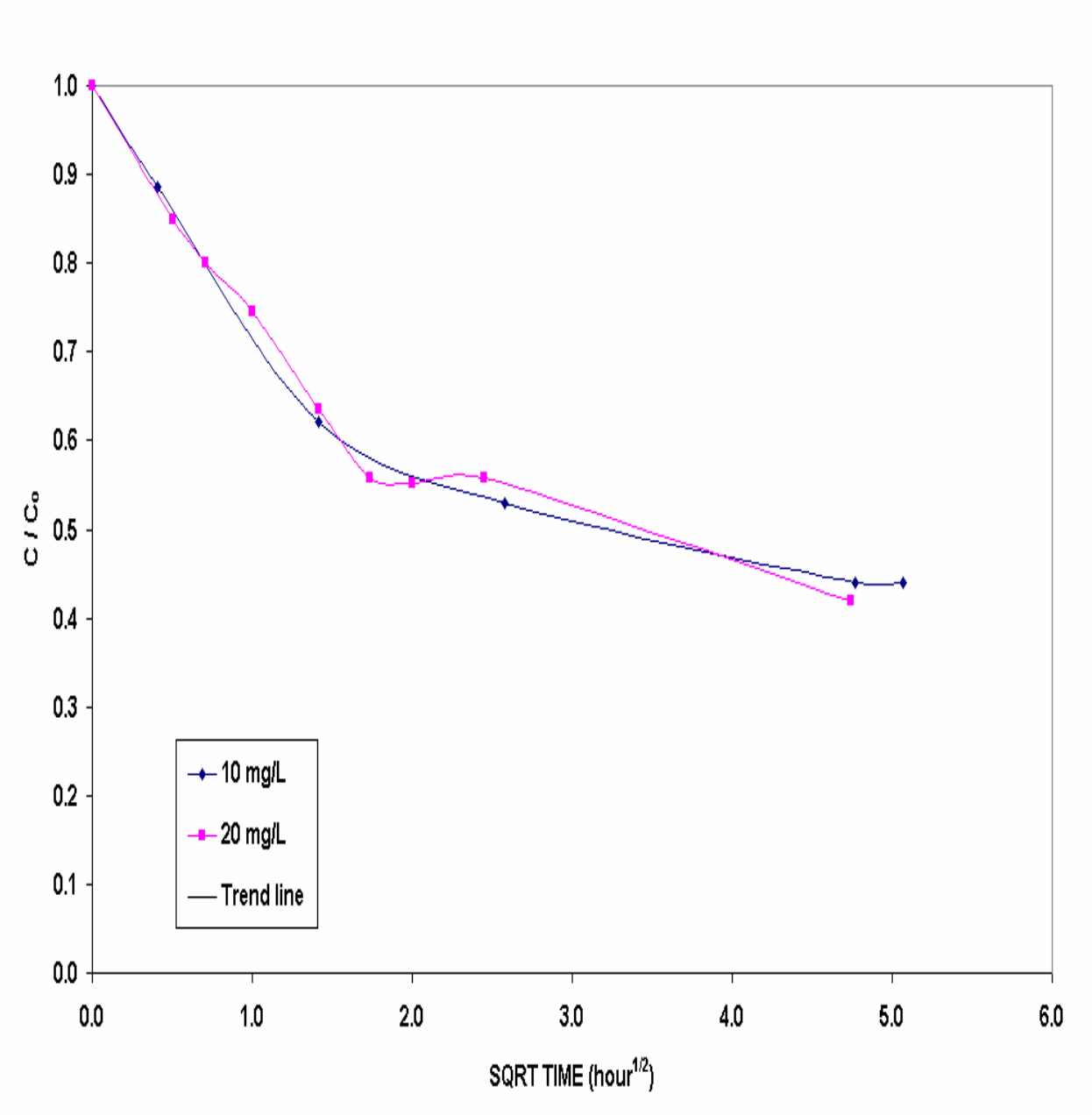

Figure 5.3: Uptake Experiment for Phosphate with 1 gram of AA400G 28x48 Mesh at T = 25 ºC and no pH Control.

The difference in D_s is due to the fact that the D_s measured is an average value for these ions , i.e.,

$$D_s = \overline{D}\ (OH^-,\ PO_4^{3-},\ SO_4^{2-})$$

The amount of 0.1 M H_2SO_4 added to the system was not monitored at it was not considered necessary at the time. It is probable that the amount added is different for 20 mg solution than the 10 mg solution and hence the weighting of the three ions in the average diffusivity calculation is different. Therefore, we should expect a different D_s and this is what is observed. For the case with no pH control, it is because D_s is only a function of OH^- and PO_4^{3-} ions, i.e.,

$$D_s = \overline{D}\ (OH^-,\ PO_4^{3-})$$

No difference is observed as no buffer solution is added.

The uptake m_t/m_∞ is plotted against square root of time in Figures 5.4 and 5.5 for the data previously presented in Figures 5.2 and 5.3. Figures 5.4 and 5.5 illustrate very clearly the nature of the phenomena. Figure 5.4 indicates different apparent diffusivities for both phosphates concentration while Figure 5.5 shows same apparent diffusivity. That may be due to the effect of the solution pH maintained throughout the experiment time by addition of the buffer solutions. For the case of 1 gram of AA400G (28x48 Mesh) with no pH control, it is observed that both uptake curves for the two different initial phosphate concentrations had almost same shape meaning that the diffusivity is independent of initial phosphate concentration as shown in Figure 5.5. Furthermore, the fractional uptake of both initial phosphate concentrations 10 mg/l and 20 mg/l under same conditions was evaluated using Equation (5.21). At 25 ºC and under controlled pH of 4.5 with 2 gram of AA400G (28x48 Mesh), fractional uptake percentages of about

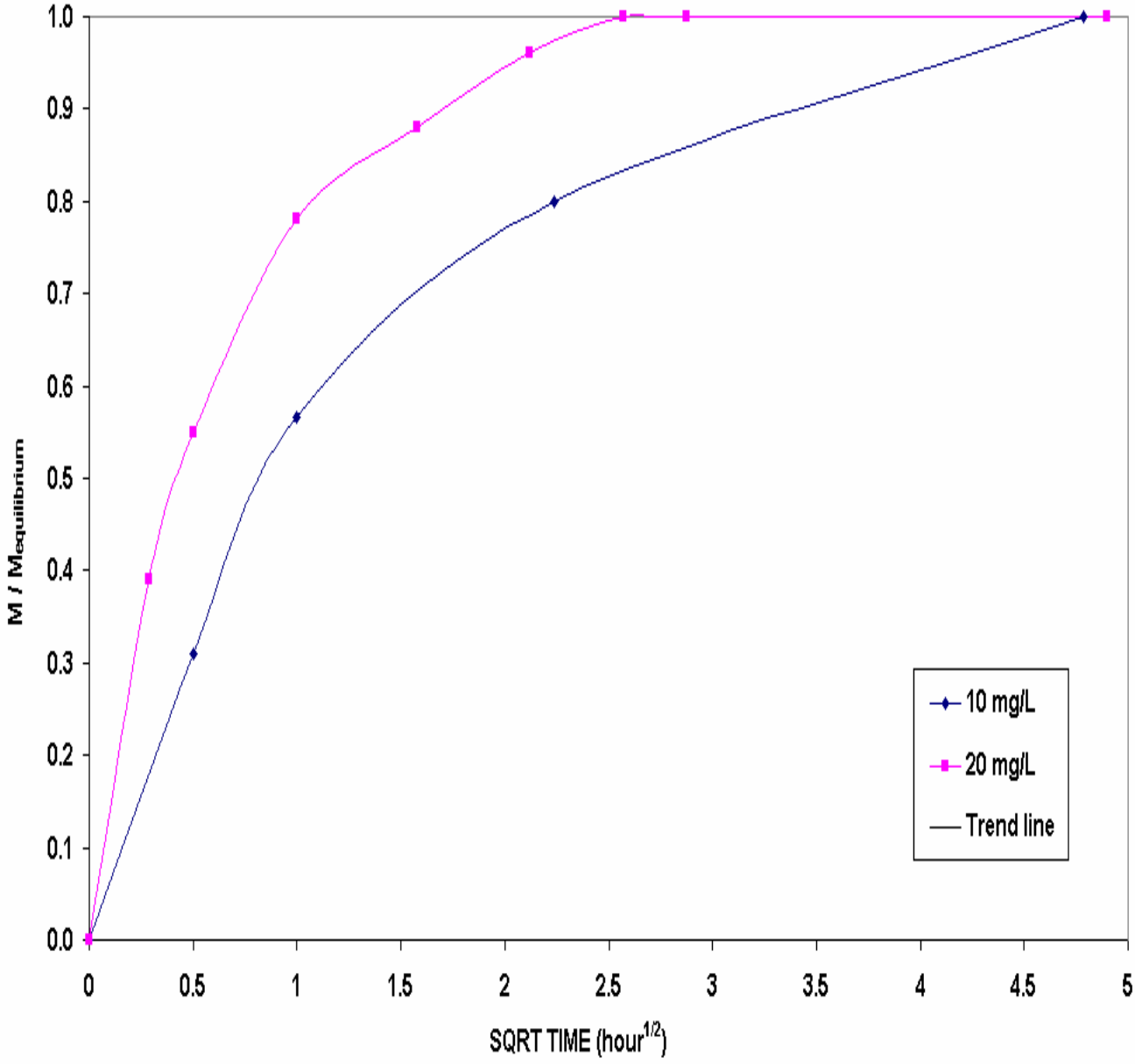

Figure 5.4: Uptake Rate for Phosphate with 2 gram of AA400G 28x48 Mesh at T = 25 ºC and Controlled pH of 4.5.

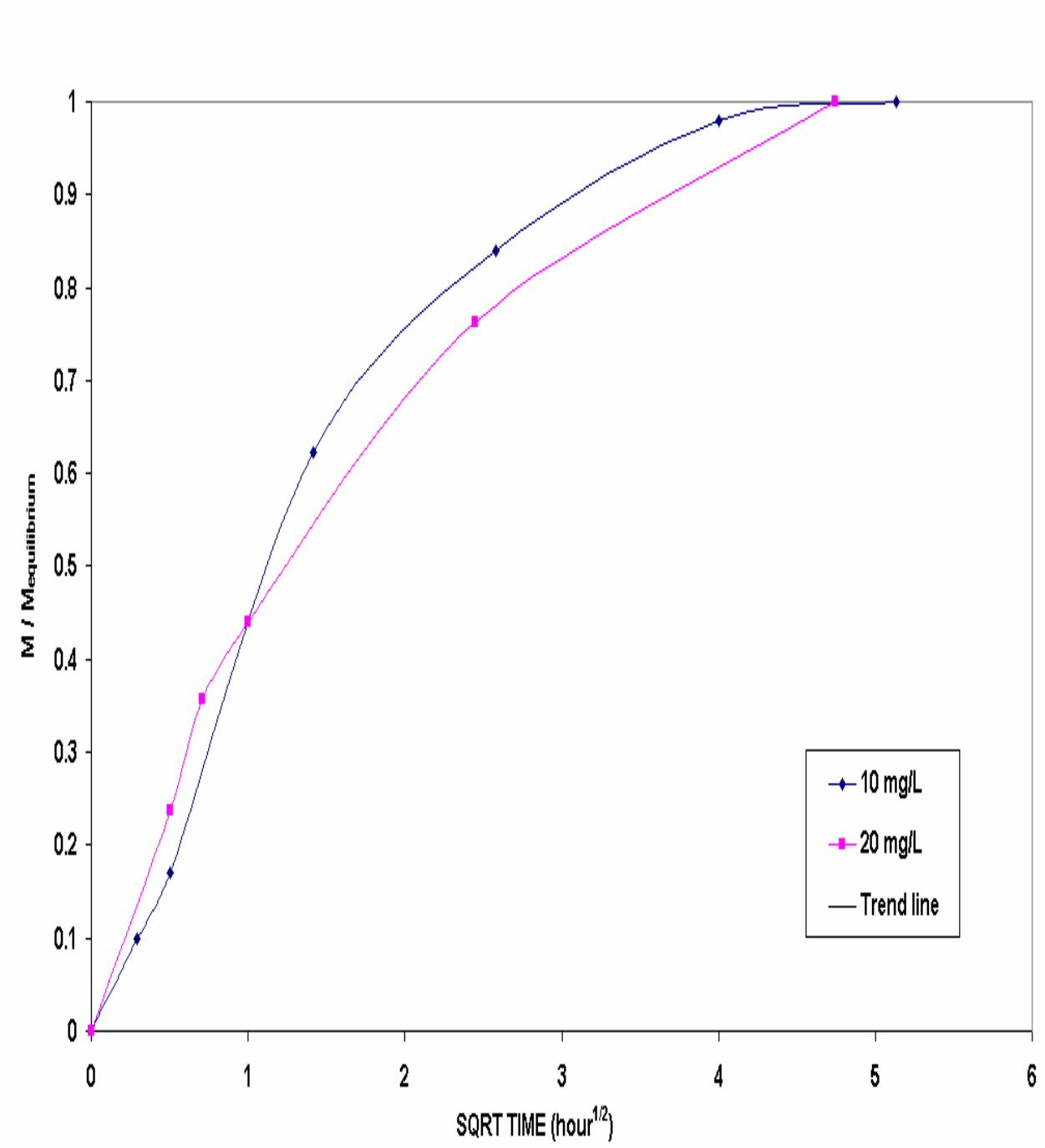

Figure 5.5: Uptake Rate of Phosphate with 1 gram of AA400G 28x48 Mesh at T = 25 ºC and no pH Control.

40% and 80% were achieved for the concentration levels of 10 and 20 mg P/L respectively. The same fractional uptake of 50% was achieved for both concentration levels for the runs with no pH control and 1 gram of AA400G (28x48 Mesh) at 25 ºC. These differences in fractional uptake may be attributed to the addition of buffer 0.1 M H_sSO_4.

Diffusion coefficients D_s as found by the HSDM model for the two phosphate concentrations and the correlation analysis results according to phosphate concentration conditions are summarized in Table 5.5. It is clear that the diffusivity coefficient increases with increasing initial phosphate concentration for the controlled pH solution. The reason is that increasing the phosphate concentration in the solution promoted the diffusion in the activated alumina adsorbent of varying amounts of buffer 0.1 M H_2SO_4 and resulted in an increase in the intraparticle diffusion rate. No significant difference was observed between the diffusivity constants for the two runs with 1 gram of AA400G (28x48 Mesh) and with no pH control. That agrees with the HSDM model that is based on the constant diffusivity assumptions. Brattebo and Odegaard (1986) found in their breakthrough experiments conducted with controlled pH condition at 25 ºC that the diffusivity increased as initial phosphate concentration increased due to the high mobility of the adsorbed phosphate at higher liquid concentrations. Note, this is probably due to the addition of buffer as above. Also, they assumed the intraparticle diffusivity is independent of concentration for HSDM model used to describe the system. Figures 5.6, 5.7, 5.8 and 5.9 show the fit of numerically exact solution to the batch kinetic data.

Table 5.5: Diffusivity Coefficients of Phosphate on AA400G 28x48 Mesh Evaluated by the HSDM Model under Different Concentrations at Temperature of 25 °C.

Run No.	pH	Concentration (mg P/L}	Adsorbent Weight (gram)	Diffusion Coefficient, D_s (cm^2/sec)
3	Controlled at 4.5	10	2	1.74E-09
4		20		2.55E-09
5	No Control	10	1	3.00E-09
9		20		3.54E-09

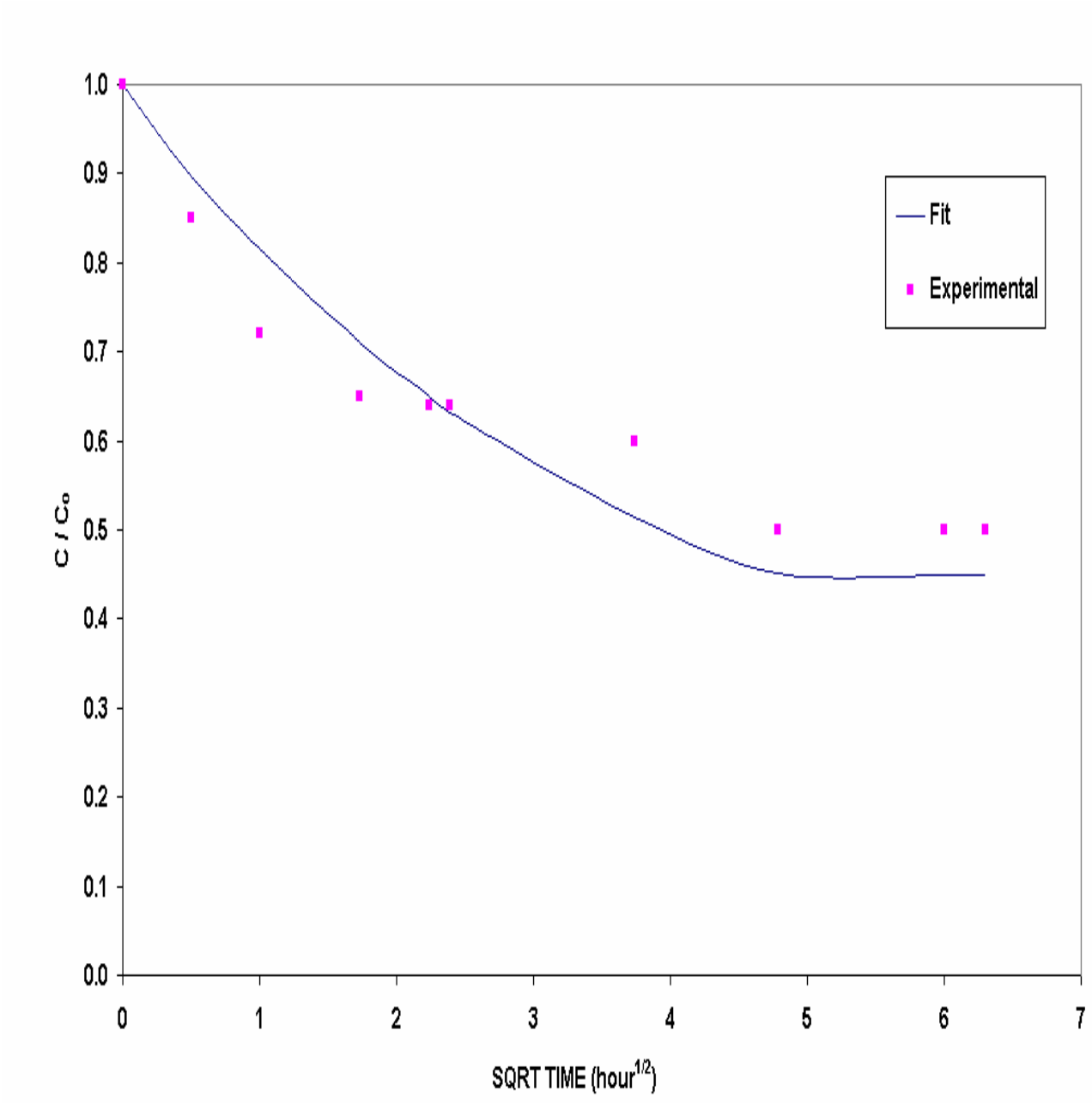

Figure 5.6: Batch Kinetic Experiment for 10 mg/L Phosphate by 2 gram AA400G 28x48 Mesh at T = 25 °C and Controlled pH of 4.5 along with HSDM Predictions [D_s= 1.74E-09 cm^2/sec, k_f = 4.85E-03 cm/sec].

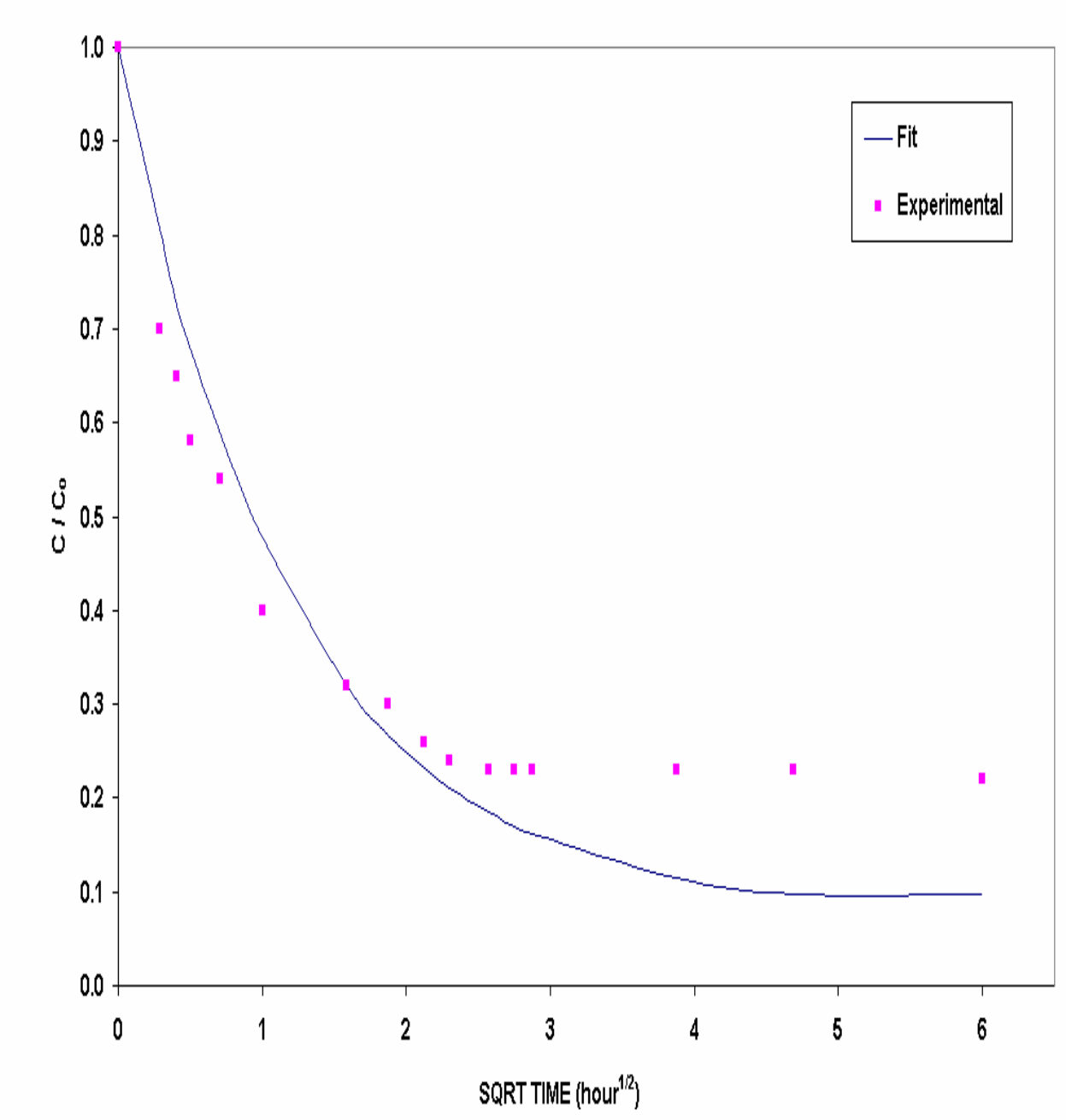

Figure 5.7: Batch Kinetic Experiment for 20 mg/L Phosphate by 2 gram AA400G 28x48 Mesh at T = 25 °C and Controlled pH of 4.5 along with HSDM Predictions [D_s= 2.55E-09 cm^2/sec, k_f = 4.85E-03 cm/sec].

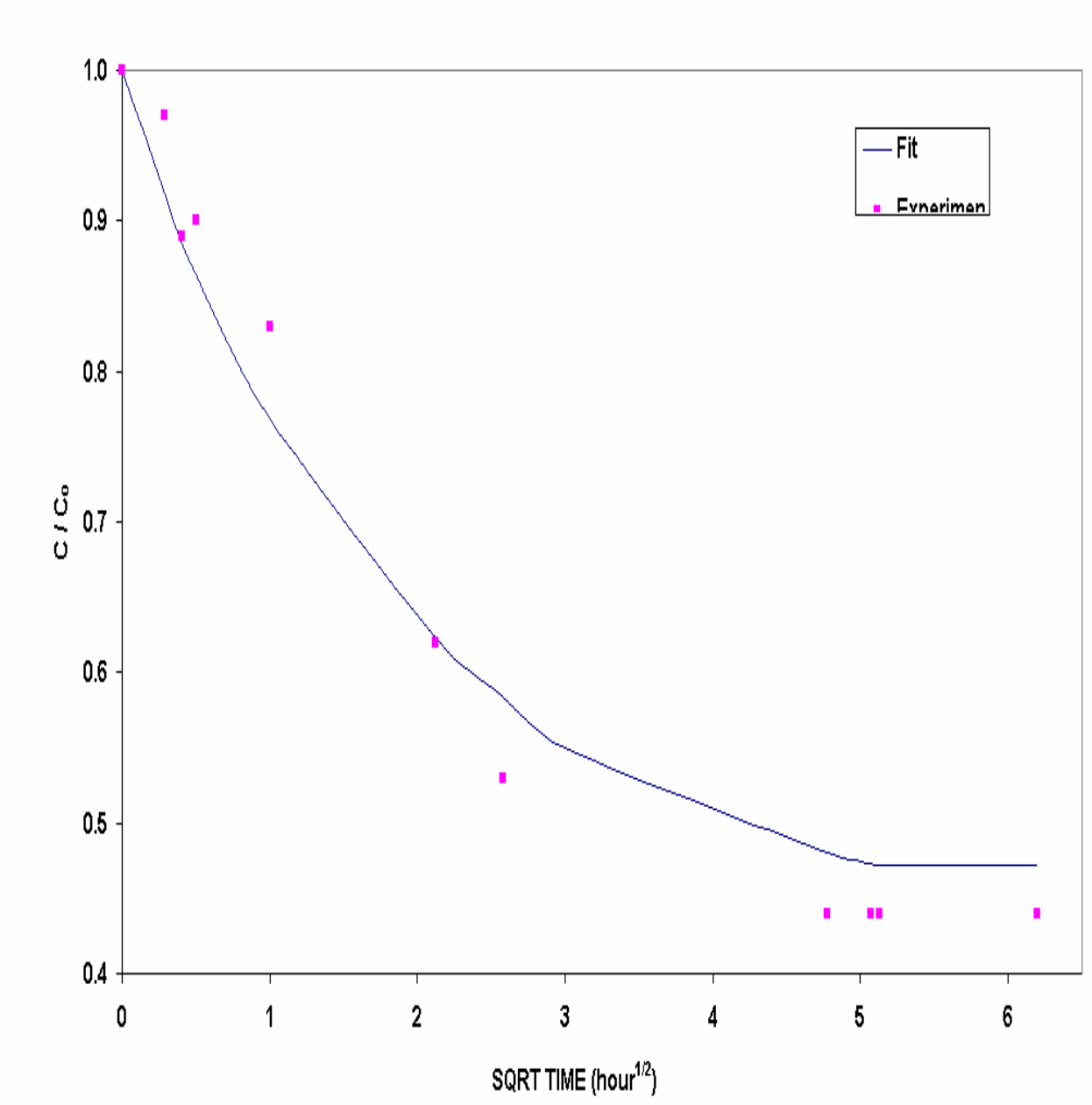

Figure 5.8: Batch Kinetic Experiment for 10 mg/L Phosphate by 1 gram AA400G 28x48 Mesh at T = 25 °C and no pH Control along with HSDM Predictions [D_s= 3.00E-09 cm^2/sec, k_f = 4.85E-03 cm/sec].

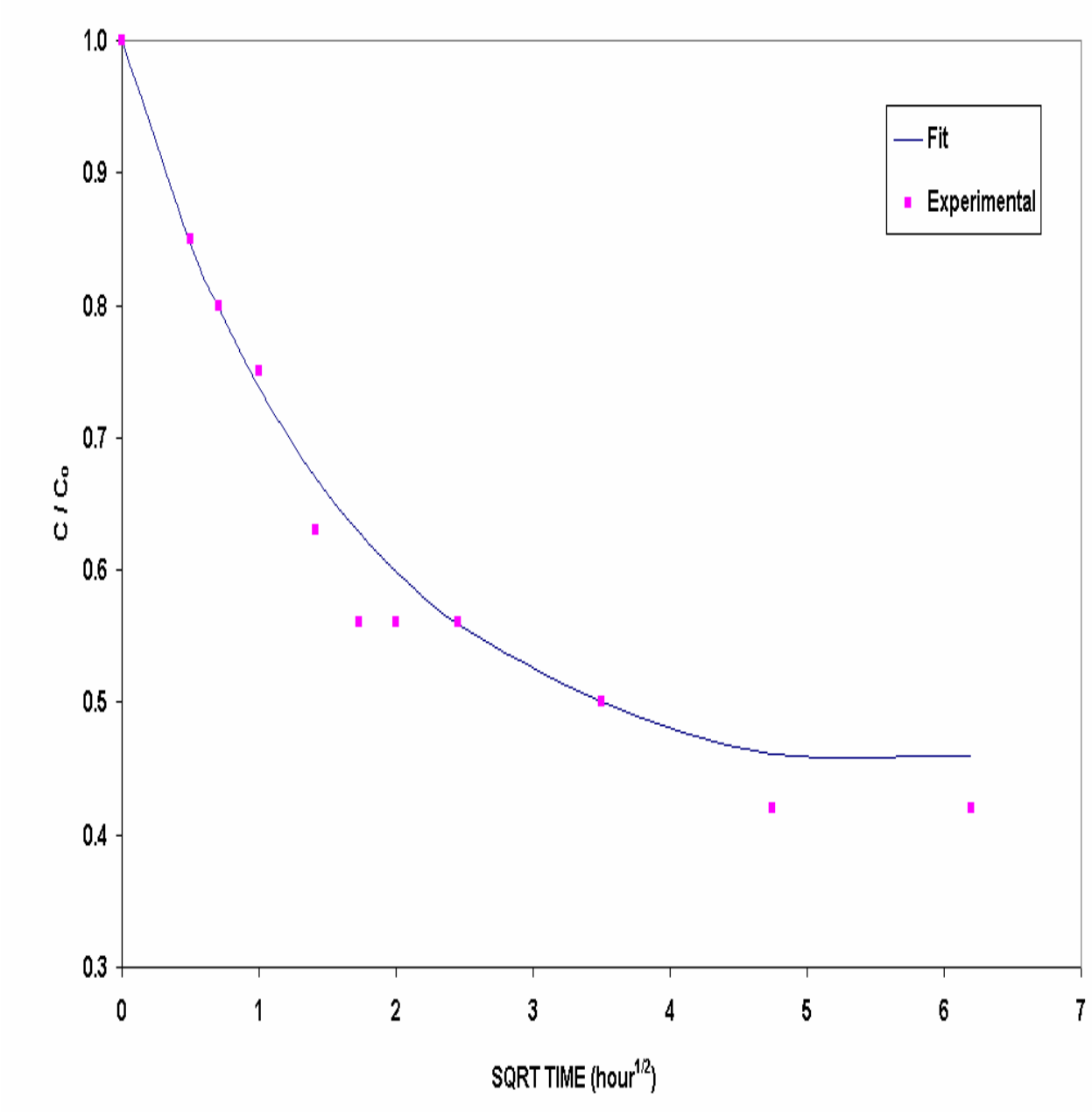

Figure 5.9: Batch Kinetic Experiment for 20 mg/L Phosphate by 1 gram AA400G 28x48 Mesh at T = 25 °C and no pH Control along with HSDM Predictions [D_s= 3.54E-09 cm^2/sec, k_f = 4.85E-03 cm/sec].

5.5.2 Effect of pH Variation

To study the effect of pH on kinetics adsorption, four runs were performed at control pH of 4.5 (runs 1 to 4) while the remainder of the runs was executed with no pH control. Frequent addition of buffer solutions of 0.1M NaOH and 0.1M H_2SO_4 to the experiment solution results in promoting the adsorption of phosphate ions at low concentrations by the activated alumina adsorbent.

The results of the batch kinetic experiments for phosphate at controlled pH of 4.5 and with no pH control are shown in Figures 5.10 and 5.11 as phosphate-reduced concentration vs. square root of time. From the figures, it is clear that the pH of both conditions affects the kinetics of adsorption. It is found that the residual phosphorous concentration decreased with no pH control compared to that with controlled pH of 4.5. The uptake curves for both conditions were different due to the effect of the solution pH at same conditions (i.e. solution concentration of 10 mg P/L, temperature of 25 ºC and circulation rate of 300 ml/min) as shown in Figures 5.10 and 5.11. Uptake curves for controlled pH of 4.5 were affected by the competing ions (H^+, OH^-, Na^+, SO_4^{2-}) released from the added buffer solutions for controlling the solution pH during the experiment time. Figure 5.10 and 5.11 show that the uptake curves of both pH conditions had different apparent diffusivity due to the different average diffusivities of the different ionic solutions, as mentioned earlier.

Furthermore, the fractional uptake percentage values under same conditions (i.e. temperature, initial phosphate concentration, particle mesh size, adsorbent weight and circulation rate) were found to be different for the two pH conditions. At 25 ºC and initial phosphate concentration 10 mg/l with 2 gram of AA400G 28x48 Mesh, a fractional

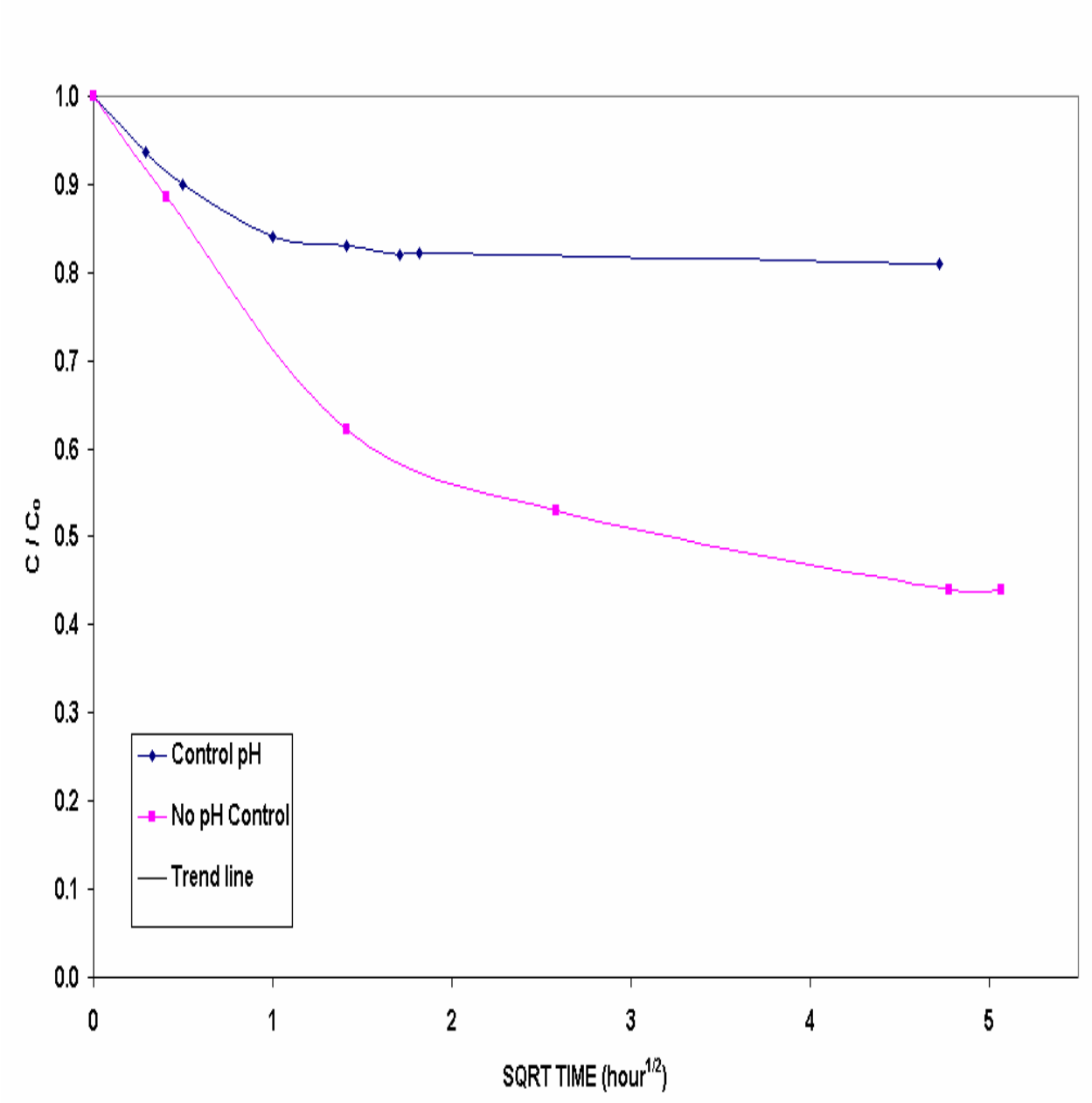

Figure 5.10: Uptake Curve for Phosphate with 1 gram of AA400G 28x48 Mesh at Temperature of 25 °C and Initial Concentration of 10 mg/L.

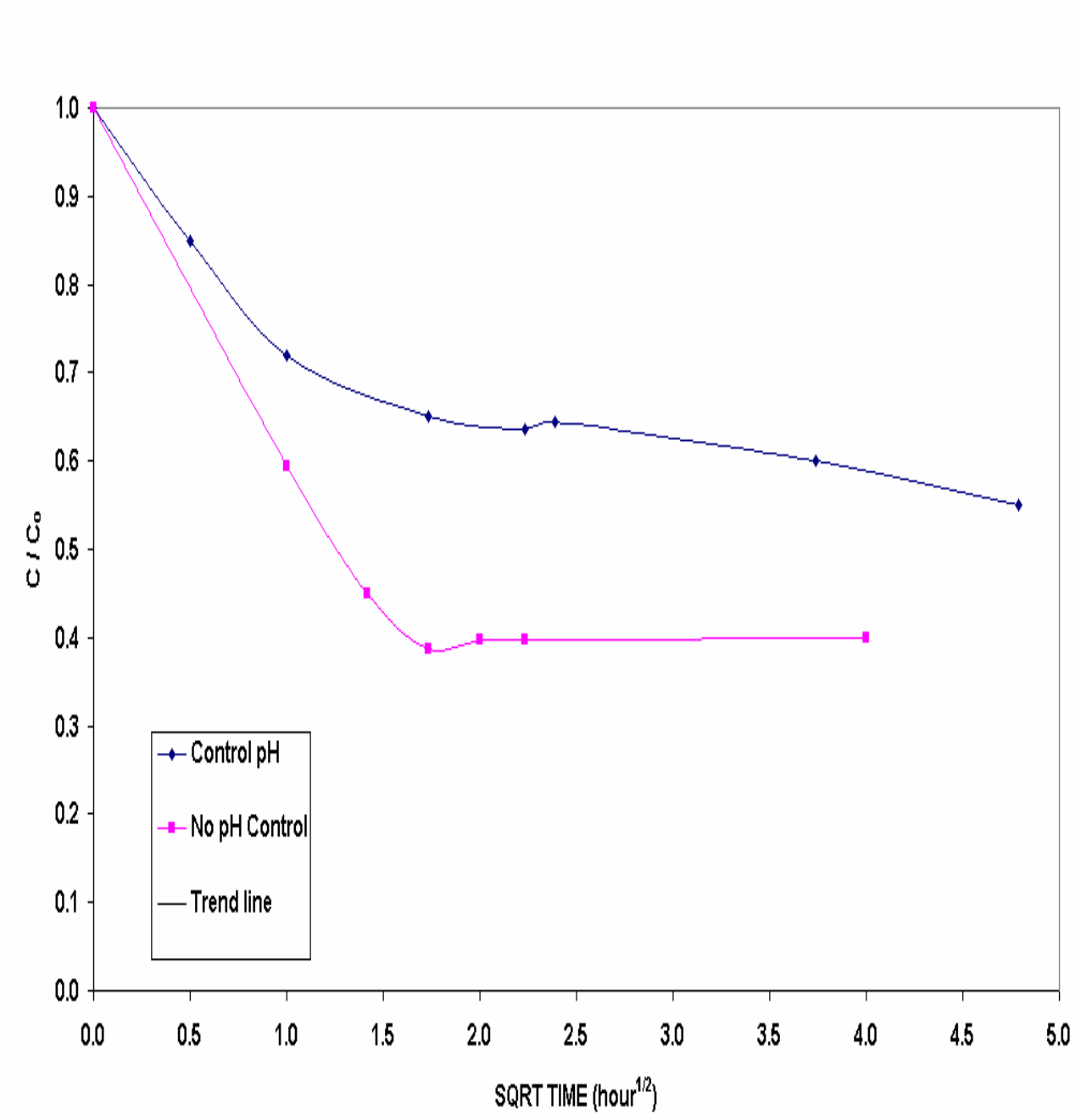

Figure 5.11: Uptake Experiment for Phosphate with 2 gram of AA400G 28x48 Mesh at Temperature of 25 °C and Initial Concentration of 10 mg/L.

uptake percentage of about 40% and 60% respectively were achieved for controlled pH of 4.5 and no pH control conditions respectively. For the case of 1 gram of AA400G 28x48 Mesh and same aforementioned conditions, fractional uptake percentages of about 20% and 50% were achieved for controlled pH of 4.5 and no pH conditions respectively.

Diffusion coefficients D_s as found by the HSDM model for both controlled pH of 4.5 and no pH control conditions are presented in Table 5.6. It can be seen from the Table that the diffusivity coefficient is higher in case of pH control compared to that with no pH control at 25 °C for both 1 or 2 gram of AA400G (28x48 Mesh). The reason is the promotion of phosphates diffusion to the adsorbent by the addition of buffer solutions that release various ions to the solution that are adsorbed by the activated alumina adsorbent. Moreover, the diffusivity is much higher in case of pH control compared to no pH control when 1 gram of AA400G (28x48 Mesh) was used because of the significant effect of the addition of buffer solutions to the lower quantity of adsorbent used in the experiment. It can be concluded that the measured diffusivity for the runs with controlled pH is an average ionic diffusivity of the phosphates plus the buffer solution ions. It can be also noticed that the diffusivities are different for the 2 gram and 1 gram adsorbent for no pH control condition because of the difference on the ratio of adsorbent weight to solution volume varying the final pH of both cases. Figures 5.12, 5.13, 5.14 and 5.15 show the fit of numerically exact solution to the batch kinetic data.

Table 5.6: Diffusivity Coefficients of 10 mg/L Phosphate Solution on AA400G 28x48 Mesh Evaluated by the HSDM Model under Different pH Control Mode at Temperature of 25 °C.

Run No.	Adsorbent Weight (gram)	pH	Diffusion Coefficient, D_s (cm^2/sec)
3	2	Controlled at 4.5	1.74E-09
7		No control	1.04E-09
2	1	Controlled at 4.5	4.21E-08
5		No control	3.00E-09

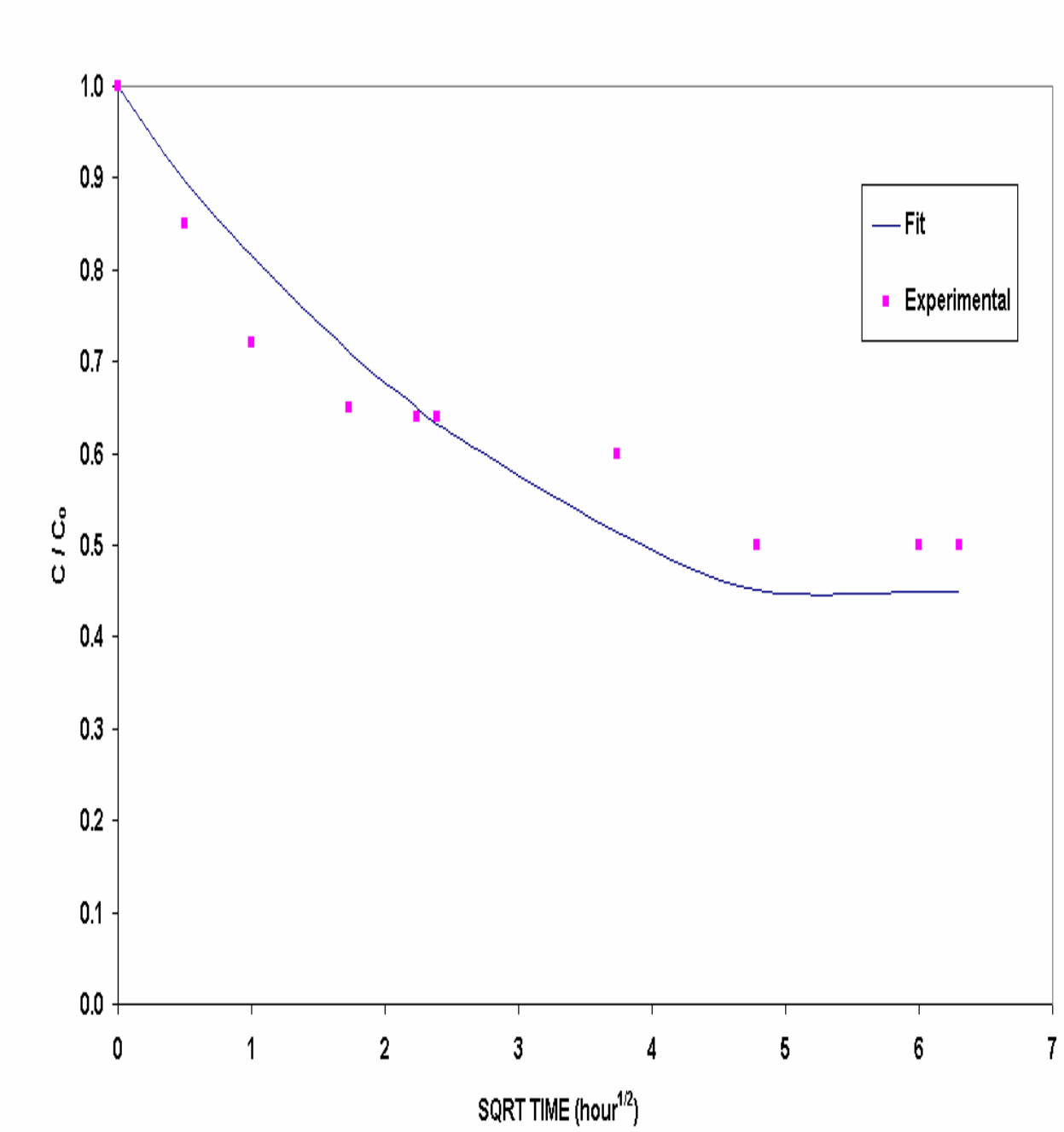

Figure 5.12: Batch Kinetic Experiment for 10 mg/L Phosphate by 2 gram AA400G 28x48 Mesh at T = 25 °C and Controlled pH of 4.5 along with HSDM Predictions [D_s= 1.74E-09 cm^2/sec, k_f = 4.85E-03 cm/sec].

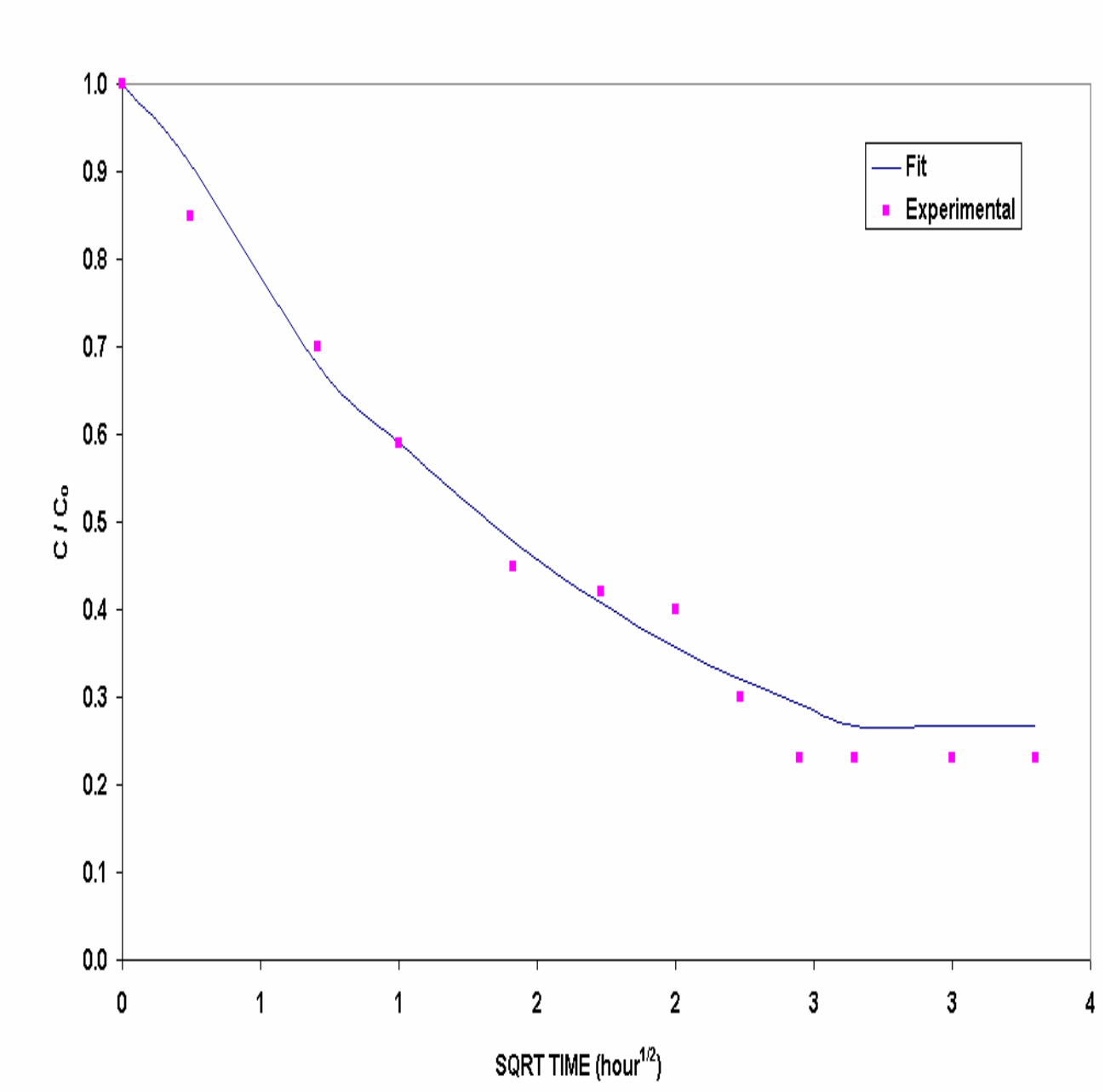

Figure 5.13: Batch Kinetic Experiment for 10 mg/L Phosphate by 2 gram AA400G 28x48 Mesh at T = 25 °C and no pH Control along with HSDM Predictions [D_s= 1.04E-09 cm^2/sec, k_f = 4.85E-03 cm/sec].

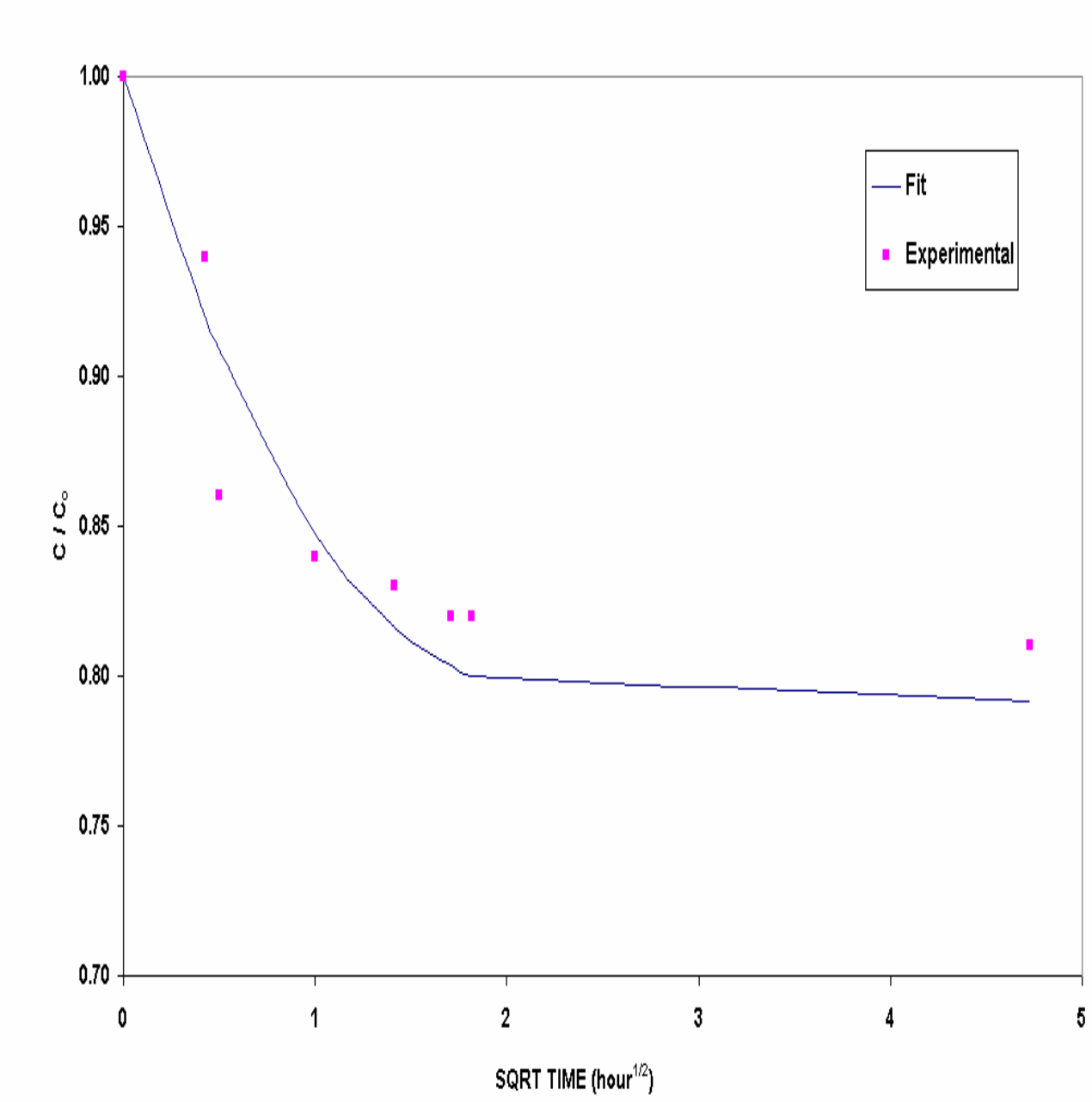

Figure 5.14: Batch Kinetic Experiment for 10 mg/L Phosphate by 1 gram AA400G 28x48 Mesh at T = 25 °C and Controlled pH of 4.5 along with HSDM Predictions [D_s= 4.21E-08 cm^2/sec, k_f = 4.85E-03 cm/sec].

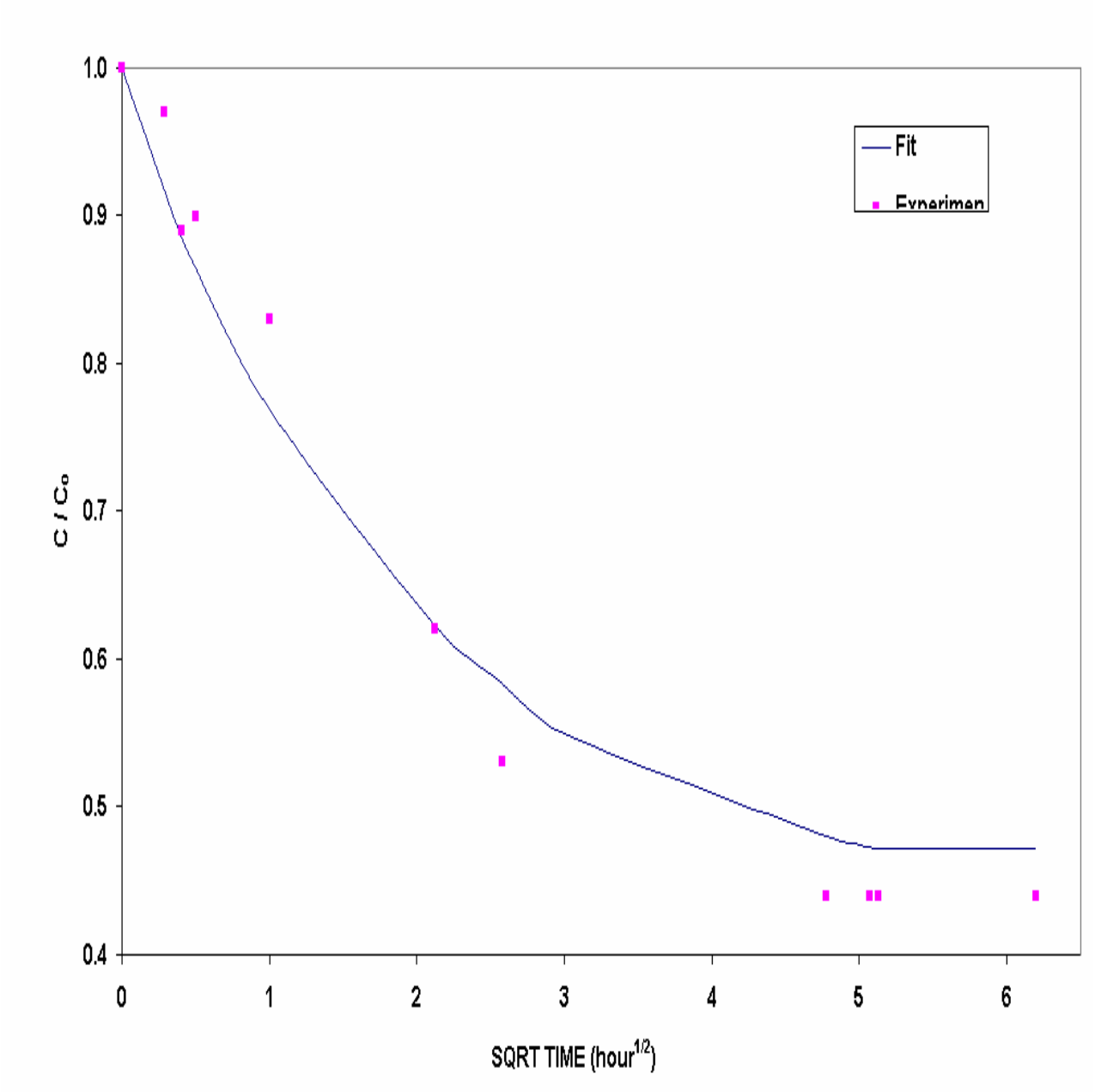

Figure 5.15: Batch Kinetic Experiment for 10 mg/L Phosphate by 1 gram AA400G 28x48 Mesh at T = 25 °C and no pH Control Along with HSDM Predictions [D_s= 3.0E-09 cm^2/sec, k_f = 4.85E-03 cm/sec].

5.5.3 Effect of Circulation Speed Variation

Variation of circulation rate (i.e. speed) on batch kinetic experiments was conducted at two values of 4.0 and 5.5 indicated in speed controller of the pump used on the kinetic experiments setup. Flow rates were calculated for the two speed values of 4.0 and 5.5 as 300 and 400 ml/min respectively. As shown on Figure 5.16, circulation rate has no effect on the uptake curves for 1 gram of AA400G 28x48 mesh at ambient temperature and with controlled pH of 4.5. This observation leads to the finding that external mass transfer resistance is not the major limiting phenomena. At 25 ºC and initial phosphate concentration 10 mg/L with 1 gram of AA400G (28x48 Mesh), a fractional uptake percentage of about 50% was achieved for both circulation rates.

Table 5.7 gives the values of Re, Sc and Sh calculated by Equations 5.15, 5.16 and 5.17 respectively at two different circulation rates of 300 and 400 ml/min. Sherwood number (Sh) seems high indicating that the external mass transfer resistance should be considered in the modeling of this system. However, for small variation in circulation rate (or Re), it is observed that no significant change was found between values of calculated Sherwood numbers (Sh) for the two cases meaning that the external mass transfer resistance is not the principle rate controlling resistance. The external mass transfer coefficients (k_f) were found to be 4.85E-09 and 5.72E-09 cm/sec for 300 and 400 ml/min respectively. It can be seen that slight difference was found between the two circulation rates in terms of external mass transfer coefficient. No significant difference was observed for the measured diffusivity constants for both circulation rates. At 25 ºC and solution concentration of 10 mg/L with no pH control and 1 gram of AA400G

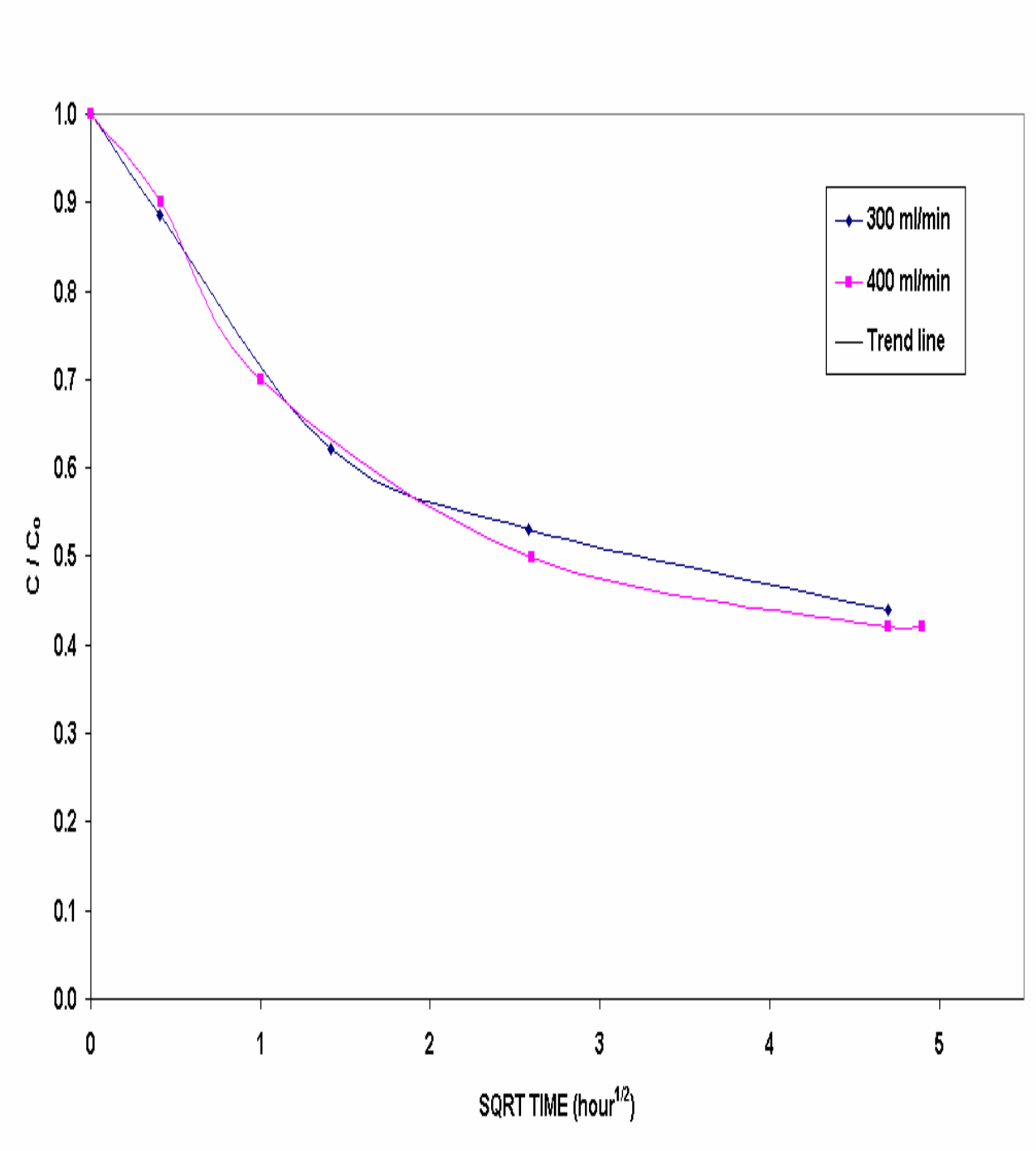

Figure 5.16: Uptake Experiment for Phosphate with 1 gram AA400G 28x48 Mesh at T = 25 °C, no pH Control and Initial Concentration of 10 mg/L.

Table 5.7: External Mass Transfer Effect of 10 mg/L Phosphate Solution on AA400G 28x48 Mesh under Different Circulation Rates at Temperature of 25 °C and no pH Control.

Run No.	Circulation Rate (ml/min)	Re (-)	Sc (-)	Sh (-)	k_f (cm/sec)	D_s (cm^2/sec)
5	300	7.31	821	35.9	4.85E-03	3.00E-09
8	400	9.75	821	42.3	5.72E-03	3.36E-09

(28x48 Mesh), the values of diffusivity constants were found to be 3.00E-09 and 3.36E-09 cm^2/sec for the circulation rates of 300 and 400 ml/min respectively. Figures 5.17 and 5.18 show the fit of numerically exact solution to the batch kinetic data.

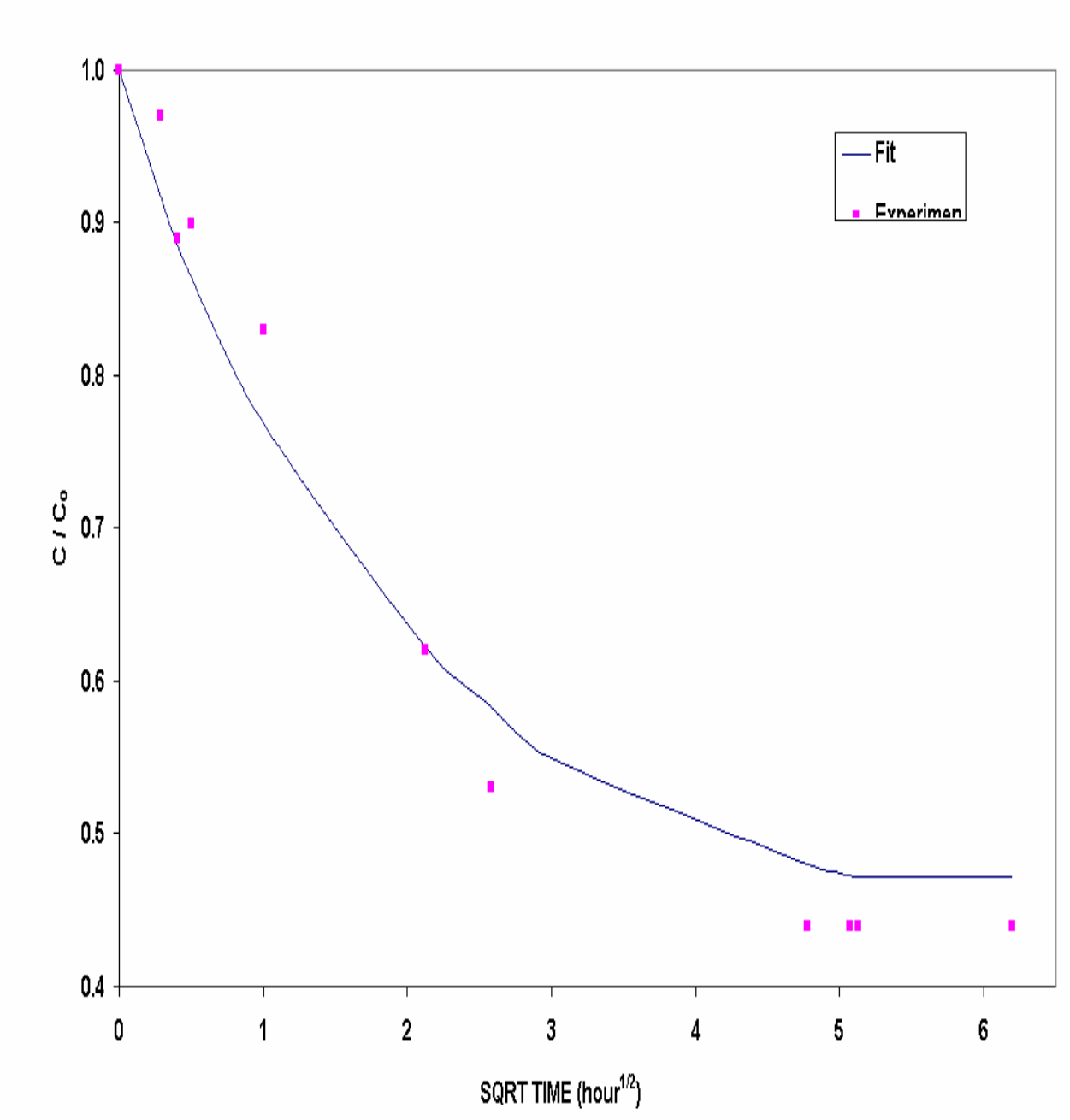

Figure 5.17: Batch Kinetic Experiment for 10 mg/L Phosphate by 1 gram AA400G 28x48 Mesh at T = 25 °C and no pH Control at Circulation Rate of 300 ml/min along with HSDM Predictions [D_s= 3.00E-09 cm^2/sec, k_f = 4.85E-03 cm/sec].

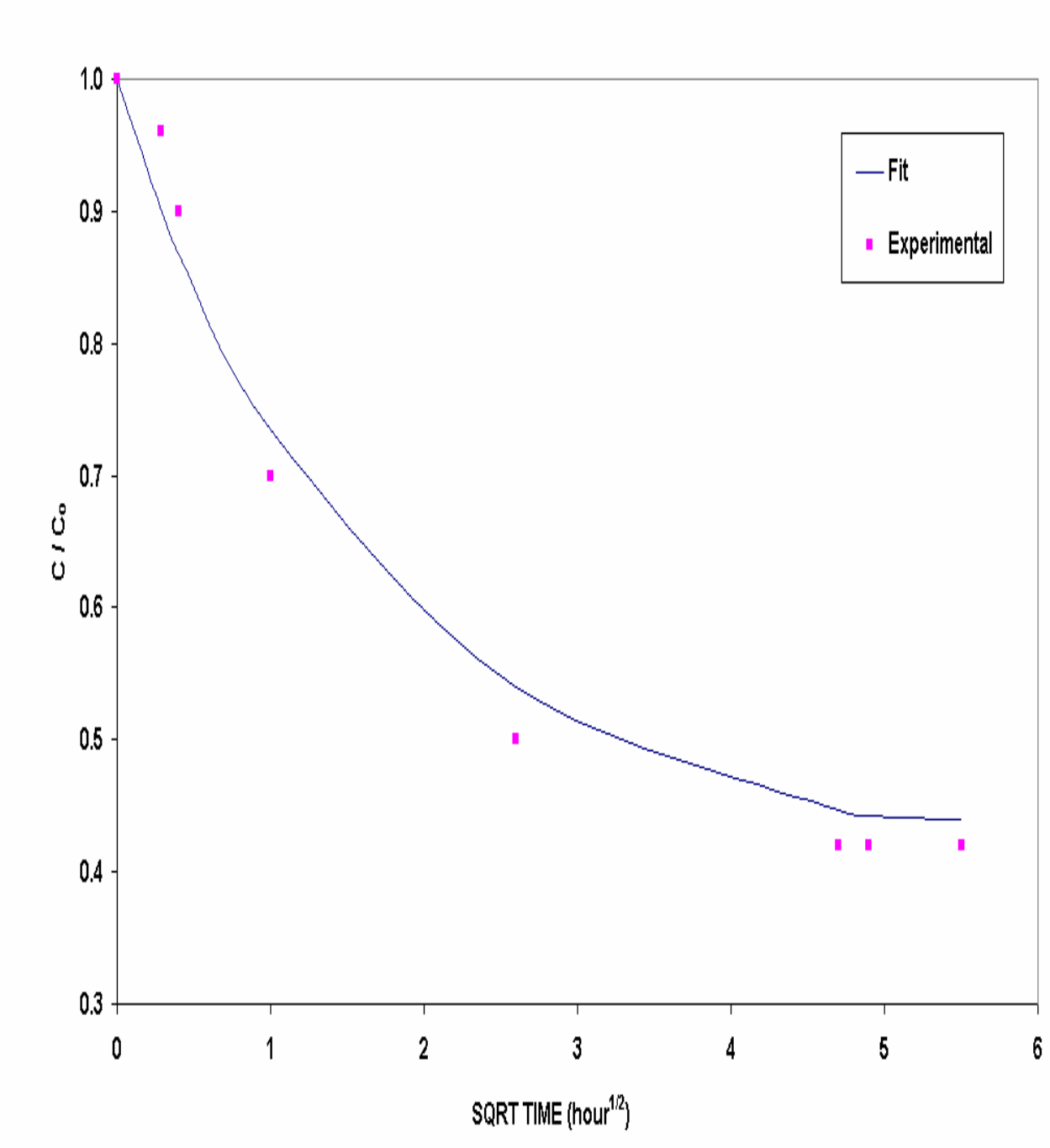

Figure 5.18: Batch Kinetic Experiment for 10 mg/L Phosphate by 1 gram AA400G 28x48 Mesh at T = 25 °C and no pH Control at Circulation Rate of 400 ml/min along with HSDM Predictions [D_s= 3.36E-09 cm^2/sec, k_f = 5.72E-03 cm/sec].

5.5.4 Effect of Temperature Variation

The results of the batch kinetic experiments for phosphate at temperatures of 25, 40 and 80 °C are shown in Figures 5.19 and 5.20 for activated alumina adsorbents AA400G (28x48 Mesh) and (14x28 Mesh) respectively with no pH control. It is clear that temperature variations affect the kinetics of adsorption of phosphate on both activated alumina adsorbents AA400G (28x48 Mesh) and (14x28 Mesh). The data show that the equilibrium time for phosphate adsorption increases with the decrease in temperature, consistent with lower values of D_s. From the figures, it is observed that the smaller mesh size adsorbent AA400G (28x48 Mesh) reached equilibrium faster than the larger particle size mesh AA400G (14x28 Mesh) as is to be expected for a macropore control particle.

The data are presented in Figures 5.21 and 5.22 in terms of uptakes. Phosphate uptake curves at different temperatures for AA400G (28x48 Mesh) and (14x28 Mesh) are plotted in Figures 5.21 and 5.22 respectively. The different long time slopes in the figures suggests the effect of temperature variation on the uptake rate.

Diffusion coefficients D_s as found by the HSDM model for the three temperatures 25, 40 and 80 °C and are presented in Table 5.8. The diffusivity coefficient increases with temperature as it is expected from Arrehenius's equation for both particle sizes. Figure 5.23 presents the relationship between the diffusivity coefficient and the temperature. From the Figure, it can be seen that the diffusivity coefficient increased with increasing temperature. The diffusivity coefficient value of 2.5E-10 cm^2/sec found by (Brattebo and

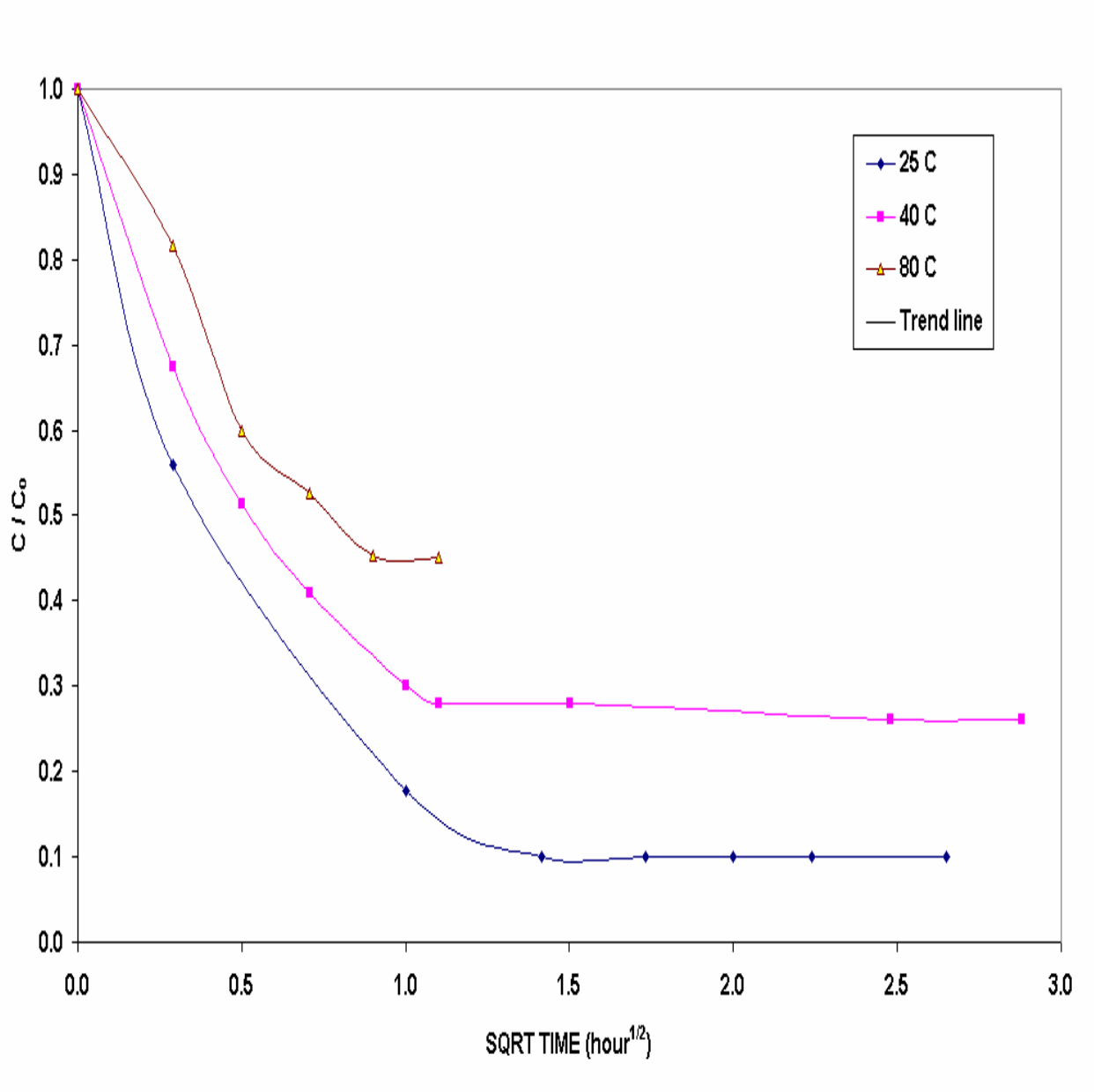

Figure 5.19: Uptake Experiment for Phosphate with 3 gram AA400G 28x48 Mesh, no pH Control and Initial Concentration of 10 mg/L.

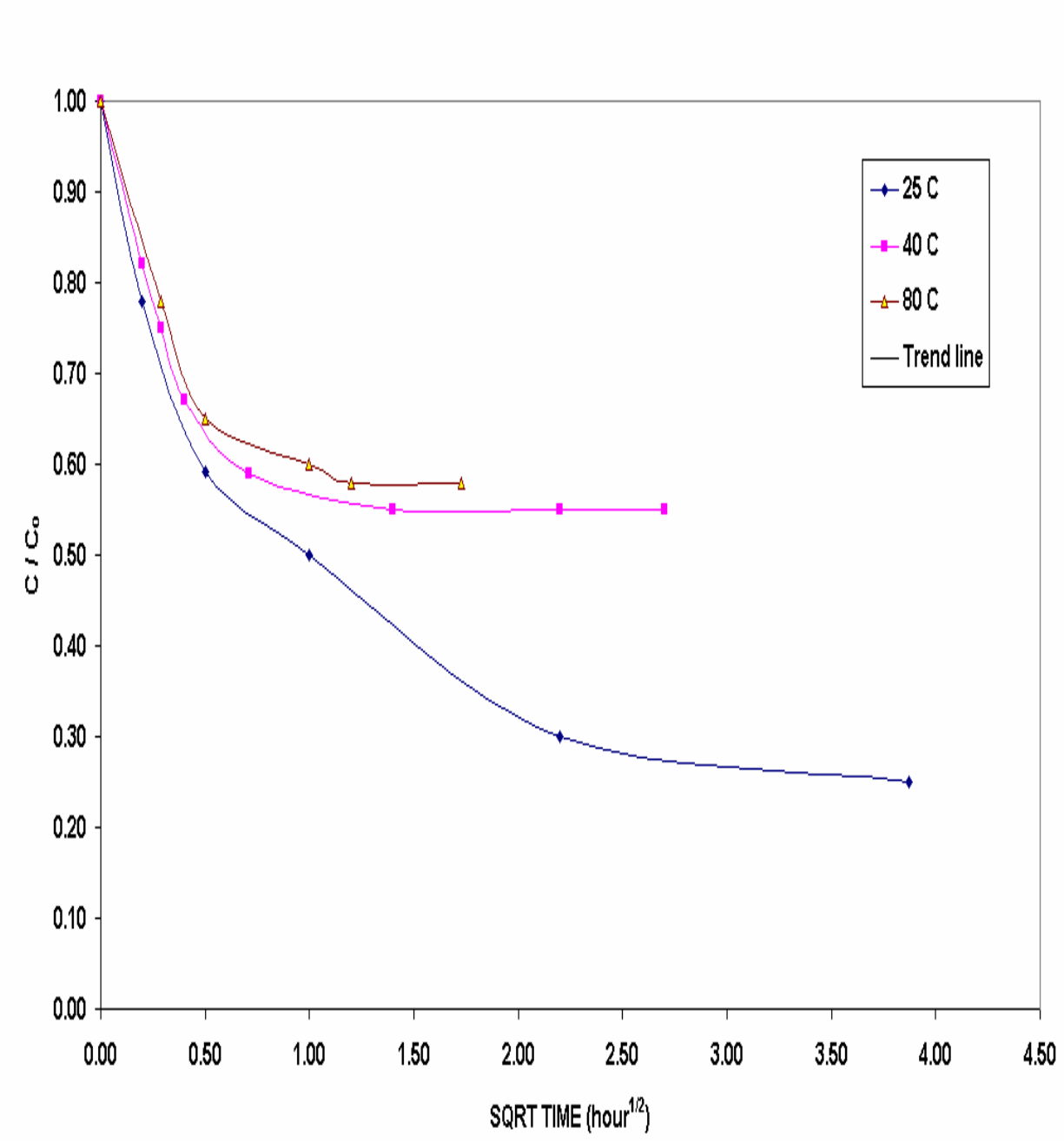

Figure 5.20: Uptake Experiment for Phosphate with 3 gram AA400G 14x28 Mesh, no pH Control and Initial Concentration of 10 mg/L.

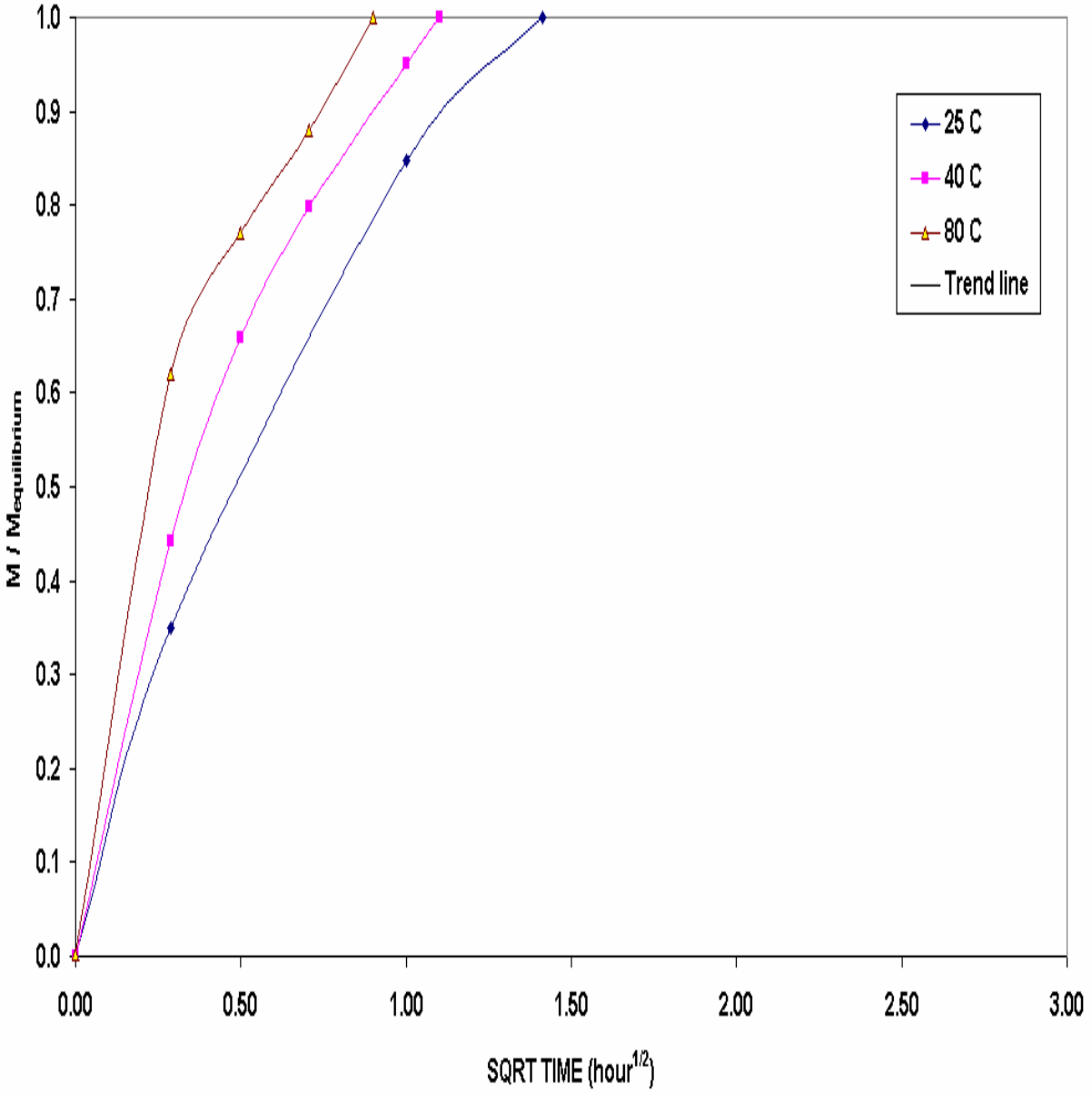

Figure 5.21: Uptake Curve for Phosphate with 3 gram AA400G 28x48 Mesh, no pH Control and Initial Concentration of 10 mg/L.

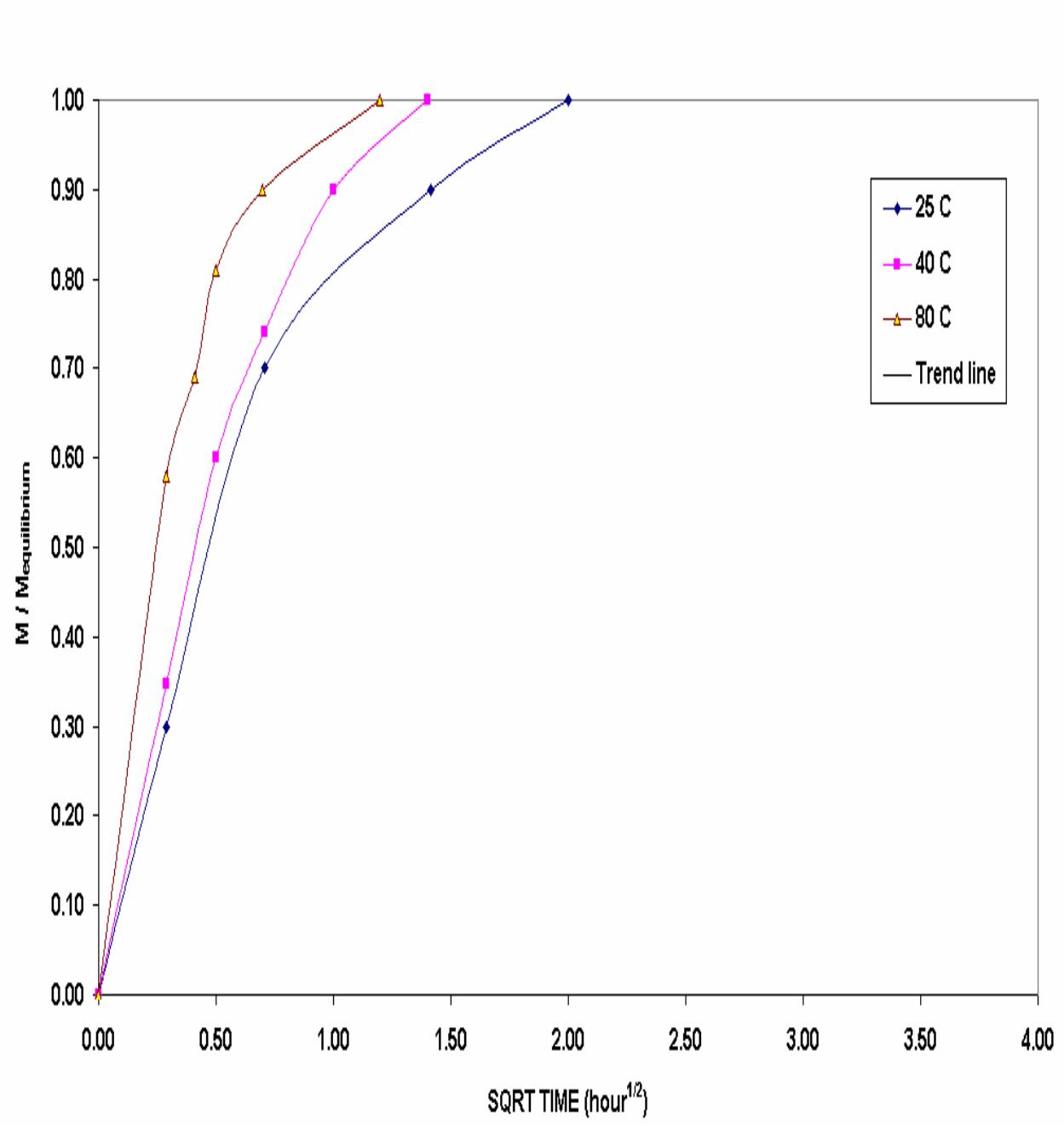

Figure 5.22: Uptake Curve for Phosphate with 3 gram AA400G 14x28 Mesh, no pH Control and Initial Concentration of 10 mg/L.

Odegaard, 1986) for this system at 25 °C is also shown in the Figure. The calculated diffusivity coefficients were found to be 28 times faster than the value reported by the literature. Different conditions and experiment setups were used for getting both values of diffusivity coefficients. Breakthrough process experiments and controlled pH condition were used to get the literature value while batch system experiments and no pH control were used in this study for finding the diffusivity coefficient. However, inspection of Brattebo and Odegaard's paper reveals that they used the long time fit to their data. Their initial data does not fit indicating that the D_s they used appears too low to fit their data in this region.

The effective pore diffusivity coefficient ($D_{eff,pore}$) is also calculated by the following equation:

$$D_{eff,pore} = \frac{D_M \varepsilon}{\tau} \tag{5.22}$$

where D_M is the molecular diffusivity of PO_4^{3-} ion in water, ε is the pore void fraction (ε = 4) and τ is the tortuosity factor (taken as τ = 5). Figure 5.23 shows the effective pore diffusivities are not equal to the surface diffusivities meaning that the pore diffusion model (PDM) can't be used alone for modeling this system. In a recent paper by (Yoshida and Galinada, 2000), parallel effect of both the pore and surface diffusion models were used for modeling an infinite volume system where the diffusivity coefficients were assumed constant and concentration independent; and the difference resulted from non-linearity of the isotherm used in the model. Figures 5.24 and 5.25 show the fit of numerically exact solution to the batch kinetic data.

Table 5.8: Diffusivity Coefficients of 10 mg/L Phosphate Solution on 3 gram of Adsorbent Evaluated by the HSDM Model under Different Temperatures and no pH Control.

Run No.	Adsorbent	Temperature (°C)	Diffusion Coefficient, D_s (cm^2/sec)
6	AA400G (28x48 Mesh)	25	7.00E-09
12		40	2.24E-08
13		80	3.84E-08
10	AA400G (14x28 Mesh)	25	6.92E-09
15		40	2.22E-08
14		80	3.72E-08

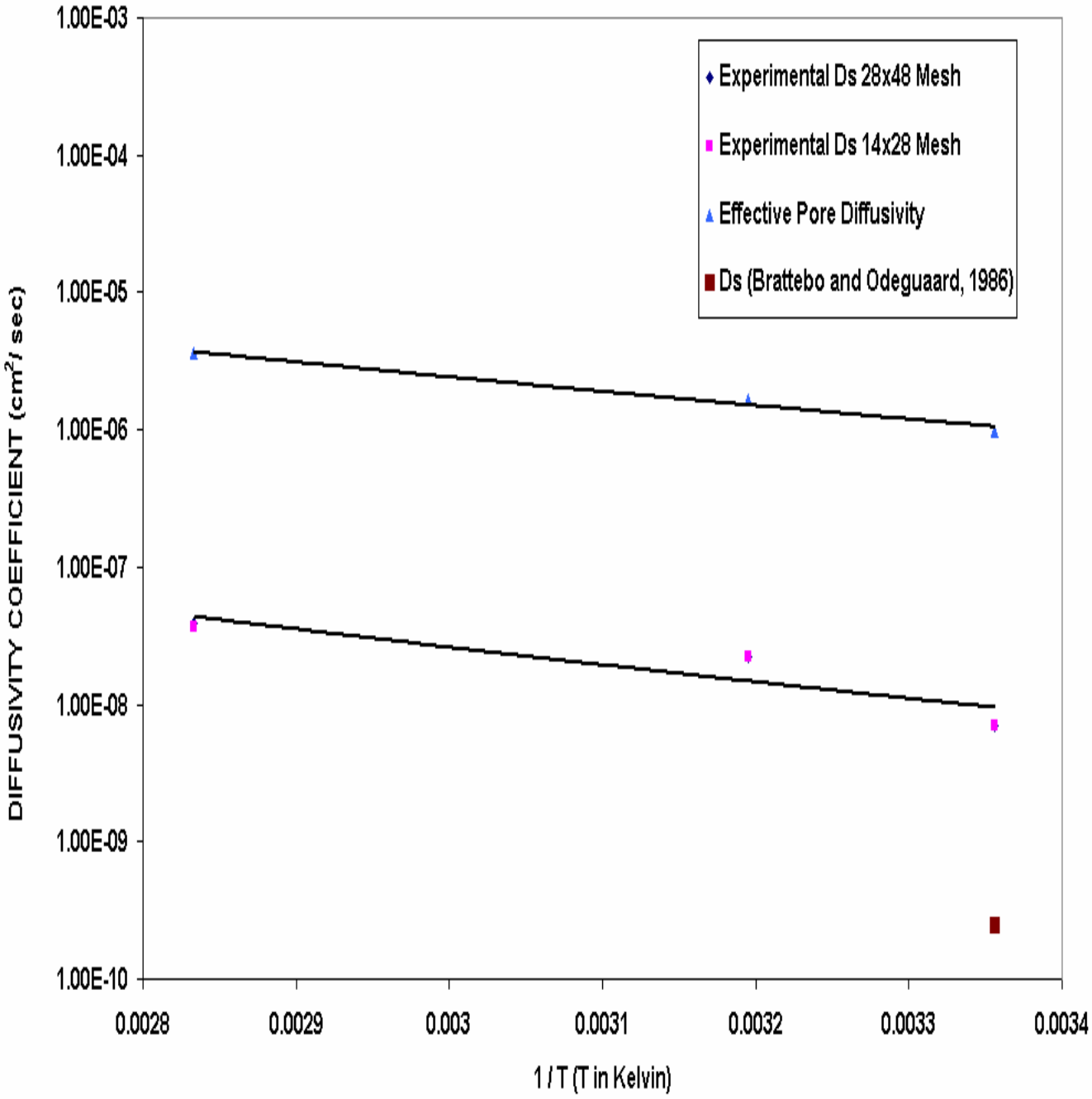

Figure 5.23: Relationship Between Diffusivities and the Temperature for AA400G with Initial Concentration of 10 mg/L along with Line of Best Fit.

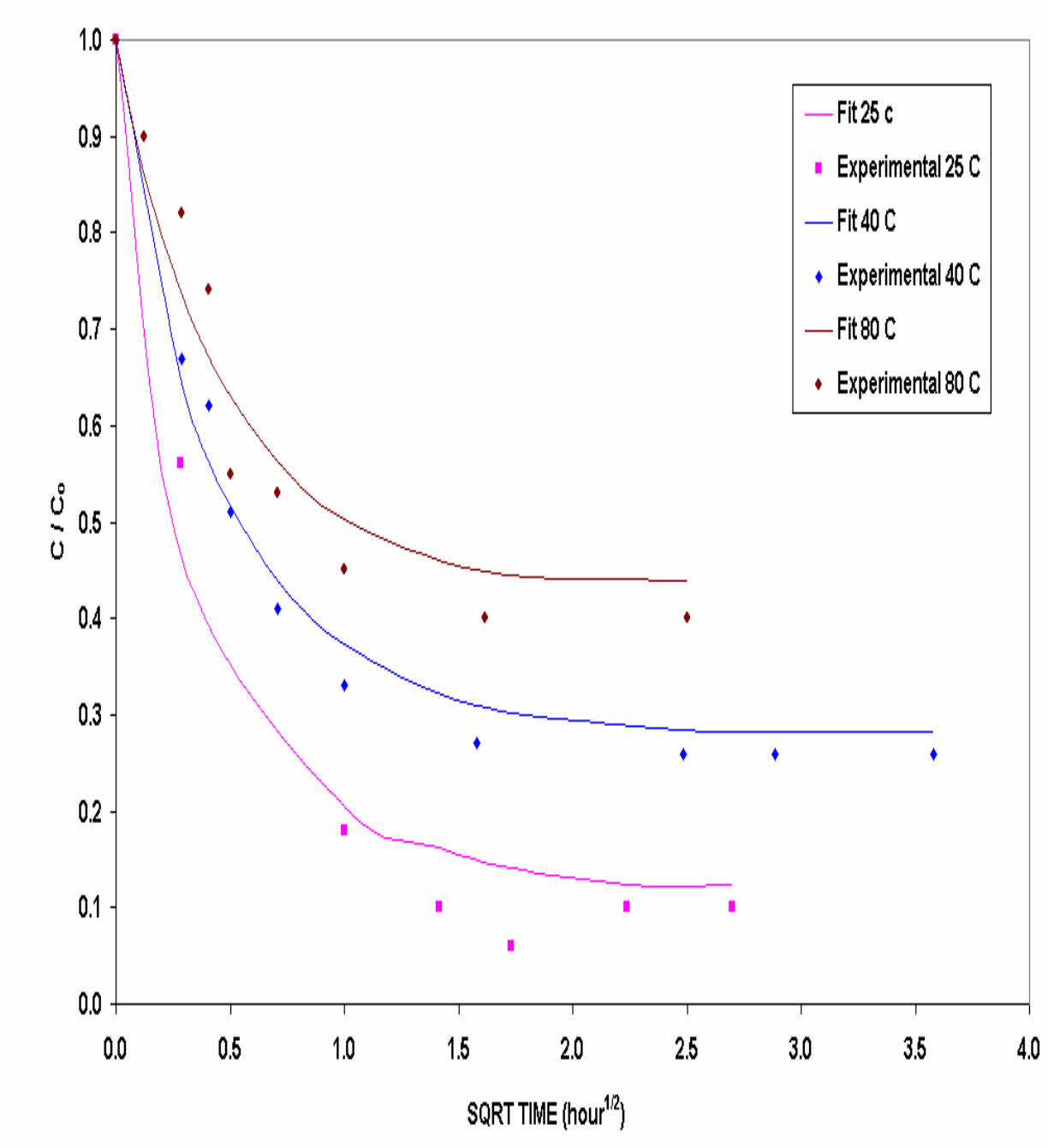

Figure 5.24: Batch Kinetic Experiment for 10 mg/L Phosphate by 3 gram AA400G 28x48 Mesh at Different Temperatures and no pH Control along with HSDM Predictions [D_s= 7.00E-09, 2.24E-08 and 3.84E-08 cm^2/sec & k_f = 4.85E-03, 7.96E-03 and 1.58E-02 cm/sec for 25, 40 and 80 °C respectively].

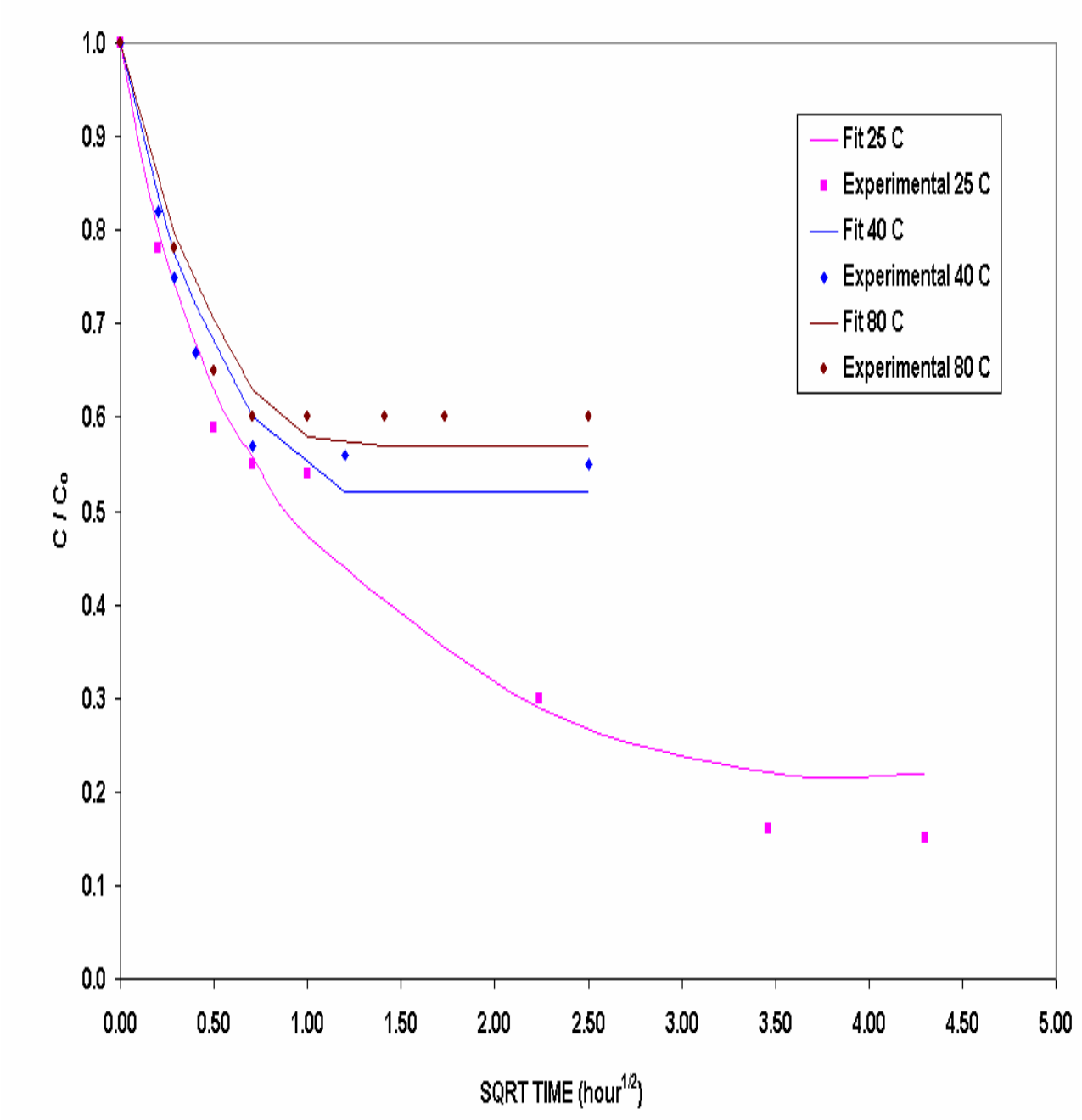

Figure 5.25: Batch Kinetic Experiment for 10 mg/L Phosphate by 3 gram AA400G 14x28 Mesh at Different Temperatures and no pH Control along with HSDM Predictions Predications [D_s= 6.92E-09, 2.22E-08 and 3.72E-08 cm^2/sec & k_f = 3.62E-03, 5.94E-03 and 1.18E-02 cm/sec for 25, 40 and 80 °C respectively].

Equilibrium Composition of kinetics Runs

The equilibrium compositions for kinetics runs were calculated from the material balance equation expressed as:

$$q = V(C_o - C_e)/W \qquad (5.23)$$

where q is the equilibrium composition (mg PO_4^{3-}/g AA400G), V is the volume of the solution (3 liters for all runs), W is the alumina adsorbent weight (gram); and C_o and C_e are the initial and final equilibrium solution concentrations (mg P/L) respectively.

The values of the equilibrium compositions found from the kinetic runs as well as isotherm runs (chapter 4) are given in Table 5.9. As it can be seen from the Table that the equilibrium compositions found from isotherms were higher than those found from kinetics. It was observed that the equilibrium composition decreased as the equilibrium concentration increased for runs 3 and 4 that would be due to the significant effect of controlled pH condition of the these kinetics runs. For the runs with no pH control at 25 ˚C [runs 5 and 11] the equilibrium composition increased with increasing the equilibrium concentration as is expected. That agrees with the relation resulting from the isotherms qualitatively not quantitatively. Runs 3 and 7 show that the equilibrium composition is inversely proportional to the equilibrium concentration. Also, runs 2 and 5 give same finding. The reason of this finding that the runs 2 and 3 were at controlled pH of 4.5 whereas runs 5 and 7 were with no pH control. Figure 5.26 indicates the equilibrium composition versus the equilibrium concentration for runs [5 to 11] of kinetics and isotherms. It is found that the equilibrium composition found from isotherms are higher than those found from kinetics. The reason might be due to different the final pH of the solution as shown in the Table 5.9. The other reason is due to the difference in normality

Table 5.9: Equilibrium Compositions for Kinetics Runs.

Run No.	Equilibrium Concentration (C_e) (mg P/L)	Equilibrium Composition (q) (mg PO_4^{3-} /g adsorbent)		Final pH	
		Kinetics (chapter-5) q= V (C_o-C_e)/W	Equilibrium (chapter 4) q =k $C_e^{1/n*}$	Kinetics (chapter-5)	Equilibrium (chapter 4)
1	1.2	26.4	20	4.5	4.5
2	8.1	17.28	51	4.5	4.5
3	6	18	43.7	4.5	4.5
4	4.6	69.3	38.3	4.5	4.5
5	4.4	50.4	117.62	4.3	4.0
6	1	27	26.34	5.28	6.0
7	4	27	106.83	4.63	4.0
8	4.2	52.2	112.23	4.47	4.1
9	8.4	104.4	226.0	3.60	3.50
10	2.5	22.5	66.46	7.66	4.0
11	3.1	31	82.58	6.97	4.0
12	2.6	22.2	71.84	6.51	5.64
13	4.5	16.2	74.53	4.2	-
14	5.8	12.6	100	6.0	-
15	5.5	13.5	161.6	4.0	-

*Runs 1 to 4 : q =17.85 $C_e^{0.50}$, Runs 5 to 11: q =26.34 $C_e^{1.01}$, Runs 12 &15: q =25.22 $C_e^{1.082}$, Runs 13 &14: q =13.05 $C_e^{1.159}$.

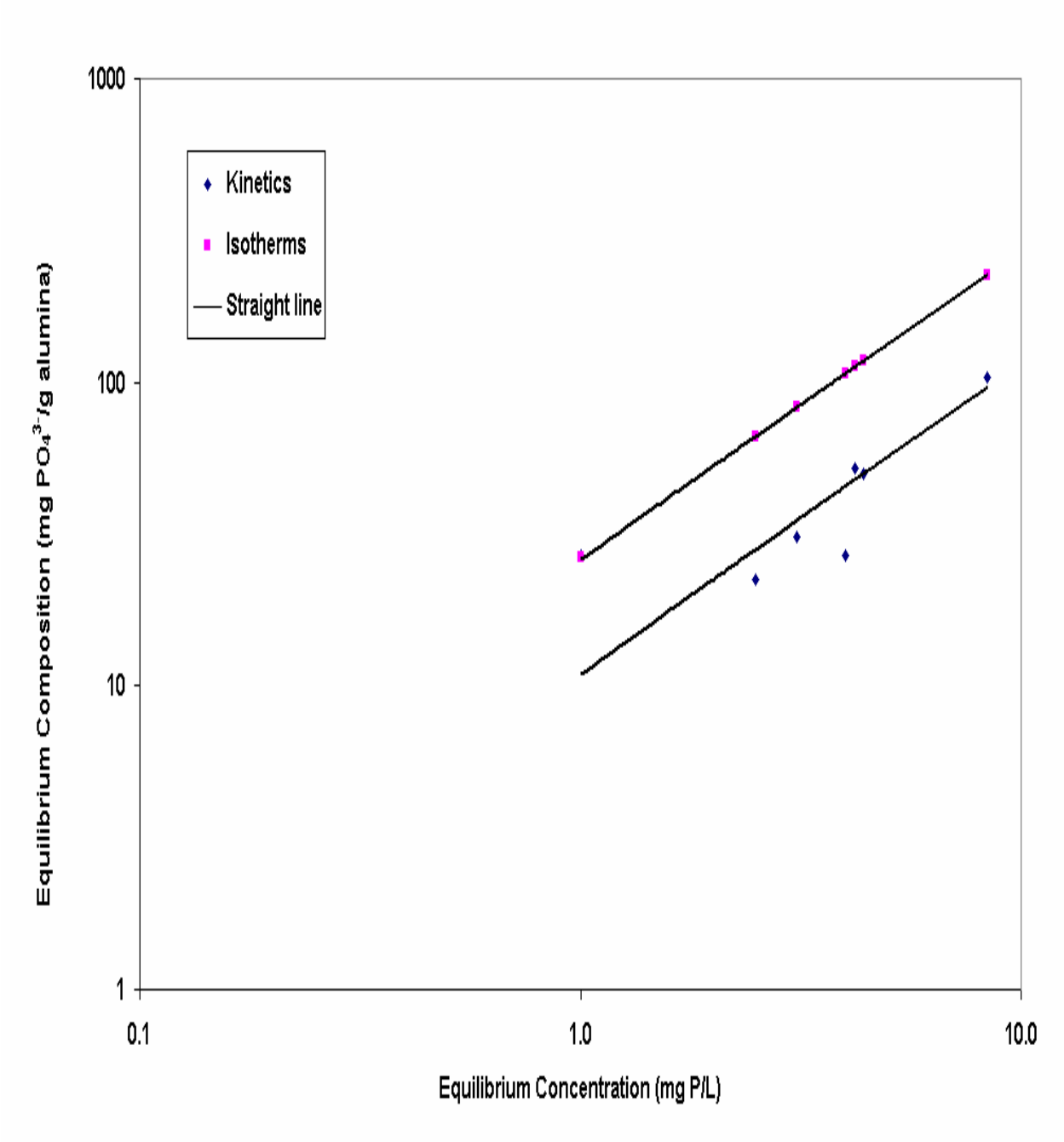

Figure 5.26: Equilibrium Composition for Kinetics and Isotherms

as ion exchangers exhibit an increasing affinity for ions of lower valence s the solution normality increases (Perry and Green, 1997).

CHAPTER SIX

CONCLUSIONS AND RECOMMENDATIONS

6.1 Conclusions

In this work equilibrium isotherms as well as kinetics of phosphate adsorption on Activated Alumina adsorbent/ion exchanger have been studied. The following are the conclusions:

1- The Freundlich isotherm fit the equilibrium isotherm data and the constants k and 1/n for all equilibrium isotherm runs are found from data fitting. Some runs with initial and final pH control may not be at steady state.

2- The adsorption capacity increases with the decrease of temperature as it is expected from Van't Hoff's relation.

3- Maximum equilibrium loading (mg PO_4^{3-}/g sorbent) was found from runs with no pH control at high phosphorous equilibrium concentration.

4- Maximum equilibrium loading at low phosphorous equilibrium concentration was found to occur with initial and final pH control of 6. This is the best pH selection for achieving the objective of reducing the phosphates concentration in the actual contaminated water stream to less than 1 ppm at 80 ºC.

5- Diffusivity coefficients are measured as the average of all ionic species present in the system.

6- The apparatus used in the kinetics set up is shown to be as a differential adsorber column.

7- Homogenous Surface Diffusion Model ‘HSDM” is used to analyze and model the experimental uptake data for all experimental batch kinetic runs. The model equations are solved numerically by orthogonal collocation method.

8- The diffusivity coefficient was found to be effected much by the solution pH and it was concentration independent in case of no pH control condition.

9- The diffusivity coefficient was higher in case of pH control compared to that with no pH control because the addition of buffer solutions 0.1M NaOH and 0.1M H_2SO_4 promoted the diffusion of the phosphate species into the alumina.

10- The external mass transfer coefficient is calculated and included in the modeling of the system.

11- The diffusivity coefficient increases with temperature as it is expected from Arrhenius’s equation.

12- The equilibrium compositions calculated from isotherms were higher than the values found by the kinetics due to the significant effect of normality.

6.2 Recommendations

1- It is recommended to perform the equilibrium studies very carefully by measuring the amount of buffer solutions added to the experiment solutions for controlling the pH.

2- It is recommended to use different lengths of packed beds equivalent to the quantity of alumina adsorbent used in the kinetics experiment.

3- It is recommended to derive a complex model combining both the pore diffusion model (PDM) and the homogeneous surface diffusion model (HSDM) for a finite volume system. An appropriate ion exchange diffusion model should also be derived to explain the diffusion phenomena.

4- It is recommended to perform regeneration studies of the packed column using caustic soda solution. Since the end result has to be a economically viable process and the literature indicates with a degree of certainty about the technical success of the process, the check for equilibrium characteristic after regeneration should be evaluated.

5- It is also recommended to study breakthrough curves for adsorption and desorption to be able to do further analyze for the system.

NOMENCLATURE

A	Total interfacial surface area, (m^2, cm^2)
a	Distance from the center of sphere to its surface (or radius), (m, cm)
a_1	Constant for solute 1
a_2	Constant for solute 2
b_1	Constant for solute 1
b_2	Constant for solute 2
B	Constant expression of the energy of adsorption
C	Equilibrium concentration of a solute in the fluid phase, (mg/m^3 of solution)
C_o	Initial solute concentration in the liquid phase, (mg of solute/m^3 of solution)
C_1	Solute 1 concentration in the fluid phase, , (mg of solute/m^3 of solution)
C_2	Solute 2 concentration in the fluid phase, (mg of solute/m^3 of solution)
C_s	Concentration of a solute at the adsorbent surface and Saturation concentration of solute, (mg of solute/m^3 of solution)
D	Diffusivity from Fick's law, (m^2/s, cm^2/s)
D_{AB}	Molecular diffusivity of solute A in liquid B, (m^2/s, cm^2/s)
D_l	Free liquid diffusivity, (cm^2/s)
$D_{eff,pore}$	Effective pore diffusivity, (cm^2/s)
D_p	Pore diffusion coefficient, (m^2/s, cm^2/s)
D_s	Surface diffusion coefficient, (m^2/s, cm^2/s)
K	Dissociation constant, (dimensionless)
k	Freundlich isotherm constant, ($mg^{1-1/n}\ L^{1/n}$ / g)
k_f	Film mass transfer coefficient, (m/s, cm/s)
n	Freundlich isotherm constant, (dimensionless)
q	Amount of solute adsorbed, (mg of solute/ g of adsorbent)
q_o	Final value of q, (mg of solute/ g of adsorbent)

q_m	Monolayer coverage of adsorbent in Langmuir isotherm, (mg of solute/ g of adsorbent)
R	Particle radius, (m, cm)
Re	Reynolds number, (dimensionless)
S_0	Surface area per unit volume of the adsorbent, (m^2, cm^2)
Sc	Schmidt number, (dimensionless)
Sh	Sherwood number, (dimensionless)
T	Temperature, (K)
t	Time, (hr, sec)
u	Reduced solid phase concentration, (dimensionless)
V	Volume of liquid solution, (m^3, cm^3)
W	Weight of adsorbent, (kg, g)
x	*Dimensionless spatial variable, (dimensionless)*
y	Dimensionless bulk concentration, (dimensionless)
τ	Tortuosity factor, (dimensionless)
θ	Fraction of surface covered, (dimensionless)
λ	Fraction of sorbate ultimately adsorbed by the adsorbent, (dimensionless)
α	Freundlich isotherm constant, (dimensionless)
μ	Viscosity of solution, (cP, kg/m.s)
ρ, ρ_l	Density of water, (cm^3/g , kg/m^3)
ε	Adsorbent bed interparticle void fraction, (dimensionless)
ε_p	Particle porosity, (dimensionless)
γ	Separation factor, (dimensionless)
ψ	Film diffusion time/surface diffusion time, (dimensionless)
ν	Superficial velocity, (cm/s, m/s)

REFERENCES

Ames, L. I. and R. B. Dean, "Phosphorous Removal from Effluents in Alumina Columns," J. Wat. Poll. Control Fed., **42(R)**, 161-172, 1970.

Annual Book of ASTM Standards, "Standard Test Methods for Phosphorous in Water", ASTM D 515-88, 11.01, 551-558, 1992.

Azizan, F., "Water Treatment Technology: Part I Chromium & Phosphate", Alcan Chemicals Limited, England, 1992.

Bhandari, V. M., V. A. Juvekar, and S. R. Patwardhan,, "Ion-exchange Studies in the Removal of Polybasic Acids. Anomalous Sorption Behavior of Phosphoric acid on Weak Base Resins," Sep. Sci. and Tech., **32(15)**, 2481-2496, 1997.

Bhaskar, G. V. and R. S. Bhamidimarri, "Adsorption of 2,4-D onto Activated Carbon: Application of Nth Order Approximation," J. Chem. Tech. Biotechnol., **53**, 297-300, 1992.

Brattebo, H., "Phosphorous Removal from Wastewater by Fixed-bed Adsorption on Granular Activated Alumina", Ph.D. Thesis, University of Trondheim, 1983.

Brattebo, H., and H. Odegaard, "Phosphorus Removal by Granular Activated Alumina", Wat. Res., **20(8)**, 977-986, 1986.

Brunauer, S., P. H. Emmett, and E. Teller, "Adsorption of Gases in Multimolecular Layers," J. Am. Chem. Soc., **60**, 309-319, 1938.

Butler, J. A. and C. Ockrent, "Studies in Electrocapillarity III," J. Phys. Chem., **34**, 2841, 1930.

Crittenden, J. C. and W. J. Weber, Jr., "Predictive Model for Design of Fixed-bed Adsorbers; Parameter Estimation and Model Development," J. Environ. Eng. Div., ASCE, **185**, 45-46, 1978.

Cooney, D. O., "Adsorption Design for Wastewater Treatment", Lewis Publishers, New York, 1999.

De Renzo, D. J., "Pollution Control Technology for Industrial Wastewater", Pollution Technology Review No. 80, Noyes Data Corporation, New Jersey, 1981.

Fatehi, A. I., "Study of Equilibrium Adsorption of Orthophosphate on Alumina Adsorbents", Research Proposal submitted to College of Graduate Studies of KFUPM, Dhaharn, 2000.

Fleming, H. L., "Application of Aluminas in Water Treatment", Environ. Prog., **5(3)**, 159-166, 1986.

Fleming, H. L., "Water Treatment Product and Processes", Alumina Chemicals, Science and Technology Handbook, Edited by D. Hart, Alcoa Canada, 1990.

Freundlich, H., Colloid and Capillary Chemistry, Matheun and Co. Ltd, London, 883, 1926.

Hayduk, W. and H. Laudie, "Prediction of Diffusion Coefficients for Non-electrolytes in Dilute Aqueous Solutions", AIChE J., **28**, 611, 1974.

Jain, J. S., and V. L. Snoeyink, "Adsorption from Bisolute Systems on Active Carbon," J. Wat. Poll. Control Fed., **45**, 2463, 1973.

Laidler, K. J. and J. H. Meiser, "Physical Chemistry", 2nd Ed., Houghton Mifflin Co., Boston, 300-301, 1995.

Langmuir, I. J., "The Adsorption of Gases on Plane Surfaces of Glass Mica, and Platinum," J. Am. Chem. Soc., **40**, 1361-1403, 1918.

Lewis, J. M. and R. A. Kydd, "Adsorption Mechanism of Phosphoric Acid on γ-alumina," J. Catal., **132(2)**, 465-471, 1991.

Narkis, N. and M. Mordehai, "Phosphorus removal by Activated Alumina", Environ. Poll., **2(B)**, 327-343, 1986.

Perry, J. H and D. W. Green, "Chemical Engineers' Handbook", 7th Ed., McGraw-Hill, New York, p.16-20, 1997.

Radke, C. J. and J. M. Prausnitz, "Adsorption of Organic Solutes from Dilute Aqueous Solution on Activated Carbon", Ind. Eng. Chem. Res., **11**, 445-446, 1972.

Reinbold, K. A., J. J. Hassett, J. C. Means, and W. L. Banwart, Adsorption of Energy-Related Organic Pollutants: A literature Review, EPA-600/3-79-086, 170, 1979.

Ronald D. N. and G. Thodos, "Removal of Orthophosphates from Aqueous Solutions with Activated Aluimna", Environ. Sci. Tech., **3(7)**, 661-667, 1969.

Ruthven, D. M., "Principles of Adsorption and Adsorption Processes", John Wily & Sons, New York, 1984.

SADAF Process Department, Personal communication, 2000.

Slejko, F. L., "Adsorption Technology: A step-by-step Approach to Process Evaluation and Application", Chemical Industries, Marcel Dekker, New York, **19**, 1985.

Urano, K. and H. Tachikawa, "Process Development for Removal and Recovery of Phosphorus from Wastewater by a New Adsorbent. 1. Preparation Method and Adsorption Capability of a New Adsorbent", Ind. Eng. Chem. Res., **30**, 1893-1896, 1991.

Wakao, N. and T. Funzkri, "Effect of Fluid Dispersion Coefficients in Dilute Solutions", Chem. Eng. Sci., **33**, 1375, 1978.

Weber W. J., Jr., and K. T. Liu, "Determination of Mass Transport Parameters for Fixed-bed Adsorbers", Chem. Eng. Comm., **6**, 49, 1980.

Weber, W. J., Jr., "Physicochemical Processes for Water Quality Control", Wiley-Interscience, New York, 640, 1972.

Williamson, J. E., K. E. Bazaire, and C. J. Geankoplis, "Liquid Phase Mass Transfer at Low Reynolds Numbers", Ind. Eng. Chem. Fund., **2**, 126-127, 1963.

Wojciechowski, B. W. and N. M. Rice, "Experimental Methods in Kinetics Studies", Elsevier Science, Amsterdam, 2003.

Yee, C. W., "Selective Removal of Mixed Phosphates by Activated Alumina,' J. Am. Wat. Works Assoc., **58**, 239-247, 1966.

Yoshida, H. and W. A. Galinada, "Intraparticle Diffusion of H_3PO_4, NaH_2PO_4, Na_2HPO_4, and Na_3PO_4 in OH-Type Strongly Basic Ion Exchanger", AIChE J., 698-702, 2000.

APPENDICES

APPENDIX A

Preparation of Experiment Solutions & the Calibration Curves

Preparation of the Stock Solution

Original solution: 0.00146 M Ortho phosphoric acid (H_3PO_4) [Purity = 85 % by weight, MW = 98 g/mol, Specific gravity = 1.69)

Mass of 1 ml of pure Orthophosphoric acid solution = 1.6934 gram * 0.85
= 1.43939 g

Mass of Total Phosphorous (P) = 1.43939 (31/98)
= 0.45532 g

Concentration of the stock solution = 455.32 mg Phosphorous/L solution

Molarity of the 455.32 mg P/L solution is 0.0046 M

Preparation of the Model Solution

Original solution: 0.0046 M Stock solution

The quantity (V) taken for preparing the model solution of 10 mg P/L into 2000 ml Erlenmeyer flask is calculated as follows:

V (ml) * (455.32mg P/L) = (2000 ml) * (10 mg P/L)

V = 44 ml

Molarity of the 10 mg P/L solution is 0.0001 M

Preparation of the Calibration Curves

- Preparation of the solution 0.2 mg P/L used for calibration curve data

Original solution: 0.0046 M Stock solution

The quantity (V) taken for preparing the model solution of 0.2 mg P/L into 2000 ml Erlenmeyer flask is calculated as follows:

$$V\ (ml) * (455.32 mg\ P/L) = (2000\ ml) * (0.2\ mg\ P/L)$$

$$V = 0.9\ ml$$

Molarity of the 0.2 mg P/L solution is 0.000002 M

- Calibration Curve Data

Phosphorous Concentration (mg P/L)	Transmittance (%)
0.00	100
0.040	92.2
0.082	83.3
0.143	79.1
0.016	76.1
0.20	71.0

A typical calibration curve is plotted on a linear graph paper as the concentration of phosphorus versus the percentage transmittance. The line fit equation resulted as:

% Transmittance = -150.37 * Phosphorous Concentration + 100

APPENDIX B

I) pH Adjustment Readings for Equilibrium Isotherms

General

* pH of initial 10 mg/L orthophosphate solution before contacting with activated alumina = 4.89 for all runs.

* Buffer solutions of 0.1 M NaOH and H_2SO_4 respectively are used to control the desired pH.

* pH before refers to the pH reading of the mixture of alumina and orthophosphate solution before adjustment by addition of buffer solutions. This was taken immediately after contacting the solution to the adsorbent. This is not at equilibrium.

* pH after refers to the pH reading of the mixture of alumina and orthophosphate solution after adjustment by addition of buffer solutions. This is not at equilibrium.

* Final pH refers to the pH reading after equilibrium condition.

* Initial pH control refers to the initial pH control upon mixing the sample solution with the activated alumina adsorbent. This is not at equilibrium.

* Final pH control refers to the final pH control of the solution one hour prior the sample analysis. This is not at complete equilibrium.

* No pH control refers to no addition of buffer solutions to the experiment solution.

* The amount of solute remaining in the solution after equilibrium is expressed as total phosphorous (P) even though it is composed of various ions of orthophosphoric acid.

* The amount adsorbed on the adsorbent after equilibrium (loading) is expressed as (mg of Total Phosphorous (P) adsorbed/g of Adsorbent). Since the actual adsorbed solute to the adsorbent is the orthophospahte ions PO_4^{3-} the loading can be converted to (mg PO_4^{3-}/g of activated alumina adsorbent) by multiplying ratio (MW of PO_4^{3-} = 95 / MW of P = 31).

Run no. 1

Type of experiment: isotherm

Adsorbent: AA400G (28x48 Mesh)

Initial concentration: 10 mg P/L

pH (control) = 4.5

Temperature: 25°C

Date started: 2/05/2002

Date ended: 4/05/2002

Time = 0 hr

Weight of Adsorbent (gram)	Quantity of Solution (ml)	pH before	pH after
0.05	100	3.66	4.69
0.10	100	3.71	4.70
0.50	100	4.01	4.30
1.00	100	6.10	4.50
0.05	200	3.61	4.47
0.10	200	3.66	4.46

Time = 3 hr

Weight of Adsorbent (gram)	Quantity of Solution (ml)	pH before	pH after
0.05	100	5.40	4.56
0.10	100	6.01	4.45
0.50	100	5.78	4.33
1.00	100	7.07	4.43
0.05	200	4.61	x
0.10	200	5.08	4.41

Time = 5 hr

Weight of Adsorbent (gram)	Quantity of Solution (ml)	pH before	pH after
0.05	100	4.72	x
0.10	100	4.56	x
0.50	100	5.30	4.42
1.00	100	5.60	4.61
0.05	200	4.69	x
0.10	200	4.52	x

Time = 6 hr

Weight of Adsorbent (gram)	Quantity of Solution (ml)	pH before	pH after
0.05	100	4.82	4.40
0.10	100	4.89	4.30
0.50	100	5.13	4.78
1.00	100	5.80	4.70
0.05	200	4.79	4.51
0.10	200	4.64	x

Time = 7 hr

Weight of Adsorbent (gram)	Quantity of Solution (ml)	pH before	pH after
0.05	100	4.54	x
0.10	100	4.54	x
0.50	100	5.47	4.45
1.00	100	5.72	4.48
0.05	200	4.59	x
0.10	200	4.77	4.38

Time = 28 hr

Weight of Adsorbent (gram)	Quantity of Solution (ml)	pH before	pH after
0.05	100	4.35	x
0.10	100	5.87	4.47
0.50	100	5.74	4.49
1.00	100	6.24	4.50
0.05	200	4.59	x
0.10	200	4.60	x

Time = 29 hr

Weight of Adsorbent (gram)	Quantity of Solution (ml)	pH before	pH after
0.05	100	5.88	4.22
0.10	100	6.04	4.45
0.50	100	6.74	4.42
1.00	100	6.92	4.38
0.05	200	4.57	x
0.10	200	5.52	4.33

Time = 45 hr

Weight of Adsorbent (gram)	Quantity of Solution (ml)	Final pH
0.05	100	4.47
0.10	100	4.86
0.50	100	5.51
1.00	100	5.72
0.05	200	4.67
0.10	200	4.49

Run no. 2

Type of experiment: isotherm

Adsorbent: AA400G (28x48 Mesh)

Initial concentration: 10 mg P/L

pH (control) = 6.0

Temperature: 25°C

Date started: 5/05/2002

Date ended: 7/05/2002

Time = 0 hr

Weight of Adsorbent (gram)	Quantity of Solution (ml)	pH before	pH after
0.05	100	3.65	6.11
0.10	100	3.71	5.83
0.50	100	4.23	6.23
1.00	100	5.98	x
0.05	200	3.67	6.14

Time = 3 hr

Weight of Adsorbent (gram)	Quantity of Solution (ml)	pH before	pH after
0.05	100	6.22	x
0.10	100	6.17	x
0.50	100	7.12	5.83
1.00	100	7.50	6.20
0.05	200	6.27	x

Time = 4 hr

Weight of Adsorbent (gram)	Quantity of Solution (ml)	pH before	pH after
0.05	100	6.38	6.05
0.10	100	6.30	x
0.50	100	6.42	6.10
1.00	100	7.24	5.87
0.05	200	6.27	6.20

Time = 9 hr

Weight of Adsorbent (gram)	Quantity of Solution (ml)	pH before	pH after
0.05	100	6.65	5.89
0.10	100	6.52	5.83
0.50	100	6.44	5.82
1.00	100	6.61	5.72
0.05	100	6.19	x

Time = 18 hr

Weight of Adsorbent (gram)	Quantity of Solution (ml)	pH before	pH after
0.05	100	6.30	x
0.10	100	6.32	x
0.50	100	6.68	6.14
1.00	100	6.95	6.18
0.05	200	6.37	x

Time = 28 hr

Weight of Adsorbent (gram)	Quantity of Solution (ml)	pH before	pH after
0.05	100	6.40	6.01
0.10	100	6.60	6.10
0.50	100	6.65	6.24
1.00	100	6.95	5.70
0.05	200	6.37	6.25

Time = 48 hr

Weight of Adsorbent (gram)	Quantity of Solution (ml)	pH before	pH after
0.05	100	6.50	6.35
0.10	100	6.52	6.19
0.50	100	6.80	6.40
1.00	100	7.10	6.40
0.05	200	6.33	x

Time = 49 hr

Weight of Adsorbent (gram)	Quantity of Solution (ml)	Final pH
0.05	100	6.60
0.10	100	6.32
0.50	100	6.60
1.00	100	6.71
0.05	200	6.38

Run no. 3

Type of experiment: isotherm

Adsorbent: AA400G (14x28 Mesh)

Initial concentration: 10 mg P/L

pH (control) = 4.5

Temperature: 25°C

Date started: 8/05/2002

Date ended: 10/05/2002

Time = 0 hr

Weight of Adsorbent (gram)	Quantity of Solution (ml)	pH before	pH after
0.05	100	3.65	4.53
0.10	100	3.81	4.67
0.50	100	5.60	4.88
1.00	100	6.72	4.80
0.05	200	3.71	4.24

Time = 2 hr

Weight of Adsorbent (gram)	Quantity of Solution (ml)	pH before	pH after
0.05	100	5.55	4.25
0.10	100	6.03	4.42
0.50	100	6.58	4.57
1.00	100	6.85	4.97
0.05	200	4.50	x

Time = 5 hr

Weight of Adsorbent (gram)	Quantity of Solution (ml)	pH before	pH after
0.05	100	4.52	x
0.10	100	5.04	4.50
0.50	100	5.91	4.58
1.00	100	6.15	4.54
0.05	200	4.61	x

Time = 12 hr

Weight of Adsorbent (gram)	Quantity of Solution (ml)	pH before	pH after
0.05	100	5.40	4.21
0.10	100	5.72	4.57
0.50	100	6.15	4.43
1.00	100	6.60	4.88
0.05	200	5.03	4.36

Time = 21 hr

Weight of Adsorbent (gram)	Quantity of Solution (ml)	pH before	pH after
0.05	100	4.74	x
0.10	100	5.74	4.86
0.50	100	6.39	4.80
1.00	100	6.72	4.49
0.05	200	4.67	x

Time = 23 hr

Weight of Adsorbent (gram)	Quantity of Solution (ml)	pH before	pH after
0.05	100	4.85	x
0.10	100	5.30	4.20
0.50	100	5.73	4.18
1.00	100	5.94	4.40
0.05	200	4.72	x

Time = 25 hr

Weight of Adsorbent (gram)	Quantity of Solution (ml)	pH before	pH after
0.05	100	5.05	4.30
0.10	100	4.62	x
0.50	100	5.22	4.33
1.00	100	5.66	4.45
0.05	200	4.84	x

Time = 45 hr

Weight of Adsorbent (gram)	Quantity of Solution (ml)	pH before	pH after
0.05	100	5.17	4.20
0.10	100	5.75	4.48
0.50	100	6.45	4.33
1.00	100	6.85	4.22
0.05	200	5.48	4.80

Time = 47 hr

Weight of Adsorbent (gram)	Quantity of Solution (ml)	Final pH
0.05	100	4.34
0.10	100	4.87
0.50	100	5.21
1.00	100	5.64
0.05	200	4.92

Run no. 4

Type of experiment: isotherm

Adsorbent: AA400G (14x28 Mesh)

Initial concentration: 10 mg P/L

pH (control) = 6.0

Temperature: 25°C

Date started: 11/05/2002

Date ended: 13/05/2002

Time = 0 hr

Weight of Adsorbent (gram)	Quantity of Solution (ml)	pH before	pH after
0.05	100	3.73	6.13
0.10	100	3.82	6.19
0.50	100	5.82	x
1.00	100	6.50	6.23
0.05	200	3.70	5.86

Time = 3 hr

Weight of Adsorbent (gram)	Quantity of Solution (ml)	pH before	pH after
0.05	100	6.25	x
0.10	100	6.40	6.25
0.50	100	7.20	6.30
1.00	100	7.82	5.90
0.05	200	6.09	x

Time = 4 hr

Weight of Adsorbent (gram)	Quantity of Solution (ml)	pH before	pH after
0.05	100	6.50	6.20
0.10	100	6.57	5.88
0.50	100	7.00	6.08
1.00	100	6.64	5.80
0.05	200	6.44	5.80

Time = 9 hr

Weight of Adsorbent (gram)	Quantity of Solution (ml)	pH before	pH after
0.05	100	6.30	x
0.10	100	6.39	x
0.50	100	6.60	5.85
1.00	100	6.16	x
0.05	200	5.94	x

Time = 18 hr

Weight of Adsorbent (gram)	Quantity of Solution (ml)	pH before	pH after
0.05	100	6.50	x
0.10	100	6.51	4.86
0.50	100	6.65	4.80
1.00	100	6.88	4.49
0.05	200	6.08	x

Time = 28 hr

Weight of Adsorbent (gram)	Quantity of Solution (ml)	pH before	pH after
0.05	100	6.06	x
0.10	100	6.26	x
0.50	100	7.20	5.86
1.00	100	6.80	6.37
0.05	200	6.30	x

Time = 48 hr

Weight of Adsorbent (gram)	Quantity of Solution (ml)	pH before	pH after
0.05	100	6.30	x
0.10	100	6.60	6.30
0.50	100	6.75	6.25
1.00	100	7.05	6.30
0.05	200	6.41	x

Time = 49 hr

Weight of Adsorbent (gram)	Quantity of Solution (ml)	Final pH
0.05	100	6.40
0.10	100	6.42
0.50	100	6.48
1.00	100	6.50
0.05	200	6.42

Run no. 5

Type of experiment: isotherm

Adsorbent: AA400G (28x48 Mesh)

Initial concentration: 10 mg P/L

pH (initial & final control) = 4.5

Temperature: 80 ºC

Date started: 10/05/2003

Date ended: 15/05/2003

Time = 0 hr (initial control)

Weight of Adsorbent (gram)	Quantity of Solution (ml)	pH before	pH after
0.05	100	3.74	4.20
0.10	100	3.75	4.10
0.50	100	4.10	x
1.00	100	4.38	x
0.10	200	3.77	4.23

Time = 120 hr (final control)

Weight of Adsorbent (gram)	Quantity of Solution (ml)	pH before	pH after
0.05	100	6.93	4.51
0.10	100	7.60	4.59
0.50	100	8.79	4.49
1.00	100	9.40	4.53
0.10	200	6.99	4.49

Run no. 6

Type of experiment: isotherm

Adsorbent: AA400G (28x48 Mesh)

Initial concentration: 10 mg P/L

pH (initial & final control) = 4.5

Temperature: 40 ºC

Date started: 10/05/2003

Date ended: 15/05/2003

Time = 0 hr initial control)

Weight of Adsorbent (gram)	Quantity of Solution (ml)	pH before	pH after
0.05	100	3.82	4.53
0.10	100	3.77	4.30
0.50	100	4.20	x
1.00	100	4.43	x
0.10	200	3.70	4.60

Time = 120 hr (final control)

Weight of Adsorbent (gram)	Quantity of Solution (ml)	pH before	pH after
0.05	100	6.89	4.57
0.10	100	7.39	4.44
0.50	100	8.20	4.30
1.00	100	9.05	4.47
0.10	200	6.90	4.31

Run no. 7

Type of experiment: isotherm

Adsorbent: AA400G (28x48 Mesh)

Initial concentration: 10 mg P/L

pH (initial & final control) = 4.5

Temperature: 25°C

Date started: 18/05/2003

Date ended: 23/05/2003

Time = 0 hr (initial control)

Weight of Adsorbent (gram)	Quantity of Solution (ml)	pH before	pH after
0.05	100	3.56	4.56
0.10	100	3.58	4.42
0.50	100	3.72	4.45
1.00	100	3.98	4.52
0.10	200	3.56	4.49

Time = 120 hr (final control)

Weight of Adsorbent (gram)	Quantity of Solution (ml)	pH before	pH after
0.05	100	6.87	4.10
0.10	100	7.40	4.05
0.50	100	8.42	4.37
1.00	100	9.25	4.57
0.10	200	7.01	4.20

Run no. 8

Type of experiment: isotherm

Adsorbent: AA400G (28x48 Mesh)

Initial concentration: 10 mg P/L

pH (initial & final control) = 6.0

Temperature: 80 ºC

Date started: 14/11/2003

Date ended: 19/11/2003

Time = 0 hr (initial control)

Weight of Adsorbent (gram)	Quantity of Solution (ml)	pH before	pH after
0.05	100	4.30	6.03
0.10	100	4.03	5.80
0.50	100	4.22	6.10
1.00	100	5.03	6.15
0.05	200	3.68	5.80

Time = 120 hr (final control)

Weight of Adsorbent (gram)	Quantity of Solution (ml)	pH before	pH after
0.05	100	6.100	x
0.10	100	7.052	6.421
0.50	100	7.577	6.721
1.00	100	8.881	6.910
0.05	200	6.250	x

Run no. 9

Type of experiment: isotherm

Adsorbent: AA400G (28x48 Mesh)

Initial concentration: 10 mg P/L

pH (initial & final control) = 6.0

Temperature: 25°C

Date started: 14/11/2003

Date ended: 1911/2003

Time = 0 hr (initial control)

Weight of Adsorbent (gram)	Quantity of Solution (ml)	pH before	pH after
0.05	100	3.48	6.00
0.10	100	3.50	5.90
0.50	100	4.10	5.20
1.00	100	4.90	6.00
0.05	200	3.44	5.80

Time = 120 hr (final control)

Weight of Adsorbent (gram)	Quantity of Solution (ml)	pH before	pH after
0.05	100	6.301	6.120
0.10	100	6.994	6.325
0.50	100	7.489	6.668
1.00	100	8.541	6.452
0.05	200	6.500	6.101

Run no. 10

Type of experiment: isotherm

Adsorbent: AA400G (28x48 Mesh)

Initial concentration: 10 mg P/L

pH (initial & final control) = 6.0

Temperature: 40ºC

Date started: 18/11/2003

Date ended: 23/11/2003

Time = 0 hr (initial control)

Weight of Adsorbent (gram)	Quantity of Solution (ml)	pH before	pH after
0.05	100	3.32	5.90
0.10	100	3.22	6.20
0.50	100	3.60	6.50
1.00	100	4.50	5.60
0.05	200	3.10	6.00

Time = 120 hr (final control)

Weight of Adsorbent (gram)	Quantity of Solution (ml)	pH before	pH after
0.05	100	6.210	x
0.10	100	6.842	6.225
0.50	100	7.458	6.329
1.00	100	8.642	6.421
0.05	200	6.421	6.145

Run no. 11

Type of experiment: isotherm

Adsorbent: AA400G (28x48 Mesh)

Initial concentration: 10 mg P/L

pH: No Control

Temperature: 25 ºC

Date started: 06/06/2004

Date ended: 11/06/2004

Weight of Adsorbent (gram)	Quantity of Solution (ml)	Final pH
0.05	100	5.78
0.30	100	7.71
0.60	100	8.20
0.90	100	8.68
0.05	200	3.9

Run no. 12

Type of experiment: isotherm

Adsorbent: AA400G (28x48 Mesh)

Initial concentration: 10 mg P/L

pH: No Control

Temperature: 40 ºC

Date started: 24/05/2004

Date ended: 29/05/2004

Weight of Adsorbent (gram)	Quantity of Solution (ml)	Final pH
0.05	100	5.64
0.10	100	6.61
0.50	100	8.00
1.00	100	8.56

Run no. 13

Type of experiment: isotherm

Adsorbent: AA400G (28x48 Mesh)

Initial concentration: 10 mg P/L

pH: No Control

Temperature: 80 ºC

Date started: 06/05/2004

Date ended: 11/05/2004

Weight of Adsorbent (gram)	Quantity of Solution (ml)	Final pH
0.05	100	5.50
0.10	100	7.05
0.50	100	8.86
1.00	100	9.26

II) Experimental Data of Adsorption Isotherms

Run no. 1

Type of experiment: isotherm

Adsorbent: AA400G (28x48 Mesh)

Initial concentration: 10 mg P/L

pH (control) = 4.5

Temperature: 25°C

Date started: 2/05/2002

Date ended: 4/05/2002

Method of analysis: UV spectrophotometer (690 wavelength)

Adsorbent Mass (gram)	Solution quantity (ml)	Trans. %	Conc. (mg P/L)	Adsorption Capacity (mg P/g Adsorbent)
0.05	100	72.0	4.52	10.96
0.10	100	89.3	1.73	8.27
0.50	100	99.3	0.11	1.98
1.00	100	98.5	0.24	0.98
0.05	200	60.1	6.44	14.24
0.10	200	74.1	4.18	11.64

Run no. 2

Type of experiment: isotherm

Adsorbent: AA400G (28x48 Mesh)

Initial concentration: 10 mg P/L

pH (control) = 6.0

Temperature: 25°C

Date started: 5/05/2002

Date ended: 7/05/2002

Method of analysis: UV spectrophotometer (690 wavelength)

Adsorbent Mass (gram)	Solution quantity (ml)	Trans. %	Conc. (mg P/L)	Adsorption Capacity (mg P/g Adsorbent)
0.05	100	71.0	4.68	10.64
0.10	100	85.8	2.29	7.70
0.50	100	97.6	0.38	1.92
1.00	100	96.6	0.54	0.94
0.05	200	57.6	6.94	12.62

Run no. 3

Type of experiment: isotherm

Adsorbent: AA400G (14x28 Mesh)

Initial concentration: 10 mg P/L l

pH (control) = 4.5

Temperature: 25°C

Date started: 8/05/2002

Date ended: 10/05/2002

Method of analysis: UV spectrophotometer (690 wavelength)

Adsorbent Mass (gram)	Solution quantity (ml)	Trans. %	Conc. (mg P/L)	Adsorption Capacity (mg P/g Adsorbent)
0.05	100	64.1	6.90	8.41
0.10	100	81.7	2.95	7.04
0.50	100	99.5	0.08	1.98
1.00	100	99.2	0.12	0.98
0.05	200	43.8	7.26	3.72

Run no. 4

Type of experiment: isotherm

Adsorbent: AA400G (14x28 Mesh)

Initial concentration: 10 mg P/L

pH (control) = 6.0

Temperature: 25°C

Date started: 11/05/2002

Date ended: 13/05/2002

Method of analysis: UV spectrophotometer (690 wavelength)

Adsorbent Mass (gram)	Solution quantity (ml)	Trans. %	Conc. (mg P/L)	Adsorption Capacity (mg P/g Adsorbent)
0.05	100	64.6	5.71	8.57
0.10	100	67.2	5.29	4.70
0.50	100	96.2	0.61	1.88
1.00	100	95.1	0.79	0.92
0.05	200	57.1	6.92	12.30

Run no. 5

Type of experiment: isotherm

Adsorbent: AA400G (28x48 Mesh)

Initial concentration: 10 mg P/L

pH (initial & final control) = 4.5

Temperature: 80 ºC

Date started: 07/06/2004

Date ended: 12/06/2004

Method of analysis: UV spectrophotometer (690 wavelength)

Adsorbent Mass (gram)	Solution quantity (ml)	Trans. %	Conc. (mg P/L)	Adsorption Capacity (mg P/g Adsorbent)
0.05	100	68.9	5.02	9.96
0.20	100	70.2	2.30	3.84
1.00	100	85.1	0.40	0.96
0.05	200	59.0	6.62	13.53

Run no. 6

Type of experiment: isotherm

Adsorbent: AA400G (28x48 Mesh)

Initial concentration: 10 mg P/L

pH (initial & final control) = 4.5

Temperature: 40 ºC

Date started: 07/06/2004

Date ended: 12/06/2004

Method of analysis: UV spectrophotometer (690 wavelength)

Adsorbent Mass (gram)	Solution quantity (ml)	Trans. %	Conc. (mg P/L)	Adsorption Capacity (mg P/g Adsorbent)
0.05	100	70.0	4.84	10.32
0.10	100	80.9	3.08	6.92
0.20	100	93.9	1.24	4.38
0.30	100	74.4	0.68	3.10
0.05	200	59.0	6.61	13.5

Run no. 7

Type of experiment: isotherm

Adsorbent: AA400G (28x48 Mesh)

Initial concentration: 10 mg P/L

pH (initial & final control) = 4.5

Temperature: 25°C

Date started: 01/06/2004

Date ended: 06/06/2004

Method of analysis: UV spectrophotometer (690 wavelength)

Adsorbent Mass (gram)	Solution quantity (ml)	Trans. %	Conc. (mg P/L)	Adsorption Capacity (mg P/g Adsorbent)
0.05	100	71.0	4.68	10.64
0.10	100	83.0	2.74	7.26
0.50	100	85.6	0.14	1.97
0.05	200	65.0	5.64	17.40

Run no. 8

Type of experiment: isotherm

Adsorbent: AA400G (28x48 Mesh)

Initial concentration: 10 mg P/L

pH (initial & final control) = 6.0

Temperature: 80 ºC

Date started: 15/05/2004

Date ended: 20/05/2004

Method of analysis: UV spectrophotometer (690 wavelength)

Adsorbent Mass (gram)	Solution quantity (ml)	Trans. %	Conc. (mg P/L)	Adsorption Capacity (mg P/g Adsorbent)
0.10	100	81.5	2.986	7.014
0.20	100	81.2	0.927	4.536
0.30	100	91.1	0.239	3.254
0.40	100	88.0	0.020	1.996
0.50	100	92.0	0.013	1.427

Run no. 9

Type of experiment: isotherm

Adsorbent: AA400G (28x48 Mesh)

Initial concentration: 10 mg P/L

pH (initial & final control) = 6.0

Temperature: 25°C

Date started: 24/05/2004

Date ended: 29/05/2004

Method of analysis: UV spectrophotometer (690 wavelength)

Adsorbent Mass (gram)	Solution quantity (ml)	Trans. %	Conc. (mg P/L)	Adsorption Capacity (mg P/g Adsorbent)
0.05	100	67.9	5.181	9.638
0.10	100	79.4	3.325	6.675
0.50	100	92.0	0.013	1.997
0.05	200	57.7	6.827	12.691

Run no.10

Type of experiment: isotherm

Adsorbent: AA400G (28x48 Mesh)

Initial concentration: 10 mg P/L

pH (initial & final control) = 6.0

Temperature: 40ºC

Date started: 01/06/2004

Date ended: 06/06/2004

Method of analysis: UV spectrophotometer (690 wavelength)

Adsorbent Mass (gram)	Solution quantity (ml)	Trans. %	Conc. (mg P/L)	Adsorption Capacity (mg P/g Adsorbent)
0.05	100	66.8	5.358	9.285
0.10	100	71.0	4.681	5.319
0.20	100	84.7	0.882	4.408
0.50	100	92.0	0.013	1.997
0.05	200	56.6	7.005	11.98

Run no. 11

Type of experiment: isotherm

Adsorbent: AA400G (28x48 Mesh)

Initial concentration: 10 mg P/L

pH: No Control

Temperature: 25 ºC

Date started: 06/06/2004

Date ended: 11/06/2004

Method of analysis: UV spectrophotometer (690 wavelength)

Adsorbent Mass (gram)	Solution quantity (ml)	Trans. %	Conc. (mg P/L)	Adsorption Capacity (mg P/g Adsorbent)
0.05	100	71.0	2.243	15.51
0.30	100	86.9	0.352	3.261
0.60	100	77.8	0.224	1.629
0.90	100	74.5	0.114	1.098
0.05	200	66.5	2.591	29.64

Run no. 12

Type of experiment: isotherm

Adsorbent: AA400G (28x48 Mesh)

Initial concentration: 10 mg P/L

pH: No Control

Temperature: 40 ºC

Date started: 24/05/2004

Date ended: 29/05/2004

Method of analysis: UV spectrophotometer (690 wavelength)

Adsorbent Mass (gram)	Solution quantity (ml)	Trans. %	Conc. (mg P/L)	Adsorption Capacity (mg P/g Adsorbent)
0.05	100	70.1	2.312	15.38
0.10	100	76.5	1.817	8.183
0.50	100	84.7	0.412	1.918
1.00	100	79.6	0.206	0.979

Run no. 13

Type of experiment: isotherm

Adsorbent: AA400G (28x48 Mesh)

Initial concentration: 10 mg P/L

pH: No Control

Temperature: 80 ºC

Date started: 06/05/2004

Date ended: 11/05/2004

Method of analysis: UV spectrophotometer (690 wavelength)

Adsorbent Mass (gram)	Solution quantity (ml)	Trans. %	Conc. (mg P/L)	Adsorption Capacity (mg P/g Adsorbent)
0.05	100	69.8	2.336	15.32
0.10	100	73.8	2.026	7.97
0.50	100	78.4	0.581	1.88
1.00	100	75.8	0.244	0.98

APPENDIX C

Kinetics Experimental Data

General

* pH control refers to continuous control of the solution pH by addition of droplets of buffer solutions of 0.1 M NaOH or H_2SO_4 respectively as required.

Run no. 1

Date started: 24/04/2003

pH (control) = 4.5

Initial concentration (C_o): 10 mg P/L

Mass of adsorbent: 3 g AA400G (28x48 Mesh)

Volume of solution: 3 L

Temperature: 25 °C

Circulation rate: 300 ml/min (0.812 cm/sec)

Method of analysis: UV spectrophotometer (690 wavelength)

Time (Hour)	Trans. (%)	Conc. (mg P/l)	C/Co
0.000	55.0	10.0	1.00
0.250	56.3	4.89	0.48
0.500	60.9	4.50	0.44
0.750	65.3	4.12	0.40
1.000	64.4	4.20	0.41
1.500	72.8	3.49	0.34
2.833	69.2	1.90	0.18
4.000	68.8	1.92	0.18
4.667	70.4	1.84	0.17
5.000	73.0	1.74	0.16
6.083	73.1	1.73	0.16
6.580	74.4	1.68	0.15
7.000	75.8	1.62	0.15
7.500	77.3	1.56	0.14
11.33	83.0	1.31	0.12
12.00	78.5	1.00	0.08
21.75	85.9	0.79	0.06
22.25	81.3	0.55	0.04

Run no. 2

Date started: 27/04/2003

pH (control) = 4.5

Initial concentration (C_o): 10 mg P/L

Mass of adsorbent: 1 g AA400G (28x48 Mesh)

Volume of solution: 3 L

Temperature: 25 °C

Circulation rate: 300 ml/min (0.812 cm/sec)

Method of analysis: UV spectrophotometer (690 wavelength)

Time (Hour)	Trans. (%)	Conc. (mg P/l)	C/Co
0.000	53.7	10.22	1.00
0.183	54.0	10.16	0.94
0.250	62.4	8.746	0.86
2.920	64.4	8.762	0.86
3.300	64.4	8.406	0.82
22.33	65.2	8.271	0.81

Run no. 3

Date started: 28/04/2003

pH (control) = 4.5

Initial concentration (C_o): 10 mg P/L

Mass of adsorbent: 2 g AA400G (28x48 Mesh)

Volume of solution: 3 L

Temperature: 25 °C

Circulation rate: 300 ml/min (0.812 cm/sec)

Method of analysis: UV spectrophotometer (690 wavelength)

Time (Hour)	Trans. (%)	Conc. (mg P/l)	C/Co
0.000	53.7	10.22	1.00
0.083	65.7	8.186	0.80
0.250	65.3	8.254	0.80
1.000	70.6	7.356	0.72
3.000	72.6	7.016	0.69
5.000	75.7	6.492	0.64
5.720	75.2	6.576	0.64
22.93	83.5	5.169	0.51

Run no. 4

Date started: 29/04/2003

pH (control) = 4.5

Initial concentration (C_o): 20 mg P/L

Mass of adsorbent: 2 g AA400G (28x48 Mesh)

Volume of solution: 3 L

Temperature: 25 °C

Circulation rate: 300 ml/min (0.812 cm/sec)

Method of analysis: UV spectrophotometer (690 wavelength)

Time (Hour)	Trans. (%)	Conc. (mg P/l)	C/Co
0.000	74.0	19.310	1.00
0.083	78.2	13.517	0.70
0.166	78.9	12.552	0.65
0.250	79.9	11.172	0.58
0.500	80.5	10.344	0.54
1.000	82.4	7.7241	0.40
2.500	83.5	6.2068	0.32
3.500	83.8	5.7931	0.30
4.500	84.3	5.1034	0.26
5.300	85.0	4.1379	0.24
6.600	84.9	4.2758	0.23
7.550	84.8	4.4138	0.22
8.250	85.2	3.8620	0.20
15.00	86.0	2.7586	0.10
22.00	86.0	2.7586	0.10

Run no. 5

Date started: 10/05/2003

pH - no control

Initial concentration (C_o): 10 mg P/L

Mass of adsorbent: 1 g AA400G (28x48 Mesh)

Volume of solution: 3 L

Temperature: 25 °C

Circulation rate: 300 ml/min (0.812 cm/sec)

Method of analysis: UV spectrophotometer (690 wavelength)

Time (Hour)	Trans. (%)	Conc. (mg P/l)	C/Co	pH
0.000	51.5	10.155	1.00	3.77
0.083	52.2	9.8837	0.97	3.81
0.166	54.5	8.9922	0.89	3.83
0.250	54.0	9.1860	0.90	3.87
1.000	55.9	8.4496	0.83	3.87
4.500	58.1	7.5968	0.62	3.94
6.660	63.8	5.3876	0.53	4.07
22.83	69.1	3.3333	0.33	4.42
25.70	69.3	3.2558	0.32	4.44
26.33	67.4	3.9922	0.32	4.47

Run no. 6

Date started: 12/05/2003

pH - no control

Initial concentration (C_o): 10 mg P/L

Mass of adsorbent: 3 g AA400G (28x48 Mesh)

Volume of solution: 3 L

Temperature: 25 °C

Circulation rate: 300 ml/min (0.812 cm/sec)

Method of analysis: UV spectrophotometer (690 wavelength)

Time (Hour)	Trans. (%)	Conc. (mg P/l)	C/Co	pH
0.000	51.5	10.000	1.00	3.54
0.083	53.6	4.6899	0.47	3.62
0.516	56.7	4.0697	0.41	3.78
1.000	68.5	1.7829	0.18	4.28
2.000	72.5	1.0078	0.10	5.28
3.000	74.7	0.5814	0.06	5.87
5.000	76.7	0.1938	0.02	6.26
7.000	76.7	0.1938	0.02	6.45
24.00	74.5	0.3100	0.02	6.99

Run no. 7

Date started: 18/05/2003

pH - no control

Initial concentration (C_o): 10 mg P/L

Mass of adsorbent: 2 g AA400G (28x48 Mesh)

Volume of solution: 3 L

Temperature: 25 °C

Circulation rate: 300 ml/min (0.812 cm/sec)

Method of analysis: UV spectrophotometer (690 wavelength)

Time (Hour)	Trans. (%)	Conc. (mg P/l)	C/Co	pH
0.000	67.0	10.638	1.00	3.55
0.300	68.1	10.248	0.96	3.77
0.433	72.8	8.5816	0.81	3.88
0.500	74.9	7.8368	0.74	4.00
1.000	79.2	6.3120	0.59	4.31
2.000	83.5	4.7872	0.45	4.42
3.000	85.4	4.1134	0.42	4.63
4.000	85.1	4.2198	0.40	4.79
5.000	85.1	4.2198	0.40	5.19
6.000	87.1	3.5106	0.33	5.39
7.000	87.0	3.5460	0.33	5.43

Run no. 8

Date started: 19/05/2003

pH - no control

Initial concentration (C_o): 10 mg P/L

Mass of adsorbent: 1 g AA400G 28x48 Mesh

Volume of solution: 3 L

Temperature: 25 °C

Circulation rate: 400 ml/min (1.083 cm/sec)

Method of analysis: UV spectrophotometer (690 wavelength)

Time (Hour)	Trans. (%)	Conc. (mg P/l)	C/Co	pH
0.000	67.0	10.638	1.00	3.45
0.366	73.8	8.2270	0.77	3.74
0.750	77.8	6.8085	0.64	3.97
1.000	81.5	5.4964	0.52	4.04
2.000	85.4	4.1134	0.39	4.47
3.000	86.0	3.9007	0.37	4.80
5.000	86.0	3.9007	0.37	5.30
7.000	87.9	3.2270	0.30	5.60
25.33	89.2	2.7660	0.26	6.52

Run no. 9

Date started: 21/05/2003

pH - no control

Initial concentration (C_o): 20 mg P/L

Mass of adsorbent: 1 g AA400G 28x48 Mesh

Volume of solution: 3 L

Temperature: 25 °C

Circulation rate: 300 ml/min (0.812 cm/sec)

Method of analysis: UV spectrophotometer (690 wavelength)

Time (Hour)	Trans. (%)	Conc. (mg P/l)	C/Co	pH
0.000	78.0	22.33	1.00	3.11
0.250	78.5	21.56	0.97	3.19
1.000	81.7	16.63	0.75	3.27
2.000	83.3	14.17	0.65	3.32
3.000	84.4	12.47	0.57	3.35
4.000	84.5	12.32	0.57	3.38
6.000	84.4	12.47	0.57	3.41
22.50	86.4	9.390	0.44	3.57

Run no. 10

Date started: 04/03/2004

pH - no control

Initial concentration (C_o): 10 mg P/L

Mass of adsorbent: 3 g AA400G 14x28 Mesh

Volume of solution: 3 L

Temperature: 25 °C

Circulation rate: 300 ml/min (0.812 cm/sec)

Method of analysis: UV spectrophotometer (690 wavelength)

Time (Hour)	Trans. (%)	Conc. (mg P/l)	C/Co	pH
0.000	57.8	9.98	1.00	3.57
0.083	65.0	8.03	0.82	3.66
0.166	69.1	6.91	0.69	3.79
0.250	72.8	5.91	0.59	3.94
0.500	71.0	5.91	0.55	4.20
1.000	74.7	5.39	0.54	5.11
2.000	76.6	4.88	0.49	6.21
3.000	77.1	4.74	0.47	6.67
4.000	78.6	4.34	0.43	6.85
5.000	78.8	4.34	0.43	6.85
6.000	81.2	3.63	0.36	7.16
25.83	84.8	2.65	0.27	7.66

Run no. 11

Date started: 03/03/2004

pH - no control

Initial concentration (C_o): 10 mg P/L

Mass of adsorbent: 2 g AA400G 14x28 Mesh

Volume of solution: 3 L

Temperature: 25 °C

Circulation rate: 300 ml/min (0.812 cm/sec)

Method of analysis: UV spectrophotometer (690 wavelength)

Time (Hour)	Trans. (%)	Conc. (mg P/l)	C/Co	pH
0.000	57.8	9.98	1.00	3.89
0.083	67.1	7.46	0.75	3.90
0.166	67.7	7.29	0.73	3.91
0.250	69.2	6.89	0.69	3.92
0.500	69.9	6.70	0.67	4.00
1.000	71.2	6.34	0.63	4.20
2.333	75.6	5.15	0.52	4.75
4.000	77.1	4.74	0.47	5.66
5.000	78.2	4.44	0.44	5.96
5.000	66.9	3.76	0.38	6.14
6.000	83.7	2.95	0.30	6.18
9.166	82.9	3.17	0.32	6.55
19.16	83.0	3.14	0.31	6.96
20.00	82.9	3.17	0.31	6.97

Run no. 12

Date started: 05/03/2004

pH - no control

Initial concentration (C_o): 10 mg P/L

Mass of adsorbent: 3 g AA400G 28x48 Mesh

Volume of solution: 3 L

Temperature: 40 °C

Circulation rate: 300 ml/min (0.812 cm/sec)

Method of analysis: UV spectrophotometer (690 wavelength)

Time (Hour)	Trans. (%)	Conc. (mg P/l)	C/Co	pH
0.000	57.8	9.98	1.00	3.66
0.083	69.8	6.72	0.67	3.85
0.166	71.7	6.21	0.62	3.97
0.250	75.7	5.12	0.51	4.15
0.500	79.5	4.09	0.41	4.67
1.000	82.5	3.28	0.33	5.53
2.500	84.8	2.65	0.27	6.51
6.166	85.0	2.60	0.26	7.01
8.333	87.0	2.06	0.22	7.16
12.83	86.0	2.33	0.21	7.30
21.83	85.0	2.60	0.21	7.48

Run no. 13

Date started: 05/03/2004

pH - no control

Initial concentration (C_o): 10 mg P/L

Mass of adsorbent: 3 g AA400G 28x48 Mesh

Volume of solution: 3 L

Temperature: 80 °C

Circulation rate: 300 ml/min (0.812 cm/sec)

Method of analysis: UV spectrophotometer (690 wavelength)

Time (Hour)	Trans. (%)	Conc. (mg P/l)	C/Co	pH
0.000	57.8	9.98	1.00	3.00
0.083	69.6	6.78	0.82	3.22
0.166	71.8	6.18	0.74	3.76
0.250	77.7	4.58	0.55	4.20
0.500	78.5	4.36	0.53	5.01
1.000	80.7	3.77	0.45	6.12
2.616	79.6	4.06	0.40	6.43

Run no. 14

Date started: 09/03/2004

pH - no control

Initial concentration (C_o) : 10 mg P/L

Mass of adsorbent: 3 g AA400G 14x28 Mesh

Volume of solution: 3 L

Temperature: 80 °C

Circulation rate: 300 ml/min (0.812 cm/sec)

Method of analysis: UV spectrophotometer (690 wavelength)

Time (Hour)	Trans. (%)	Conc. (mg P/l)	C/Co	pH
0.000	57.8	9.98	0.00	3.20
0.083	66.5	7.62	0.99	3.60
0.166	68.0	7.21	0.72	3.92
0.250	72.2	6.07	0.61	4.34
0.500	72.7	5.94	0.59	6.00
1.000	72.7	5.94	0.59	6.66

Run no. 15

Date started: 10/03/2004

pH - no control

Initial concentration (C_o): 10 mg P/L

Mass of adsorbent: 3 g AA400G 14x28 Mesh

Volume of solution: 3 L

Temperature: 40 °C

Circulation rate: 300 ml/min (0.812 cm/sec)

Method of analysis: UV spectrophotometer (690 wavelength)

Time (Hour)	Trans. (%)	Conc. (mg P/l)	C/Co	pH
0.000	61.0	9.11	1.00	3.66
0.083	68.3	7.13	0.65	3.76
0.166	72.5	5.99	0.45	3.80
0.500	75.3	5.23	0.32	4.25
1.000	76.2	4.99	0.28	5.13
2.000	82.0	3.41	0.37	6.22
3.000	82.0	3.41	0.37	6.60
4.000	82.0	3.41	0.37	6.60
5.000	82.0	3.41	0.37	6.79

APPENDIX D

Calculation Procedure for the Model

The following steps summarize the calculation procedure of the model (chapter 5)

1. Calculation of Parameters

With the given values of constants such as velocity, viscosity, density, void ratio, particle size for each run given in Table 5.3 (chapter 5), the following parameters are calculated:

- Molecular diffusivity is calculated by the following equation (Hayduk and Laudie, 1974)

$$D_{AB} = 13.26E\text{-}05\ (\mu_B^{-1.14})\ (V_A^{-0.589})$$

Where μ_B is the solution B (water) viscosity in centipoises at a given temperature and V_A is the molar volume of the solute A (PO_4^{3-}) in cm^3 $g\text{-}mole^{-1}$.

- Mass transfer coefficient is calculated by equation (5.14)
- Fractional uptake (λ) is calculated using the experimental data as follows:

$$\lambda = \frac{C_o - C_\infty}{C_o}$$

where C_o and C_∞ are the initial and the equilibrium concentrations respectively.

- Parameters of the model equations (γ and α) which are calculated as follows:

$$\gamma = (1/\lambda) - 1$$

and α is found from the Freundlich isotherm equations (chapter 4). Table 5.3 gives values of γ and α for each run.

2. The partial differential equations (5.7 and 5.8) with the given initial and boundary conditions equations (5.9-5.11) are solved numerically using orthogonal collocation method.

3. The experimental data is fit using the function called “Lsqcurvefit” that minimizes the sum of the square difference between the theoretical and experimental data (uptake values). Values of D_s are used as initial guess for the fit .

APPENDIX E

Computer Program Used in the Numerical Analysis

```
**************************************************************
C     ** PURPOSE AND COMPUTER PROGRAM NAME:
C
C     **In order to determine the surface diffusion coefficient and fit the
C     experimental data the following programs are used:
C     ** Main program: falqi_main
C     ** Subroutine programs: falqi1, falqi2, falqi3
C
C     ** DESCRIPTION OF PARAMETERS:
C
C     ** u          : Dimensionless solute concentration at the adsorbent particle
C     ** y          : Dimensionless solute concentration at the liquid phase
C     ** param1     : Initial guess value of Ds / R^2
C     ** psi        : Dimensionless variable; ratio of film diffusion to solid
C                     Diffusion
C     ** gamma      : Dimensionless variable; separation factor
C     ** alpha      : Freundlich isotherm constant
C     ** con_data   : Experimental uptake data  (C/Co)
C                                   ** yvec       : Vector representing dimensionless solute
concentration at the
C                     liquid phase
C     ** time_vec   : Vector representing dimensionless time
C     ** time       : Experimental time data
C     ** den        : Density of the solution
C     ** vis        : Viscosity of the solution
C     ** Va         : Molar volume of solute PO4^3-
C     ** Dl         : Molecular diffusivity of solute into the solution
C     ** Ds_R2      : Diffusion time constant Ds / R^2
C     **************************************************************
```

```
C     ***************************************************************
C     **      MAIN PROGRAM: "falqi_main"
C     ***************************************************************
global N A B alpha psi gamma u y
format long

datano=input('Enter run no >>')
alpha=input('Enter alpha >>')
gamma=input('Enter gamma >>')

switch datano
case 1
   load data1.txt
   M=data1;
case 2
   load data2.txt
   M=data2;
case 3
   load data3.txt
   M=data3;
case 4
   load data4.txt
   M=data4;
case 5
   load data5.txt
   M=data5;
case 6
   load data6.txt
   M=data6;
case 7
   load data7.txt
   M=data7;
case 8
   load data8.txt
   M=data8;
case 9
  load data9.txt
   M=data9;
case 10
   load data10.txt
   M=data10;
case 11
   load data11.txt
   M=data11;
case 12
   load data12.txt
```

```
   M=data12;
case 13
   load data13.txt
   M=data13;
case 14
   load data14.txt
   M=data14;
case 15
   load data15.txt
   M=data15;
case 16
   load data16.txt
   M=data16;
end

time=[M(:,1)];
con_data=[M(:,2)];
param1=3.0e-7;
ub=[];
lb=[0];
[param]=lsqcurvefit('falgi1',param1,time,con_data,lb,ub)


global N A B alpha psi gamma u y

[N,X,W,A,B] = abxwSP8;

Ds_R2 = param;

options =
odeset('InitialStep',eps,'RelTol',sqrt(eps),'AbsTol',20*eps)
;

time_vec = Ds_R2.*time*3600;

[t c] = ode15s('falgi2',time_vec,[zeros(1,N) 1],options);

yvec = c(:,end);

dev=(100*abs(con_data-yvec))./con_data;
max_dev=max(dev);
mean_dev=mean(dev);

r_bar=mean(con_data);
R2=1-(sum((con_data-yvec).^2)/sum((con_data-r_bar).^2))
t = time_vec/Ds_R2/3600;
max_time=max(time);
```

```
timefit = time.^0.5;
plot(timefit,yvec,timefit,con_data,'b*')
legend('Fit','Experimental')
xlabel('square time (square hour)')
ylabel('C/Co')

C  ************************************************************

C     ************************************************************
C     **      SUBROUTINE PROGRAM: "falqi1"
C     ************************************************************


function yvec = falgi1(param1,time)

global N A B alpha psi gamma u y

[N,X,W,A,B] = abxwSP8;

Ds_R2 = param1;

options =
odeset('InitialStep',eps,'RelTol',sqrt(eps),'AbsTol',20*eps)
;

den=1;vis=0.01;
%void=0.4;
velocity=0.812;
Va=17;
R=0.045;
Dl=13.26e-5*(1^-1.14)*(Va^-0.589);
Re=(2*den*R*velocity)/(vis);
Sc=vis/den/Dl;
kf=[(2+1.1*Re^0.6*Sc^0.333)*Dl]/(R*2)
C1=(kf*254e4/3000);
psi=C1/Ds_R2;
time_vec = Ds_R2.*time*3600;


[t c] = ode15s('falgi2',time_vec,[zeros(1,N) 1],options);

yvec = c(:,end);


C  ************************************************************
```

```
C     ************************************************************
C     **     SUBROUTINE PROGRAM: "falqi2"
C     ************************************************************
function dc = falgi2(t,c)

global N A B alpha psi gamma u y

u = c(1:N);
y = c(end);

us_guess = (y^alpha + u(end))/2;
[us fvec ifail] = c05nbf('falgi3',us_guess);

if ifail~=0
   error('Not Converged')
end

du = B(1:N,:)*[u;us];
dy = -psi*(y - us^(1/alpha));
dc = [du;dy];


C     ************************************************************
C     **     SUBROUTINE PROGRAM: "falqi"
C  ************************************************************
function [fvec,iflag] = falgi3(n,us,iflag)

global N A B alpha psi gamma u y

fvec = A(end,:)*[u;us] - psi*gamma/3*(y - us^(1/alpha));


C     ************************************************************
C     **     Orthogonal collocation Points:
C     ************************************************************

function [NSP,XXSP,WXSP,AXSP,BXSP] = abxwSP8
          NSP= 8;
          XXSP( 1)=  .1691860E+00;
          XXSP( 2)=  .3335048E+00;
          XXSP( 3)=  .4882293E+00;
          XXSP( 4)=  .6289081E+00;
          XXSP( 5)=  .7514942E+00;
          XXSP( 6)=  .8524606E+00;
          XXSP( 7)=  .9289015E+00;
          XXSP( 8)=  .9786118E+00;
          XXSP( 9)=  .1000000E+01;
```

```
WXSP( 1)=  .4796125E-02;
WXSP( 2)=  .1782844E-01;
WXSP( 3)=  .3537711E-01;
WXSP( 4)=  .5231507E-01;
WXSP( 5)=  .6342936E-01;
WXSP( 6)=  .6477107E-01;
WXSP( 7)=  .5468958E-01;
WXSP( 8)=  .3427863E-01;
WXSP( 9)=  .5847953E-02;
AXSP( 1, 1)= -.8865981E+01;
AXSP( 1, 2)=  .1556880E+02;
AXSP( 1, 3)= -.1264388E+02;
AXSP( 1, 4)=  .1132233E+02;
AXSP( 1, 5)= -.1019516E+02;
AXSP( 1, 6)=  .8975397E+01;
AXSP( 1, 7)= -.7520016E+01;
AXSP( 1, 8)=  .5632024E+01;
AXSP( 1, 9)= -.2273523E+01;
AXSP( 2, 1)= -.2124686E+01;
AXSP( 2, 2)= -.4497686E+01;
AXSP( 2, 3)=  .1081853E+02;
AXSP( 2, 4)= -.7578744E+01;
AXSP( 2, 5)=  .6251002E+01;
AXSP( 2, 6)= -.5280024E+01;
AXSP( 2, 7)=  .4329022E+01;
AXSP( 2, 8)= -.3206206E+01;
AXSP( 2, 9)=  .1288795E+01;
AXSP( 3, 1)=  .5940037E+00;
AXSP( 3, 2)= -.3724237E+01;
AXSP( 3, 3)= -.3072327E+01;
AXSP( 3, 4)=  .9732716E+01;
AXSP( 3, 5)= -.6166260E+01;
AXSP( 3, 6)=  .4724198E+01;
AXSP( 3, 7)= -.3698837E+01;
AXSP( 3, 8)=  .2678385E+01;
AXSP( 3, 9)= -.1067642E+01;
AXSP( 4, 1)= -.2792394E+00;
AXSP( 4, 2)=  .1369615E+01;
AXSP( 4, 3)= -.5109356E+01;
AXSP( 4, 4)= -.2385086E+01;
AXSP( 4, 5)=  .9780039E+01;
AXSP( 4, 6)= -.5728472E+01;
AXSP( 4, 7)=  .4064550E+01;
AXSP( 4, 8)= -.2818267E+01;
AXSP( 4, 9)=  .1106217E+01;
AXSP( 5, 1)=  .1735533E+00;
AXSP( 5, 2)= -.7797386E+00;
```

```
AXSP( 5, 3)=  .2234354E+01;
AXSP( 5, 4)= -.6750542E+01;
AXSP( 5, 5)= -.1996023E+01;
AXSP( 5, 6)=  .1063851E+02;
AXSP( 5, 7)= -.5786603E+01;
AXSP( 5, 8)=  .3661706E+01;
AXSP( 5, 9)= -.1395216E+01;
AXSP( 6, 1)= -.1319026E+00;
AXSP( 6, 2)=  .5685856E+00;
AXSP( 6, 3)= -.1477811E+01;
AXSP( 6, 4)=  .3413481E+01;
AXSP( 6, 5)= -.9184201E+01;
AXSP( 6, 6)= -.1759612E+01;
AXSP( 6, 7)=  .1253670E+02;
AXSP( 6, 8)= -.6164030E+01;
AXSP( 6, 9)=  .2198793E+01;
AXSP( 7, 1)=  .1201156E+00;
AXSP( 7, 2)= -.5066767E+00;
AXSP( 7, 3)=  .1257584E+01;
AXSP( 7, 4)= -.2632402E+01;
AXSP( 7, 5)=  .5429570E+01;
AXSP( 7, 6)= -.1362587E+02;
AXSP( 7, 7)= -.1614811E+01;
AXSP( 7, 8)=  .1634129E+02;
AXSP( 7, 9)= -.4768803E+01;
AXSP( 8, 1)= -.1362340E+00;
AXSP( 8, 2)=  .5682938E+00;
AXSP( 8, 3)= -.1379067E+01;
AXSP( 8, 4)=  .2764155E+01;
AXSP( 8, 5)= -.5203142E+01;
AXSP( 8, 6)=  .1014580E+02;
AXSP( 8, 7)= -.2474724E+02;
AXSP( 8, 8)= -.1532784E+01;
AXSP( 8, 9)=  .1952022E+02;
AXSP( 9, 1)=  .3154644E+00;
AXSP( 9, 2)= -.1310374E+01;
AXSP( 9, 3)=  .3153318E+01;
AXSP( 9, 4)= -.6223729E+01;
AXSP( 9, 5)=  .1137244E+02;
AXSP( 9, 6)= -.2076041E+02;
AXSP( 9, 7)=  .4142664E+02;
AXSP( 9, 8)= -.1119734E+03;
AXSP( 9, 9)=  .8400000E+02;
BXSP( 1, 1)= -.9989137E+02;
BXSP( 1, 2)=  .1275532E+03;
BXSP( 1, 3)= -.4079580E+02;
BXSP( 1, 4)=  .2088386E+02;
```

```
BXSP( 1, 5)= -.1286935E+02;
BXSP( 1, 6)=  .8701261E+01;
BXSP( 1, 7)= -.6100357E+01;
BXSP( 1, 8)=  .4102481E+01;
BXSP( 1, 9)= -.1583931E+01;
BXSP( 2, 1)=  .3431378E+02;
BXSP( 2, 2)= -.1237711E+03;
BXSP( 2, 3)=  .1135115E+03;
BXSP( 2, 4)= -.3556170E+02;
BXSP( 2, 5)=  .1838727E+02;
BXSP( 2, 6)= -.1144447E+02;
BXSP( 2, 7)=  .7683274E+01;
BXSP( 2, 8)= -.5053001E+01;
BXSP( 2, 9)=  .1934436E+01;
BXSP( 3, 1)= -.5530744E+01;
BXSP( 3, 2)=  .5720460E+02;
BXSP( 3, 3)= -.1475810E+03;
BXSP( 3, 4)=  .1209435E+03;
BXSP( 3, 5)= -.3689672E+02;
BXSP( 3, 6)=  .1889323E+02;
BXSP( 3, 7)= -.1156707E+02;
BXSP( 3, 8)=  .7271747E+01;
BXSP( 3, 9)= -.2737562E+01;
BXSP( 4, 1)=  .1914584E+01;
BXSP( 4, 2)= -.1211906E+02;
BXSP( 4, 3)=  .8178581E+02;
BXSP( 4, 4)= -.1873294E+03;
BXSP( 4, 5)=  .1453922E+03;
BXSP( 4, 6)= -.4351545E+02;
BXSP( 4, 7)=  .2187931E+02;
BXSP( 4, 8)= -.1261168E+02;
BXSP( 4, 9)=  .4603728E+01;
BXSP( 5, 1)= -.9730984E+00;
BXSP( 5, 2)=  .5168209E+01;
BXSP( 5, 3)= -.2057879E+02;
BXSP( 5, 4)=  .1199161E+03;
BXSP( 5, 5)= -.2610292E+03;
BXSP( 5, 6)=  .1974684E+03;
BXSP( 5, 7)= -.5834803E+02;
BXSP( 5, 8)=  .2801210E+02;
BXSP( 5, 9)= -.9635670E+01;
BXSP( 6, 1)=  .6443051E+00;
BXSP( 6, 2)= -.3150125E+01;
BXSP( 6, 3)=  .1031924E+02;
BXSP( 6, 4)= -.3514708E+02;
BXSP( 6, 5)=  .1933779E+03;
BXSP( 6, 6)= -.4164193E+03;
```

```
      BXSP( 6, 7)=  .3139346E+03;
      BXSP( 6, 8)= -.9099179E+02;
      BXSP( 6, 9)=  .2743226E+02;
      BXSP( 7, 1)= -.5349845E+00;
      BXSP( 7, 2)=  .2504696E+01;
      BXSP( 7, 3)= -.7482403E+01;
      BXSP( 7, 4)=  .2092936E+02;
      BXSP( 7, 5)= -.6767246E+02;
      BXSP( 7, 6)=  .3718054E+03;
      BXSP( 7, 7)= -.8306760E+03;
      BXSP( 7, 8)=  .6403283E+03;
      BXSP( 7, 9)= -.1292018E+03;
      BXSP( 8, 1)=  .5740023E+00;
      BXSP( 8, 2)= -.2628084E+01;
      BXSP( 8, 3)=  .7504776E+01;
      BXSP( 8, 4)= -.1924759E+02;
      BXSP( 8, 5)=  .5183376E+02;
      BXSP( 8, 6)= -.1719332E+03;
      BXSP( 8, 7)=  .1021607E+04;
      BXSP( 8, 8)= -.2693303E+04;
      BXSP( 8, 9)=  .1805592E+04;
      BXSP( 9, 1)=  .5264537E+02;
      BXSP( 9, 2)= -.2181765E+03;
      BXSP( 9, 3)=  .5226565E+03;
      BXSP( 9, 4)= -.1023073E+04;
      BXSP( 9, 5)=  .1840175E+04;
      BXSP( 9, 6)= -.3246194E+04;
      BXSP( 9, 7)=  .5875670E+04;
      BXSP( 9, 8)= -.8563703E+04;
      BXSP( 9, 9)=  .4760000E+04;
C     ************************************************************
```

VITA

Name:	Fahad Hussain Falqi
Date & Place of Birth:	November 10, 1977 & Taif, K.S.A.
Religion:	ISLAM
Permanent Address:	P.O. Box 11425, Al- Jubail Industrial City 31961, Saudi Arabia
Nationality:	Saudi Arabia

Education Qualification:

B.Sc. Chemical Engineering, (May 2000)
King Fhad University of Petroleum & Minerals, Dhahran, Saudi Arabia

Professional Experience:

Process Engineer (Sep 2000-June 2002)
Ethylene Plant, SADAF Company, One of SABIC companies, Al-Jubail Industrial City.

Process Engineer (June 2002-Feb 2003)
UNITED Ethylene Plant Project, Yokohama, Japan, One of SABIC companies, Al-Jubail Industrial City.

Process and Production Engineer (Feb 2003-Aug 2004)
UNITED Ethylene Plant Project, One of SABIC companies, Al-Jubail Industrial City.

Process Engineer (Oct 2004-date)
UNITED II Ethylene Plant Project, Reading, UK, One of SABIC companies, Yanbu Industrial City.